平成 25 年度博士論文

Studies on heat, water and carbon exchanges between atmosphere and forest at a tropical deciduous forest in Northern Thailand

（タイ北部・熱帯落葉林における大気-森林間での熱・水・炭素交換に関する研究）

Yasunori Igarashi

（五十嵐　康記）

Contents

Contents

List of Abbreviations

Chapter 1
General introduction

Chapter 2
Micrometeorology and eddy flux observation at a teak plantation in Northern Thailand

Chapter 3
Seasonal and inter-annual variation of stomatal conductance and its controlling factors at a teak plantation in Northern Thailand

Chapter 4
Modeling of stomatal conductance and estimation of evapotranspiration at tropical deciduous forest in Northern Thailand

List of Abbreviations

A_c	available energy at the canopy	LAI	leaf area index
A_s	available energy at the soil surface	LE	latent heat flux
c_p	specific heat of air at a constant pressure	LE_c	latent heat flux from the canopy
EI	total interception	LE_s	latent heat flux from the soil surface
d	zero-plane displacement	NEE	net ecosystem exchange
E_i	canopy interception	P	rainfall
E_{it}	trunk interception	P_G	annual rainfall
E_p	evaporation from wet surface	P_{max}	maximum photosynthesis
E_{ps}	transpiration from wet canopy	R	Gas constant
E_{pt}	evaporation from soil surface	R_e	night time respiration
ET	evapotranspiration	RH	relative humidity
E_{tc}	transpiration	R_s	downward short wave radiation
E_{ts}	soil evaporation	SAT	sonic anemometer
F_c	CO_2 flux	S_b	downward short wave radiation at a forest floor
F_s	storage flux	T_a	air temperature
G	ground heat flux	U	wind velocity
G_a	aero dynamic conductance	u^*	friction velocity

G_c	canopy conductance	v	dimensional curve parameter
G_s	surface conductance	VPD	vapor pressure deficit
g_s	stomatal conductance	z_0	roughness length
GSL	growing season length	γ	psychometric constant
g_{smax}	maximum stomatal conductance	Δ	ratio of charge of saturation water vapor pressure with temperature
g_{sref}	reference conductance	Θ_{0-60}	averaged soil moisture
H	sensible heat flux	ρ	density
IBR	imbalance ratio	σ_u	standard derivation of horizontal turbulence intensity
IRGA	infra-red gas analyzer	σ_w	standard derivation of vertical turbulence intensity
κ	Von Karman coefficient	τ	the term of available energy transmitted downwards at LAI
L	Monin-Obukhov length	$\emptyset_m$	momentum stability correction function

Chapter 1

General introduction

1.1 Energy, water and carbon cycle in tropical forest

Tropical forests are an important latent energy source (e.g. Choudhury et al., 1998; Fisher et al., 2009) and having a strong influence on both regional and global climate (e.g. Mabuchi et al., 2005a and b; vad der Molen et al., 2006). Tropical forests also play a significant role in the global carbon budget (e.g. Melillo et al., 1993; Malhi and Grace, 2000). Because tropical forests contain ~ 25% of the carbon in the terrestrial biosphere, account for ~ 33% of terrestrial net primary production (Sabine et al., 2004), and can sequester large amounts of carbon (Bonan, 2008). Therefore, accurate prediction of heat, water and carbon exchanges between atmospheres and tropical forests is a critical to our understanding of these processes under changing climate.

In the tropical forest, several different types of forest which include evergreen and deciduous forests are distributed depending on the annual rainfall and its seasonality (e.g. Kuraji et al., 1995; Tanaka et al., 2008). A number of filed studies have investigated of the hydrological and carbon exchanges between forests and atmospheres in Amazonian and Southeast Asian tropical forest, by using an eddy covariance method. Eddy covariance method, a micrometeorological technique, provides a direct measure of heat, water and carbon fluxes between atmosphere and forest canopy (Baldocchi et al. 1988; Foken and Wichura 1996; Aubinet et al. 2000). With current technology, the eddy covariance method is able to measure mass and energy fluxes over short and long timescales (hour, days, seasons, and years) with minimal disturbance to the underlying vegetation. Another attribute of the eddy covariance method is its ability to sample a relatively large area of land. Typical footprints have longitudinal length scales of 100 - 2000 m (Schmid 1994). Using an eddy covariance method, previous studies have been revealing the water balance in tropical forests after 1990's. Major results that used eddy covariance method were listed as Table.1.1 (e.g. Shutleworth et al., 1984; Hodnet et al., 1995; Grace te al., 1995; Leopoldo et al., 1995; Williams et al., 1998; Malhi et al., 2002; Vourlists et al., 2002; Carswell e al., 2002; Scotto et al., 2003; da Rocha et al., 2004; Tani et al., 2003; Kumagai et al., 2004, 2005 and 2006;

Table 1.1 List of water balance in Amazonian and Southeast Asian tropical forests based on the eddy covariance method.

Region	Site	Latitude / Longtide	Vegetation	Rainfall (mm)	Q (mm)	ET (mm)	Observation year	Method	Citation
South America	Reserva Biologica do Cuieiras Manaus, Brazil	2 ° 35 ' S / 60 ° 06 ' W	Evergreen tropical rainforest	2089	-	1123	1995 - 1996	EC	Malhi et al. (2002)
South America	Tapajos National Forest Santarem Para, Brazil	2 ° 51 ' S / 54 ° 58 ' W	Evergreen tropical rainforest	2106	-	1124	2002 - 2006	EC	Hutyra et al. (2007)
South America	Reserva Ducke Manaus, Brazil	2 ° 57 ' S / 59 ° 57 ' W	Evergreen tropical rainforest	2648	-	1311	1983 -1985	EC & Model	Shuttleworth (1988)
South America	Floresta Na- cional do Tapajos Para, Brazil	3 ° 01 ' S / 54 ° 58 ' W	Evergreen tropical rainforest	3200	-	1281	2000 - 2001	EC	da Rocha et al. (2004)
South America	Cantao State Park Tocantins, Brazil	9 ° 46 ' S / 50 ° 08 ' W	Mixed semi-deciduous forests	1692	-	1332	2003 - 2006	EC	Borma et al. (2009)
South America	Rebio Jarn Rondonia, Brazil	10 ° 10 ' S / 61 ° 40 ' W	Evergreen tropical rainforest	2200	-	1359	2001 - 2002	EC	von Randow et al. (2004)
South America	Sinop Matto Grosso, Brazil	11 ° 24 ' S / 55 ° 19 ' W	Evergreen tropical rainforest	2095	-	1029	1999 - 2000	EC	Vourlitis et al. (2001)
South America	Eucalyptus plantation São Paulo, Brazil	21 ° 35 ' S / 47 ° 36 ' W	Evergreen eucalyptus plantation	1329	-	1179	2006 - 2007	EC	Carbral et al. (2010)
Asia	Palangkaraya Central Kalimantan, Indonesia	2 ° 20 ' S / 114 ° 02 ' E	Evergreen tropical peat swamp forest	1856	-	1244	2002	EC	Hirano et al. (2005)
Asia	Pasoh Negeri Sembilan, Malaysia	2 ° 58 ' N / 102 ° 18 ' E	Evergreen lowland mixed dipterocarp	1733	-	1318	2003 - 2005	EC	Takanashi et al. (2010)
Asia	Lambir Sarawaku, Malaysia	4 ° 12 ' N / 114 ° 02 ' E	Evergreen lowland forest	2154	-	1303	2001 - 2002	EC	Kumagai et al (2004)
Asia	O Thom I Central Cambodia	12 ° 544 ' N / 105 ° 28 ' E	Evergreen broad-leaved evergreen trees	1700	-	1140	2004	EC	Nobuhiro et al. (2009)
Asia	KogMa Chaing Mai, Thailand	18 ° 48 ' N / 98 ° 54 ' E	Evergreen Hill evergreen forest	1575	425	850	1998 - 1999	EC, WS & Model	Tanaka et al. (2003)
Asia	Xishuangbanna Southwest China	21 ° 55 ' N / 101 ° 15 ' E	Evergreen tropical rainforest	1322	-	1029	2003 - 2006	EC	Li et al. (2006)

※ Q: annual runoff, ET: annual evapotranspiration, EC : eddy covariance method, WS : catchment water balance, Model : hydrological model which was validated observed eddy covariance data.

Saitoh et al., 2005; Takanashi et al., 2005; Kosugi et al., 2008; Ohkubo et al., 2008; Hirata et al., 2008; Takanashi et al., 2010). These previous studies mainly conducted at tropical evergreen forest. On the other hands, studies on the water and carbon exchanges between forests and atmosphere at a tropical deciduous-type forest are less relative rather than that of tropical evergreen forest (Kuraji, 1996). A vegetation surface of deciduous forest changes with vegetation phonology, such as leaf-out and leaf-fall. These seasonal surface changes would influence energy partitioning and carbon exchanges thorough the transpiration and photosynthesis on vegetation surface. And the tropical forest, deciduous types of forests account for significant portion of the area. Tropical moist deciduous forests and tropical dry forests represent 43 % of the total tropical forest area (FAO, 2001). Furthermore, the total area of tropical deciduous forests is estimated to be larger than that of temperate deciduous forests (Melillo et al., 1993). Therefore, it is required to investigate heat, water and carbon exchanges of tropical deciduous forests and their response to the environmental variables based on the field measurements.

1.2 Characteristics of heat and water exchanges in topical deciduous forest

Deciduous forests in temperate and/or boreal region retain leaves on the canopy during from spring to autumn and fall leaves in the winter, on the other hands, deciduous forests in tropical region retain leaves on the canopy in the wet season and fall in the dry season. The clear seasonal changes of canopy surface may influence, energy partitioning between the canopy and the soil surface, the boundary layer of the canopy, water storage on the canopy and the transpiration periods. Kelliher et al. (1995) showed that leaf area index (LAI) play a important role to distribute available energy for the canopy and the soil surface. According to Nakai et al. (2008), forest structure and canopy condition can change the vertical profile of wind speed above the canopy. Wilson and Baldocchi (2000) showed that energy partitioning of sensible heat flux (H) and latent heat flux (LE) was strongly dependent on whether leaves were present or not in temperate deciduous forest. In temperate and/or boreal deciduous forests, incident radioactive energy is relatively small during from autumn to spring because of low solar elevation; on the other hand, high incident radioactive is available throughout the year in tropical deciduous forests. Therefore, it can be considered that the effect of canopy condition to land surface processes in tropical deciduous forest is larger than that of temperate and boreal deciduous forests. There is a typical tropical deciduous forest in mainland Southeast Asia due to the Asian monsoon climate. The Asian monsoon climate is characterized by strong seasonal variations with dry and rainy seasons.

According to review by Tanaka et al. (2008), the clear seasonality of rainfall and interannual variations in onset and offset of monsoon were observed in that region. Yoshifuji et al. (2006) showed that the interannual variations in onset and offset of monsoon, length of rainy season, influence growing-season length (leafy-season) and transpiration period at a tropical deciduous forest in northern Thailand. These interannual variations are larger than that of temperate and/or boreal deciduous forest (Goulden et al., 1996; Wilson and Baldocchi, 2000; Granier et al., 2002a and 2002b; Saigusa et al., 2002; Barr et al., 2004; Yoshifuji et al., 2006; Hirata et al., 2007; Yoshifuji et al., 2011).

Land-surface regulation of evapotranspiration is mainly determined by surface conductance and aerodynamic conductance. Surface conductance is a major factor to regulate LE relative to aerodynamic conductance in a forest due to the large surface roughness. Therefore, to know the relationship between surface conductance and environmental variables and phonological and physiological changes is important to understand the characteristic of evapotranspiration in tropical deciduous forests.

In general, annual evapotranspiration from forest ecosystem around world was mainly determined by the annual rainfall and annual mean air temperature (e.g. Zhang et al., 1999 and 2001; Komatsu et al., 2012). As the author mentioned above, interannual variation of growing season length is large. Therefore, it can be considered that not only the annual rainfall but also the growing season length might influence evapotranspiration in tropical deciduous forest. The growing season length must be taken into consideration when to evaluate the annual evapotranspiration and its interannual variation.

1.3 The effect of leaf maturing and aging to transpiration and photosynthesis in a topical deciduous forest

In deciduous forest, it has been indicated that the effect of leaves maturing and aging to water and carbon exchanges (e.g. Kitajima et al., 1997; Wilson et al. 2000; Kitajima et al., 2002). Photosynthetic capacity of a leaf generally exhibits a monotonic, often linear, decline after full expansion (Koike, 1988; Zotz and Winter, 1994; Ackerly and Bazzaz, 1995; Kitajima, Mulkey, and Wright, 1997). This decline is not an uncontrolled physiological deterioration, but is caused by a redistribution of resources, especially nitrogen, to younger leaves for optimization of whole-shoot photosynthetic income (Field and Mooney, 1983; Hikosaka, Terashima, and Katoh, 1994). Consideration of the effect of leaf age on photosynthetic capacity is necessary to estimate the long-term carbon budget of a leaf and of the whole crown. For temperate deciduous species, the maximum carboxylation rates of mature individual leaves are often strongly controlled by leaf age rather than ambient

environmental factors (Wilson et al., 2001). Kitajima et al. (1997 and 2002) also showed that photosynthetic capacity decreased with leaf age in a tropical seasonal dry forest in Panama. Therefore, considering the effect of leaf maturing and aging to transpiration and photosynthesis in tropical deciduous forest is greatly important.

1.4 Objectives

Because of these backgrounds, studies on energy, water and carbon exchange between the atmosphere and tropical deciduous forests in Southeast Asia is the critical issue. This study aimed to investigate the relationship between seasonal and interannual variation of evapotranspiration and interannual variation of environmental variables and growing season length, and the effect of maturing and aging of leaves to photosynthesis at a deciduous forest under the Asian monsoon climate. This study was conducted in teak (*Tectona grandis* Linn.f.) plantation in northern Thailand. Teak is one of the major deciduous tree species of Southeast Asia, and its plantation are widely distributed over tropical Asia. Simple species components and forest structure of plantation provides an advantage to evaluate the energy, water and carbon exchanges between atmosphere to forest.

Objective in Chapter 2 is to show the outlines of the sites and the characteristics of seasonal and interannual variation in meteorological factors and seasonal and interannual variation of sensible heat and latent heat flux and net ecosystem exchanges using eddy covariance technique at a teak plantation in northern Thailand. The quality check like a spectrum analysis and footprint for eddy flux measurement was also examined.

Objective in Chapter 3 is to reveal the characteristic of seasonal and interannual variation of transpiration, surface, canopy and stomatal conductance and its controlling factor. To this objective, soil evaporation was modeled using the latent heat flux in dry (leaf-less) season to divide the latent heat flux into canopy transpiration and soil evaporation.

Objective in Chapter 4 is to estimate of interannual variation of evapotranspiration by using a big-leaf model which contained Jarvis-type stomatal conductance model and Rutter-type interception model, and to examine how the rainfall and the growing season length affect the evapotranspiration in a tropical deciduous forest.

Objective in Chapter 5 is to reveal the relationship between water and carbon exchanges. The water and carbon exchanges and the timing of teak phenology such as leaf-out and leaf-fall, as well as leaf ageing was discussed.

This study is concluded in chapter 6.

References

Ackerly, D. D., & Bazzaz, F. A. (1995). Leaf Dynamics, Self-Shading and Carbon Gain in Seedlings of a Tropical Pioneer Tree. Oecologia, 101(3), 289–298. doi:10.2307/4220887

Almeida, A. C., Soares, J. V., Landsberg, J. J., & Rezende, G. D. (2007). Growth and water balance of Eucalyptus grandis hybrid plantations in Brazil during a rotation for pulp production. Forest Ecology and Management, 251(1-2), 10–21. doi:10.1016/j.foreco.2007.06.009

Aubinet, M., Heinesch, B., Longdoz, B. (2002). Estimation of the carbon sequestration by a heterogeneous forest: night flux corrections, heterogeneity of the site and inter-annual variability. Global Change Biology, 8(11), 1053–1071. doi:10.1046/j.1365-2486.2002.00529.x

Barr, A. G., Black, T. a., Hogg, E. H., Kljun, N., Morgenstern, K., & Nesic, Z. (2004). Inter-annual variability in the leaf area index of a boreal aspen-hazelnut forest in relation to net ecosystem production. Agricultural and Forest Meteorology, 126(3-4), 237–255. doi:10.1016/j.agrformet.2004.06.011

Black, T. A., Chen, W. J., Barr, A. G., Arain, M. A., Chen, Z., Nesic, Z., Hogg, E. H., et al. (2000). Increased carbon sequestration by a boreal deciduous forest in years with a warm spring. Geophysical Research Letters, 27(9), 1271. doi:10.1029/1999GL011234

Bonan, G. B. (2008). Forests and climate change: forcings, feedbacks, and the climate benefits of forests. Science, 320(5882), 1444–1449. doi:10.1126/science.1155121

Cabral, O. M. R., Rocha, H. R., Gash, J. H. C., Ligo, M. a. V., Freitas, H. C., & Tatsch, J. D. (2010). The energy and water balance of a Eucalyptus plantation in southeast Brazil. Journal of Hydrology, 388(3-4), 208–216. doi:10.1016/j.jhydrol.2010.04.041

Carrara, A., Kowalski, A. S., Neirynck, J., Janssens, I. A., Yuste, J. C., & Ceulemans, R. (2003). Net ecosystem CO_2 exchange of mixed forest in Belgium over 5 years. Agricultural and Forest Meteorology, 119(3-4), 209–227. doi:10.1016/S0168-1923(03)00120-5

Carswell, F. E., Costa, A. L., Palheta, M., Malhi, Y., Meir, P., Costa, J. de P. R., Ruivo, M. de L., et al. (2002). Seasonality in CO_2 and H_2O flux at an eastern Amazonian rain forest. Journal of Geophysical Research, 107(D20), 8076. doi:10.1029/2000JD000284

Else,M.A., Tiekstra, A.E., Croker, S.J., Davies, W.J. & Jackson, M.B. (1996) Stomatal closure in flooded tomato plants involves abscisic acid and a chem- ically unidentified antitranspirant in xylem sap. Plant Physiology, 112,239– 247.

Field, C., & Mooney, H. a. (1983). Leaf age and seasonal effects on light, water, and nitrogen use efficiency in a California shrub. Oecologia, 56(2-3), 348–355. doi:10.1007/BF00379711

Goulden, M. L., Munger, J. W., Fan, S.-M., Daube, B. C., & Wofsy, S. C. (1996). Measurements of carbon sequestration by long-term eddy covariance: methods and a critical evaluation of accuracy. Global Change Biology, 2(3), 169–182. doi:10.1111/j.1365-2486.1996.tb00070.x

Grace, J., Lloyd, J., Mcintyre, J., Miranda, A., Meir, P., Miranda, H., Moncrieff, J., et al. (1995). Fluxes of carbon dioxide and water vapour over an undisturbed tropical forest in south-west Amazonia. Global Change Biology, 1(1), 1–12. doi:10.1111/j.1365-2486.1995.tb00001.x

Hikosaka, K., Terashima, I., & Katoh, S. (1994). , nitrogen nutrition and photon flux density on the distribution of nitrogen among leaves of a vine (Ipomoea tricolor Cav.) grown horizontally to avoid mutual shading of. Oecologia, 93, 451 – 457.

Hirata, R., Saigusa, N., Yamamoto, S., Ohtani, Y., Ide, R., Asanuma, J., Gamo, M., et al. (2008). Spatial distribution of carbon balance in forest ecosystems across East Asia. Agricultural and Forest Meteorology, 148(5), 761–775. doi:10.1016/j.agrformet.2007.11.016

Hodnetta, M. G., Silvab, L. P., Rochac, H. R., & Sennad, R. C. (1995). Seasonal soil water storage changes beneath central Amazonian rainforest and pasture, 170, 233–254.

Kanae, S., Oki, T., & Musiake, K. (2001). Impact of Deforestation on Regional Precipitation over the Indochina Peninsula. Journal of Hydrometeorology, 2(1), 51–70. doi:10.1175/1525-7541(2001)002<0051:IODORP>2.0.CO;2

Kelliher, F., Leuning, R., Raupach, M. R., & Schulze, E.-D. (1995). Maximum conductances for evaporation from global vegetation types. Agricultural and Forest Meteorology, 73(1-2), 1–16. doi:10.1016/0168-1923(94)02178-M

Kitajima, K., Mulkey, S. S., & Wright, S. J. (1997). Seasonal leaf phenotypes in the canopy of a tropical dry forest: photosynthetic characteristics and associated traits. Oecologia, 109(4), 490–498. doi:10.1007/s004420050109

Kitajima, K., Mulkey, S. S., & Wright, S. J. (1997). Decline of Photosynthetic Capacity with Leaf Age in Relation to Leaf Longevities for Five Tropical Canopy Tree Species. American Journal of Botany, 84(5), 702 – 708.

Kitajima, K., Mulkey, S. S., Samaniego, M., & Joseph Wright, S. (2002). Decline of photosynthetic capacity with leaf age and position in two tropical pioneer tree species. American journal of botany, 89(12), 1925–32. doi:10.3732/ajb.89.12.1925

Koike, T. (1988). Leaf Structure and Photosynthetic Performance as Related to the Forest Succession of Deciduous Broad-Leaved Trees1. Plant Species Biology, 3(2), 77–87. doi:10.1111/j.1442-1984.1988.tb00173.x

Kosugi, Y., Takanashi, S., Ohkubo, S., Matsuo, N., Tani, M., Mitani, T., Tsutsumi, D., et al. (2008). CO_2 exchange of a tropical rainforest at Pasoh in Peninsular Malaysia. Agricultural and Forest Meteorology, 148(3), 439–452. doi:10.1016/j.agrformet.2007.10.007

Kumagai, T., Saitoh, T. M., Sato, Y., Morooka, T., Manfroi, O. J., Kuraji, K., & Suzuki, M. (2004). Transpiration, canopy conductance and the decoupling coefficient of a lowland mixed dipterocarp forest in Sarawak, Borneo: dry spell effects. Journal of Hydrology, 287(1-4), 237–251. doi:10.1016/j.jhydrol.2003.10.002

Kumagai, T., Saitoh, T. M., Sato, Y., Takahashi, H., Manfroi, O. J., Morooka, T., Kuraji, K., et al. (2005). Annual water balance and seasonality of evapotranspiration in a Bornean tropical rainforest. Agricultural and Forest Meteorology, 128(1-2), 81–92. doi:10.1016/j.agrformet.2004.08.006

Kumagai, T., Ichie, T., Yoshimura, M., Yamashita, M., Kenzo, T., Saitoh, T. M., Ohashi, M., et al. (2006). Modeling CO_2 exchange over a Bornean tropical rain forest using measured vertical and horizontal variations in leaf-level physiological parameters and leaf area densities. Journal of Geophysical Research, 111(D10), 1–16. doi:10.1029/2005JD006676

Kume, T., Kuraji, K., Yoshifuji, N., Morooka, T., Sawano, S., Chong, L., & Suzuki, M. (2006). Estimation of canopy drying time after rainfall using sap flow measurements in an emergent tree in a lowland mixed-dipterocarp forest in Sarawak, Malaysia. Hydrological Processes, 20(3), 565–578. doi:10.1002/hyp.5924

Kuraji, K. (1996). Water balance studies on moist tropical forested catchments. Journal of the Japanese forestry science [in Japanese], 78(1), 89–99.

Lean, J., Warrilow, D. A. (1989). Simulation of the regional climatic impact of Amazon deforestation. Nature, 342(6248), 411–413. doi:10.1038/342411a0

Leopoldo, P. R., Franken, W. K., & Villa Nova, N. A. (1995). Real evapotranspiration and transpiration through a tropical rain forest in central Amazonia as estimated by the water balance method. Forest Ecology and Management, 73(1-3), 185–195. doi:10.1016/0378-1127(94)03487-H

Okubo, S., Kosugi, Y. (2007). Amplitude and seasonality of storage fluxes for CO_2 heat and water vapour in a temperate Japanese cypress forest. Tellus B, 60(1), 11–20. doi:10.1111/j.1600-0889.2007.00321.x

Mabuchi, K., Sato, Y., & Kida, H. (2005a). Climatic Impact of Vegetation Change in the Asian Tropical Region. Part I: Case of the Northern Hemisphere Summer. Journal of Climate, 18(3), 410–428. doi:10.1175/JCLI-3273.1

Mabuchi, K., Sato, Y., & Kida, H. (2005b). Climatic Impact of Vegetation Change in the Asian Tropical Region. Part II: Case of the Northern Hemisphere Winter and Impact on the Extratropical Circulation. Journal of Climate, 18(3), 429–446. doi:10.1175/JCLI-3274.1

Van der Molen, M., Dolman, a, Waterloo, M., & Bruijnzeel, L. (2006). Climate is affected more by maritime than by continental land use change: A multiple scale analysis. Global and Planetary Change, 54(1-2), 128–149. doi:10.1016/j.gloplacha.2006.05.005

Malhi, Y., & Grace, J. (2000). Tropical forests and atmospheric carbon dioxide. Trends in Ecology & Evolution, 15(8), 332–337. doi:10.1016/S0169-5347(00)01906-6

Malhi, Y., Pegoraro, E., Nobre, A. D., Pereira, M. G. P., Grace, J., Culf, A. D., & Clement, R. (2002). Energy and water dynamics of a central Amazonian rain forest. Journal of Geophysical Research, 107(D20), 1–17. doi:10.1029/2001JD000623

Melillo, J. M., McGuire, A. D., Kicklighter, D. W., Moore, B., Vorosmarty, C. J., & Schloss, A. L. (1993). Global climate change and terrestrial net primary production. Nature, 363(6426), 234–240. doi:10.1038/363234a0

Morris, J., Ningnan, Z., Zengjiang, Y., Collopy, J., & Daping, X. (2004). Water use by fast-growing Eucalyptus urophylla plantations in southern China. Tree physiology, 24(9), 1035–44.

Nakai, T., Sumida, A., Daikoku, K., Matsumoto, K., Van der Molen, M. K., Kodama, Y., Kononov, A. V, et al. (2008). Parameterisation of aerodynamic roughness over boreal, cool- and warm-temperate forests. Agricultural and Forest Meteorology, 148(12), 1916–1925. doi:10.1016/j.agrformet.2008.03.009

Nobuhiro, T. (2009). Evapotranspiration Characteristics of a Lowland Dry Evergreen Forest in Central Cambodia Examined Using a Multilayer Model. Journal of Water Resource and Protection, 01(05), 325–335. doi:10.4236/jwarp.2009.15039

Da Rocha, H. R., Goulden, M. L., Miller, S. D., Menton, M. C., Pinto, L. D. V. O., De Freitas, H. C., & e Silva Figueira, A. M. (2004). Seasonality of water and heat fluxes over a tropical forest in eastern Amazonia. Ecological Applications, 14(sp4), 22–32.

Sabine CL, Heimann M, Artaxo P et al. (2004) Current status and past trends of the global carbon cycle. In: The Global Carbon Cycle (eds Field CB, Raupach MR), pp. 17–44. Island Press, Washington.

Saigusa, N., Yamamoto, S., Murayama, S., Kondo, H., & Nishimura, N. (2002). Gross primary production and net ecosystem exchange of a cool-temperate deciduous forest estimated by the eddy covariance method. Agricultural and Forest Meteorology, 112(3-4), 203–215. doi:10.1016/S0168-1923(02)00082-5

Saigusa, N., Yamamoto, S., Murayama, S., Kondo, H. (2005). Inter-annual variability of carbon budget components in an AsiaFlux forest site estimated by long-term flux measurements. Agricultural and Forest Meteorology, 134(1-4), 4–16. doi:10.1016/j.agrformet.2005.08.016

Saitoh, T. M., Kumagai, T., Sato, Y., & Suzuki, M. (2005). Carbon dioxide exchange over a Bornean tropical rainforest. Journal of Agricultural Meteorology, 60(5), 553–556.

Saleska, S. R., Miller, S. D., Matross, D. M., Goulden, M. L., Wofsy, S. C., Rocha, H. R. Da, Camargo, P. B. De, et al. (2003). Carbon in Amazon forests: Unexpected seasonal fluxes and disturbance-induced losses. Science, 302(5650), 1554–1557. doi:10.1126/science.1091165

Shuttleworth, W. J., Gash, J. H. C., Lloyd, C. R., Moore, C. J., Roberts, J., Filho, A. D. O. M., Fisch, G., et al. (1984). Eddy correlation measurements of energy partition for Amazonian forest. Quarterly Journal of the Royal Meteorological Society, 110(466), 1143–1162. doi:10.1002/qj.49711046622

Shuttleworth, W. J., Leuning, R., Black, T. A., Grace, J., Jarvis, P. G., Roberts, J., & Jones, H. G. (1989). Micrometeorology of Temperate and Tropical Forest [and Discussion]. Philosophical Transactions of the Royal Society B: Biological Sciences, 324(1223), 299–334. doi:10.1098/rstb.1989.0050

Takanashi, S., Kosugi, Y., Tani, M., Matsuo, N., Mitani, T., & Nik, A. (2005). Characteristics of the gas exchange of a tropical rain forest in Peninsular Malaysia. Phyton(Horn), 45(4), 61–66.

Takanashi, S., Kosugi, Y., Tanaka, Y., Yano, M., Katayama, T., Tanaka, H., & Tani, M. (2005). CO_2 exchange in a temperate Japanese cypress forest compared with that in a cool-temperate deciduous broad-leaved forest. Ecological Research, 20(3), 313–324. doi:10.1007/s11284-005-0047-8

Tanaka, K., Takizawa, H., Tanaka, N., Kosaka, I., Yoshifuji, N., Tantasirin, C., Piman, S., et al. (2003). Transpiration peak over a hill evergreen forest in northern Thailand in the late dry season: Assessing the seasonal changes in evapotranspiration using a multilayer model. J. Geophys. Res., 108(D17), 4533. doi:10.1029/2002JD003028

Tanaka, N., Kume, T., Yoshifuji, N., Tanaka, K., Takizawa, H., Shiraki, K., Tantasirin, C., et al. (2008). A review of evapotranspiration estimates from tropical forests in Thailand and adjacent regions. Agricultural and Forest Meteorology, 148(5), 807–819. doi:10.1016/j.agrformet.2008.01.011

Tani, M. (2003). Long-term estimation of evapotranspiration from a tropical rain forest in Peninsular Malaysia. Water Resources Systems - Water Availability and Global Change, 267–274.

Vourlitis, G. L., Priante Filho, N., Hayashi, M. M. S., Nogueira, J. D. S., Caseiro, F. T., & Holanda Campelo, J. (2001). Seasonal variations in the net ecosystem CO_2 exchange of a mature Amazonian transitional tropical forest (cerradao). Functional Ecology, 15(3), 388–395. doi:10.1046/j.1365-2435.2001.00535.x

White, M. A., Running, S. W., & Thornton, P. E. (1999). The impact of growing-season length variability on carbon assimilation and evapotranspiration over 88 years in the eastern US deciduous forest. International Journal of Biometeorology, 42(3), 139–145. doi:10.1007/s004840050097

Williams, M., Malhi, Y., Nobre, A. D., Rastetter, E. B., Grace, J., & Pereira, M. G. P. (1998). Seasonal variation in net carbon exchange and evapotranspiration in a Brazilian rain forest: a modelling analysis. Plant, Cell and Environment, 21(10), 953–968. doi:10.1046/j.1365-3040.1998.00339.x

Wilson, K. B. (2000). Factors controlling evaporation and energy partitioning beneath a deciduous forest over an annual cycle. Agricultural and Forest Meteorology, 102(2-3), 83–103. doi:10.1016/S0168-1923(00)00124-6

Wilson, K. B., Baldocchi, D. D., & Hanson, P. J. (2001). Leaf age affects the seasonal pattern of photosynthetic capacityand net ecosystem exchange of carbon in a deciduous forest. Plant, Cell and Environment, 24(6), 571–583. doi:10.1046/j.0016-8025.2001.00706.x

Li, Z., Zhang, Y., Wang, S., Yuan, G., Yang, Y., & Cao, M. (2010). Evapotranspiration of a tropical rain forest in Xishuangbanna, southwest China. Hydrological Processes, 24(17), 2405 – 2416. doi:10.1002/hyp.7643

Zotz, G., & Winter, K. (1994). Photosynthesis of a tropical canopy tree, Ceiba pentandra, in a lowland forest in Panama. Tree physiology, 14(11), 1291–301.

Chapter 2

Micrometeorology and eddy flux observation at a tropical deciduous forest in Northern Thailand

2.1. Introduction

This chapter highlights how the data collection of this study was conducted. It includes site location, type of the scientific instruments used, micrometeorology measurements, and explanation of eddy flux measurements.

2.2 Material and methods

2.2.1 Study site

Measurements were conducted in an even-aged teak (*Tectona grandis* Linn. f.) stand planted in 1968 in Mae Moh plantation, Lampang province, northern Thailand (18 ° 25 N, 99 ° 43E, 380 m above sea level, Fig. 2.1 A and B). Teakwood has high market value and thus teak plantations have been widely established throughout the tropics in Indochina and India (Krishnapillay, 2000). Until the 1960 - 70s, drastic decreases in forested area had been occurring in SE Asia; recently, however, forest rehabilitation and plantations have been increasingly promoted in the region. In Thailand, teak plantations have primarily been established in the northern part of the country by the Forest Industry Organization (FIO). The Mae Moh study site had a mean annual temperature of 25 °C, and a mean annual precipitation of 1387 mm for the period 2001 - 2006 (Yoshifuji, 2006). The climate of this area is influenced by the Asian monsoon, which produces highly seasonal variation in precipitation. There was a clear dry season period from November to March, during which the mean monthly rainfall was below 100mm. Due to the clear seasonality of rainfall, canopy surface condition changes drastically (Fig. 2.1 C). The soil at the MaeMoh plantation is classified as loamy paleustults (Thai classification). The study site was located within an area of flat terrain, where the stand structure was almost homogenous. The tree density in the study site was 400 trees ha^{-1}, and the mean tree height and diameter at breast height in

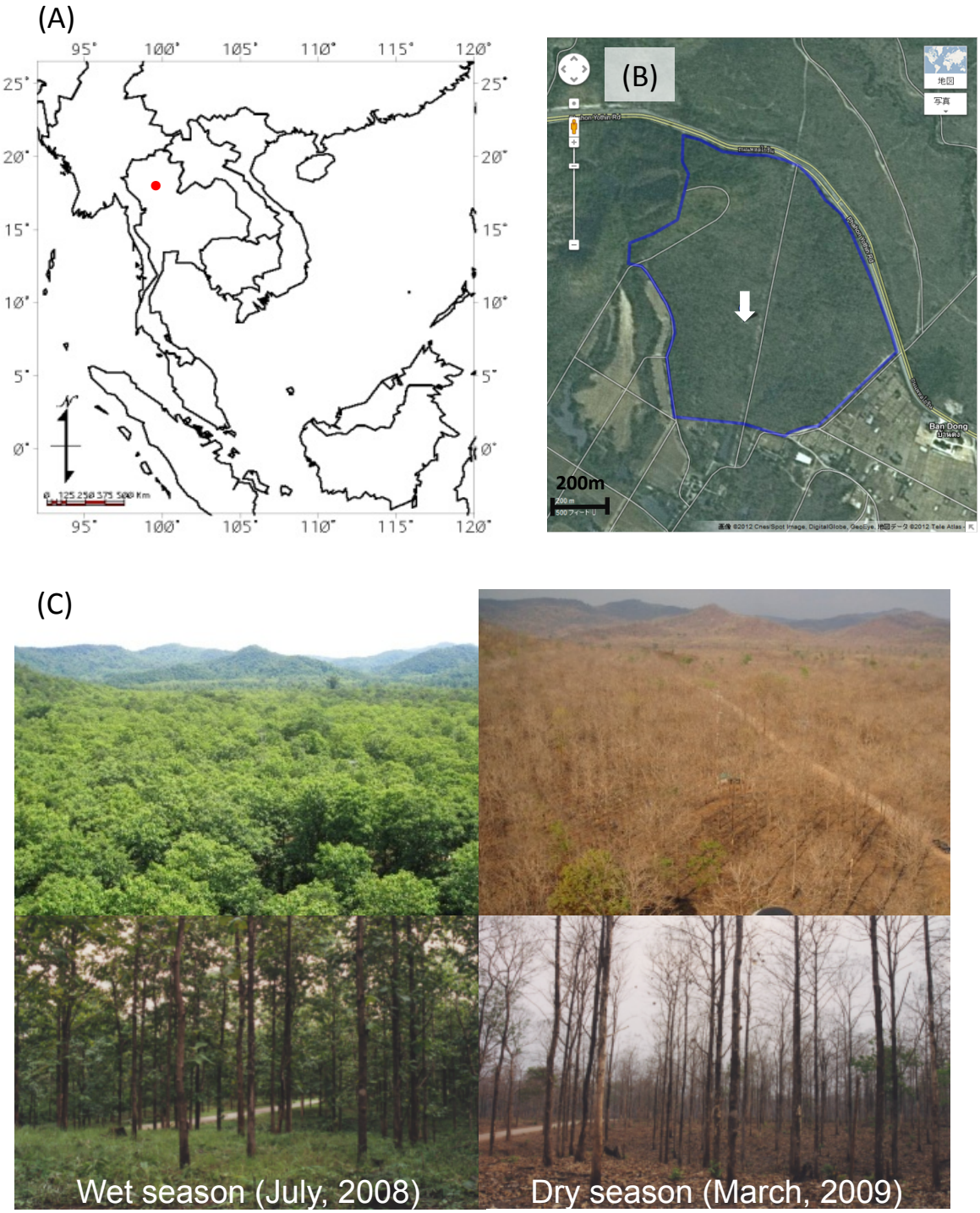

Fig.2.1 (A) Location of MaeMoh teak plantation, (B) boundary line of study site and (C) canopy and understory condition in wet season and dry season. ●in (A) represents study site. Blue line and white arrow in (B) represent boundary line of study site and location of meteorological tower.

Feb. 2012 were 21.0 m and 23.5 cm, respectively. Grasses, woody plants, and bamboo grass mainly dominated the understory vegetation of the study site.

2.2.2 Micrometeorological measurements

The micrometeorological and soil moisture observation at this site was described in Table 2.1. Rainfall was measured using a self-made storage-type rain gauge in an open site about 500m from the tower. A tipping bucket-type rain gauge (No. 34T; Ohta-Keiki, Tokyo, Japan) equipped with a data logger (Hobo Event; Onset Computer) was also installed next to the rain gauge, and the time of each tip was recorded to give the time distribution of rainfall. Volumetric soil water content (θ_i: m^3 m^{-3}) was measured near the tower at depths of 0.1, 0.2, 0.4 and 0.6 m with domain reflectometer (CS-615; Campbell Scientific) at 10-min intervals (CR10X; Campbell Scientific). Solar radiation below the canopy (S_b) was measured on the forest floor at the height of approximately 0.5 m with a pyranometer (MS401; EKO, Tokyo, Japan). G and θ_i were recorded, 40m from the tower, with a data logger (CR10X; Campbell Scientific). Soil water content was represented by the relative extractable water in the 0-60 cm soil layer (Θ_{0-60}) following Kugamai et al. (2004) and Yoshifuji et al. (2011):

$$\theta_i = \frac{\theta_i - \theta_{imin}}{\theta_{imax} - \theta_{imin}} \quad (2.1)$$

$$\Theta_{0-60} = \frac{10\times\theta_{10} + 30\times\theta_{20} + 20\times\theta_{40} + 10\times\theta_{60}}{60} \quad (2.2)$$

where θ_i, θ_{imax}, and θ_{imin} were soil water content in each layer, maximum and minimum values over the entire observation period (2006 - 2012), respectively. Meteorological variables were monitored at 40m height on a scaffold tower. Downward shortwave radiation (R_d) (MS801; EKO, Tokyo, Japan) and longwave radiation (MS42; EKO, Tokyo, Japan) were measured at the top of the tower. Upward shortwave (CM21; Kipp & Zonen, Delft, The Netherlands) and longwave (PIR; Eppley, Newport, RI, USA) radiation were measured at 30 m. Net radiation (R_n) was calculated as the sum of these radiation values. Air temperature (T_a) and relative humidity (RH) above the canopy were measured at a height of 39 m, with an aspirated psychrometer (HMP45D; Vaisala, Helsinki, Finland). Vapor pressure deficit (VPD) was calculated from T_a and RH. Those data were measured every 5 s and their 10-min averages were recorded with a data logger (CR23X and CR1000; Campbell Scientific, Logan, UT, USA). Ground heat flux (G) was measured with heat sensor (MF81; EKO, Tokyo, Japan).

Table 2.1 Equipments and data acquisitions for meteorological observation in MaeMoh plantation, and measurement period of data used in this study.

Item	Position	Height (m)	Sensor		Data logger	Measurment interval (sec)	Logging interval (min)	Period
Rainfall	Open site	0.5	0.5 tipping bucket	No.34T, Ohta Keiki Co.	HOBO event	event	event	Jun 01 -
	Open site	0.0	Storage bottle	Self-made	manual	daily	daily	Jun 01 -
Downword Shortwave radiation	Scaffold tower	41.4	Phyranometer	CMP21, Kipp & Zonen	CR23X, Campbell Scientific Inc.	5	10	Jun 01 -
Downword longwave radiation	Scaffold tower	41.4		PIR, The Eppley Laboratory, Inc.	CR23X, Campbell Scientific Inc.	5	10	Jun 01 -
Upword Shortwave radiation	Scaffold tower	36.6	Infrared radiometer	CMP21, Kipp & Zonen	CR23X, Campbell Scientific Inc.	5	10	Jun 01 -
Upword longwave radiation	Scaffold tower	36.6		PIR, The Eppley Laboratory, Inc.	CR23X, Campbell Scientific Inc.	5	10	Jun 01 -
Net radiation	-	-	Calculated *	-	-	-	-	Jun 01 -
Downword Shortwave radiation on the forest floor	Sub-plot	0.5	Phyranometer	CMP21, Kipp & Zonen	CR10X, Campbell Scientific Inc.	5	10	Jun 01 -
Air temperature & Water vapor **	Scaffold tower	31.9	Relative humidity and temperature Probes	HMP45D, Vaisala	CR1000, Campbell Scientific Inc.	5	10	Jun 01 -
Volumetric soil water content	Sub-plot	-0.1	Time domain reflector	CS615, Campbell Scientific, Inc.	CR1000, Campbell Scientific Inc.	5	10	Jun 01 -
	Sub-plot	-0.2	Time domain reflector	CS615, Campbell Scientific, Inc.	CR1000, Campbell Scientific Inc.	5	10	Jun 01 -
	Sub-plot	-0.4	Time domain reflector	CS615, Campbell Scientific, Inc.	CR1000, Campbell Scientific Inc.	5	10	Jun 01 -
	Sub-plot	-0.6	Time domain reflector	CS615, Campbell Scientific, Inc.	CR1000, Campbell Scientific Inc.	5	10	Jun 01 -
Sonic anemometer	Scaffold tower	28	Sonic anemometer	USA-1, METEK	CR5000, Campbell Scientific Inc.	0.1	1/600	Nov 05 -
Gas analyser	Scaffold tower	28	Gas analyser	LI7500, Li-Cor	CR5000, Campbell Scientific Inc.	0.1	1/600	Nov 05 -

*Net radiation was calculated with downward and upward shortwave radiation and downward and upward long wave radiation.
** Water vapor and vapor pressure deficit were calculated from air temperature and relative humidity measurements.

Table 2.2 Annual value of meteorological elements and canopy condition.

Period	2006-2007	2007-2008	2008-2009	2009-2010	2010-2011	2011-2012	Average (mm)	S.D. (mm)
Rainfall (mm)	1720.4	1130	1204.7	1306.5	1278.9	1852.4	1415.5	296.8
Growing season length (d)	297	285	315	318	312	333	310	16.8
Maximum LAI (m^2 m^{-2})	3.2	2.8	2.8	2.9	3.0	3.2	3.0	0.2
R_n (MJ d^{-1})	11.7	12.0	11.9	12.1	12.5	11.4	11.9	0.4
T_a (°C)	25.2	25.4	24.8	25.4	25.8	24.5	25.2	0.5
VPD (hPa)	10.4	11.5	10.4	11.7	13.4	10.0	11.2	1.2

* It should be noted that hydrological year and annual statistic values were defined and calculated period from March and next February.

2.2.3 Monitoring of leaf area index

To estimate seasonal changes of LAI, Irradiative transmittance, which decreased exponentially with increasing LAI from the top of the canopy, was used. In this study site, LAI was calculated as follow

$$\mathrm{LAI} = 2.7\times[-\ln(R_s/S_b)] - 1.43 \quad (2.3)$$

According to Yoshifuji et al. (2011), Here, S_b is solar radiation below the canopy. S_b was measured on the forest floor at the height of approximately 0.5 m with a pyranometer (MS401; EKO, Tokyo, Japan). A more complete description of the LAI estimation is available in Yoshifuji et al. (2006, 2011).

2.2.4 Eddy flux measurements and calculation

The eddy covariance technique (e.g. Baldocchi et al., 1988) is useful for measuring exchanges of heat, water and carbon fluxes between atmospheres and terrestrial ecosystem (Lee et al., 2004). In this study, eddy fluxes of sensible heat flux (H), latent heat flux (LE) and CO_2 flux (F_c) were measured on the scaffold tower at the height of 28.0 m (white arrow in Fig. 2.1 B and Fig. 2.3 A) using eddy covariance method (beginning in November 2005). Air temperature and three-dimensional wind speeds were measured using a three-dimensional sonic anemometer (SAT) (USA-1; METEK, Elmshorn, Germany). Concentrations of H_2O and CO_2 were measured using an open-path H_2O/CO_2 infrared gas analyzer (IRGA) (LI7500; Li-Cor, Lincoln, NE, USA). USA-1 and LI7500 were installed southeast corner of the tower (Fig. 3.2B and C). Analogue signals from the sonic anemometer and IRGA were collected at 10Hz on a data logger (CR5000; Campbell Scientific). In addition, a vertical profile of CO_2 concentrations was also derived from measurements at several heights on the same tower to assess fluxes of CO_2 storage in the air layer below the canopy (F_s). Air samples for CO_2 measurements were drawn continuously at a flow rate of 2000 ml min^{-1} through a 4-mm internal diameter polyethylene tube at each inlet from five heights (2, 8, 14, 20 and 28 m) by an IRGA (LI-800; Li-Cor). The vertical profile of CO_2 concentration system was controlled and logged by a data logger (CR10; Campbell Scientific).

Eddy flux is computed as a covariance between instantaneous deviation in vertical wind speed (w') from the mean value ($\overline{w}$) and instantaneous deviation in gas concentration, mixing ratio

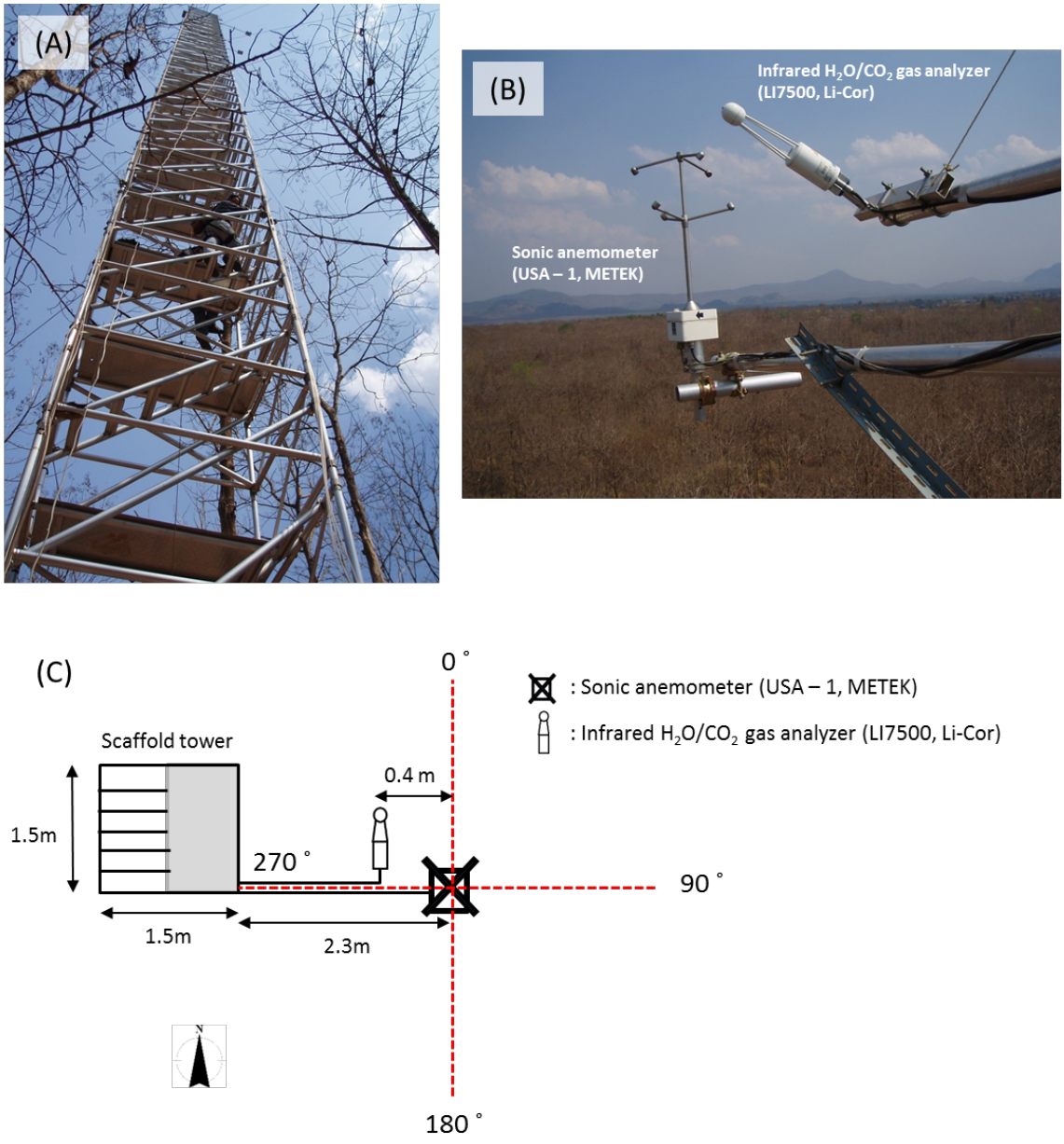

Fig.2.2 (A) Scaffold tower at Mae Moh site, view from the ground. (B) Sonic anemometer and infrared gas analyzer at 28m height, view from the northeast corner of the tower. (C) position of sensors.

(c'), from its mean value ($\bar{c}$), multiplied by mean air density (ρ). Several mathematical operations and assumptions, including Reynolds decomposition, are involved in getting from physically complete equations of the turbulent flow to practical equations for computing eddy flux, as shown below.

In turbulent flow, vertical flux can be presented as:

$$F = \overline{\rho w c} \tag{2.4}$$

Reynolds decomposition is used then to break in to means and deviation:

$$F = \overline{\rho(\bar{w} + w')(\bar{c} + c')} \tag{2.5}$$

$$w = \bar{w} + w' \tag{2.6}$$

$$c = \bar{c} + c' \tag{2.7}$$

Open parenthesis:

$$F = \overline{\rho(\bar{w}\bar{c} + \bar{w}c' + w'\bar{c} + w'c')} \tag{2.8}$$

Equation is simplified:

$$F = \rho\left(\bar{w}\bar{c} + \bar{w}\overline{c'} + \overline{w'}\bar{c} + \overline{w'c'}\right) \tag{2.9}$$

Then important assumption is made for conventional eddy covariance, density fluctuations are assumed negligible. And, mean vertical wind velocity is also negligible for horizontal homogeneous terrain.

Eddy flux was defined as:

$$F = \rho\left(\overline{w'c'}\right) \tag{2.10}$$

H, LE and F_c were calculated using 30-min averages. Linear trends in air temperature, H_2O and CO_2 were removed, and the Webb correction (Webb et al., 1980) was applied. If the 30-min- interval data contained spikes or out-of-range data, that 30-min portion of flux data was rejected for quality purposes. Non-stationary and integral turbulence tests (Foken and Wichura, 1996) were applied to remove unfavorable data. Net ecosystem exchange (NEE)

quantifies the exchange of carbon between an ecosystem and the atmosphere. NEE is estimated as the sum of F_c and the rate of exchange of F_s:

$$\mathrm{NEE} = F_c + F_s \tag{2.11}$$

$$F_s = \int_0^z \left(\frac{dc}{dt}\right) dz \tag{2.12}$$

where c is the CO_2 concentration below the canopy. z is the height from the ground to the top of canopy, and t is time. NEE is positive when the atmosphere is gaining carbon from the ecosystem (in situations when the atmospheric flux is the only important mechanism for carbon gain or loss by the ecosystem).

2.2.5 Spectrum analysis

To check the accuracy of SAT and IRGA, spectrum analysis (Baldocchi and Meyers, 1991) was applied. Base on the 30-min 10Hz (18000 data), double rotation was applied. Fast Fourier Transform (FFT; Niho, 1977) method is most common an can also be used. Although, calculation time required for this method is substantially less than that required for Blackman-Turkey, the current method is subject to the restriction that the data consist of 2^n data points. Furthermore, the use of this method is difficult if the number of missing value (e.g. spikes and noise) is large and/or if these exists a significant scattr in the high frequency side of the spectra. The number of data N needs to be the factorial of 2, and for 10 Hz turbulence data, a typical total number of the data analyzed with FFT is either 2^{14} = 16384 data (about 27 min 20s).

2.2.6 Footprint analysis

A value of vertical flux at some point is possible to think the total of fluxes carried by the turbulent flow at windward various points. To check the source area and fetch of this site, footprint analysis was conducted. To calculate the footprint, Footprint model (Schuepp et al., 1990) modified by Lloyd (1995) was used. The model which calculates for the relative contribution of fluxes at z is given by:

$$\frac{1}{Q}\frac{dQ}{dx} = \frac{-2x_{\max}}{x^2}\phi_m \exp\left[\left(\frac{-2x_{\max}}{x^2}\right)\phi_m\right] \tag{2.13}$$

Here, left side of the equation is relative contribution of flux per unit area. x is horizontal distance from the tower. $x_{\max}$ is horizontal distance from the tower which the flux footprint is a maximum, and ϕ_m is a momentum stability correction function. Following Dyer (1974), ϕ_m is expressed as

$$\phi_m = \left[1 - 16\frac{(z_s - d)}{L}\right]^{-\frac{1}{4}} \tag{2.14}$$

z is the measurement height, L is the Monin-Obukhov length [m]. The ratio z / L was directly measured with the eddy flux. x_{max} is expressed as:

$$x_{\max} = \frac{U(z_s - d)}{u^* 2k} \tag{2.15}$$

U is a mean wind velocity, u^* is friction velocity, k is a Von Karman coefficient (0.41). $x_{\max}$ can rewrite below by Schumid and Oke (1990):

$$x_{\max} = \frac{U(z_s - d)}{u^* 2k}$$

$$x_{\max} \approx \frac{1.7 {z_s}^{1.03}\left[\ln\left(\frac{z_s}{z_0}\right) - \psi\ln\left(\frac{z_s}{L}\right)\right]}{\left(1 - \frac{z_s}{L}\right)^{\frac{1}{2}}} \tag{2.16}$$

Here, z_0 is a roughness length. As a function of z_s, $\psi(z_s/L)$ is expressed below:

$$\psi\left(\frac{z_s}{L}\right) = \left(1 - \frac{76 z_s}{L}\right)^{-\frac{1}{4}} - 1 \tag{2.17}$$

To calculate the integral of Eq(2.14), integration relative source intensity from some point to tower is expressed as:

$$\frac{Q}{Q_0} = \int \frac{-2x_{\max}}{x^2}\phi_m \exp\left[\left(\frac{-2x_{\max}}{x^2}\right)\phi_m\right] dx = \exp\left(\frac{-2x_{\max}}{x^2}\phi_m\right) \tag{2.18}$$

The relative source intensity and integration relative source intensity depends on L.

2.3Results and discussions

2.3.1 Seasonal and interannual variation of meteorological variables and LAI

Fig. 2.3 showed Temporal variations in (a) Rainfall and soil water contents (Θ_{0-60}) (b) downward short-wave radiation (R_s), (c) temperature (T_a), and vapor pressure deficit (VPD) and (d) leaf area index (LAI), in the period from January 2006 to August 2012. Based on previous studies in tropical deciduous forest under Asian monsoon climate (Yoshifuji et al., 2006; Tanaka et al., 2008; Yoshifuji et al., 2011), hydrological year and annual statistic values were defined and calculated period from March and next February. Table.2.3 showed an annual value of meteorological elements and canopy condition. According to previous studies (e.g. Yoshifuji et al., 2006), the season of this site can be roughly divided into the wet season and the dry season. Furthermore dry season can be divided into the cool and hot dry season, although a clear criterion of season separation in this site does not exist. One of the most important things of this study is to consider the effect of LAI to energy partitioning and/or evapotranspiration. Therefore, this study concentrated to separate obvious wet season or not. Shaded columns in Fig. 2.3 represent the month (monthly rainfall exceeded 100 mm) which was considered to be obvious wet season.

The annual rainfall in this site was 1415.5 mm (S.D. ± 296 mm) with large inter-annual variation. Seasonal variation in rainfall was clear in every year. Rainfall was increasing from mid/end of April and decreasing from end of October and first of November. The season of this site can be roughly divided into the rainy season and the dry season.

R_s showed seasonal variation caused by the changes of solar elevation. R_s largely decreased sometime in wet season due to the effect of rainfall and this phenomenon was observed even if it is dry season when after rainfall. The most characteristic about R_s in this site was that seasonal amplitude of R_s was small relative to its temperate and boreal forest. In fact, compared to the previous results (e.g. Wilson and Baldocchi, 2000; Davis et al., 2003), the reduction in R_s during the dry season (corresponding to the Northern Hemisphere winter) in this site was not drastic. Mean annual air temperature and vapor pressure deficit were 25.2 ˚C and 1.1 kPa, respectively, and also showed clear seasonality. VPD increased in the late dry season in response to the increase in T_a, and showed maximum value in the late dry season. Then, VPD decreased in the beginning of the wet season following to the decrease in T_a, and kept the lowest value during the wet season. In the early dry season, the value of VPD was almost same as those in the wet season, as a result of the decrease in T_a. Based on the changes in T_a and VPD, in the dry season can be separated into cool dry season which

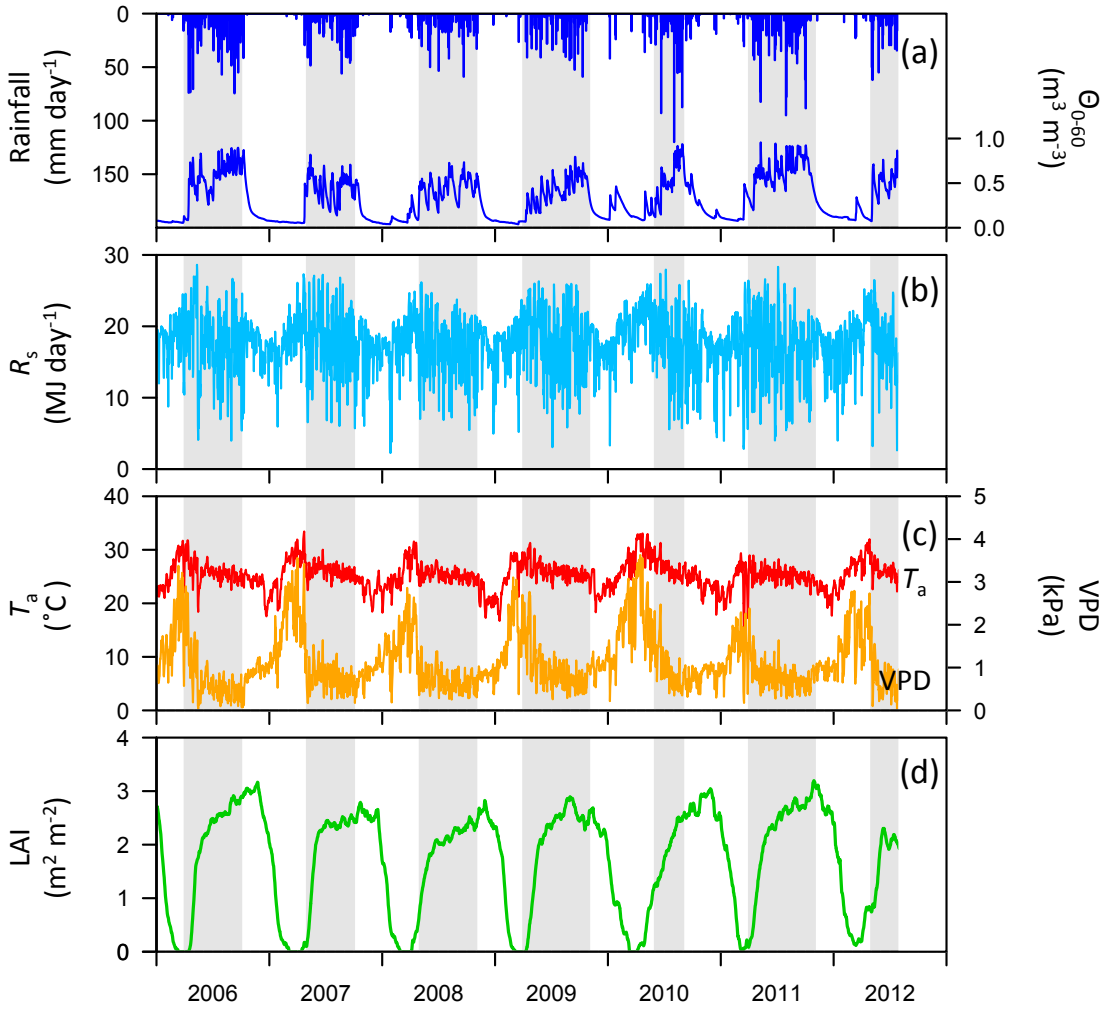

Fig.2.3 Temporal variations in (a) Rainfall and soil water contents ($\Theta_{0\text{-}60}$) (b) downward short-wave radiation (R_s), (c) temperature (T_a), and vapor pressure deficit (VPD), (d) leaf area index (LAI), in the period from January 2006 to August 2012. Shaded columns represent the month (monthly rainfall exceeded 100 mm) which was considered to be obvious wet season.

occurs first and presents a relatively low T_a and followed by the hot dry season, which presents a high T_a and VPD.

Leaf area index (LAI) was also monitored. LAI increased rapidly with onset of wet season following to the increase $\Theta_{0\text{-}60}$ and decreased with end of wet season. Mean maximum LAI value was 3.0 ± 0.2 (m^2 m^{-2}) during from 2006 to 2011 with range between 2.8 and 3.2 (m^2 m^{-2}). The timing of leaf-out and leaf-fall showed interannual variation due to the length of wet season although the maximum LAI in each year was almost constant approximately 3.0 (m^2 m^{-2}). Based on the previous study that examined the timing of sap flow and LAI increasing conducted by Yoshifuji et al. (2011), the growing season was defined as the period LAI gather than 0.2 (m^2 m^{-2}). The mean growing season length was 310 ± 16.8 (days) with range between 285 and 333 (days). Dantec et al. (2000) compered maximum LAI during four years and over 420 ha of a deciduous temperate forest across a range of stand structure and site scale. They had shown that maximum LAI was relatively stable between years. Wilson and Baldocchi (2000) also reported that maximum LAI in temperate deciduous forest in Oak ridge, TN, USA was 5.5 and interannual variation of maximum LAI was small. According to Dantec et al. (2000), water stress is one of the most important parameter that likely to influence LAI and showed that water stress can just affect to the length of leaf expansion period not maximum LAI. In this study, interannual variation of maximum LAI and interannual variation of growing season length were small and large, respectively. This findings support previous findings in temperate desirous forest.

2.3.2 Characteristics of rainfall

To examine about the interception in after chapter, characteristics of rainfall was clarified in this section. Fig. 2.4 showed number of rain events (A) and annual rainfall (B) between 2006 and 2012. Number of rain events and annual rainfall was 86.2 ± 10.9 (times). The number of average rainfall events of ≤ 10 mm was 50.7 (58.6%) although rainfall values in events of ≤10 mm were 165.0 mm (12.1 % of total). Also, the number of average rainfall events of > 40 mm was 9.3 (11.0%) although cumulative rainfall values with events of > 40 mm was 707.1 mm (47.5 % of total). The difference the number of annual rainfall event was mainly caused by the number of small rainfall event (≤ 10mm) although the difference annual rainfall was mainly caused the amount of heavy rainfall event (>40mm) because about half of rainfall was supplied by the heavy intensity rainfall event (> 40 mm). The characteristic of rainfall in this site was similar to that of tropical rainforest in Borneo, Malaysia. According to Kume et al. (2011), small rainfall events occupied approximately 80 % of total rainfall events but the cumulative values of small rainfall events was approximately under 20%.

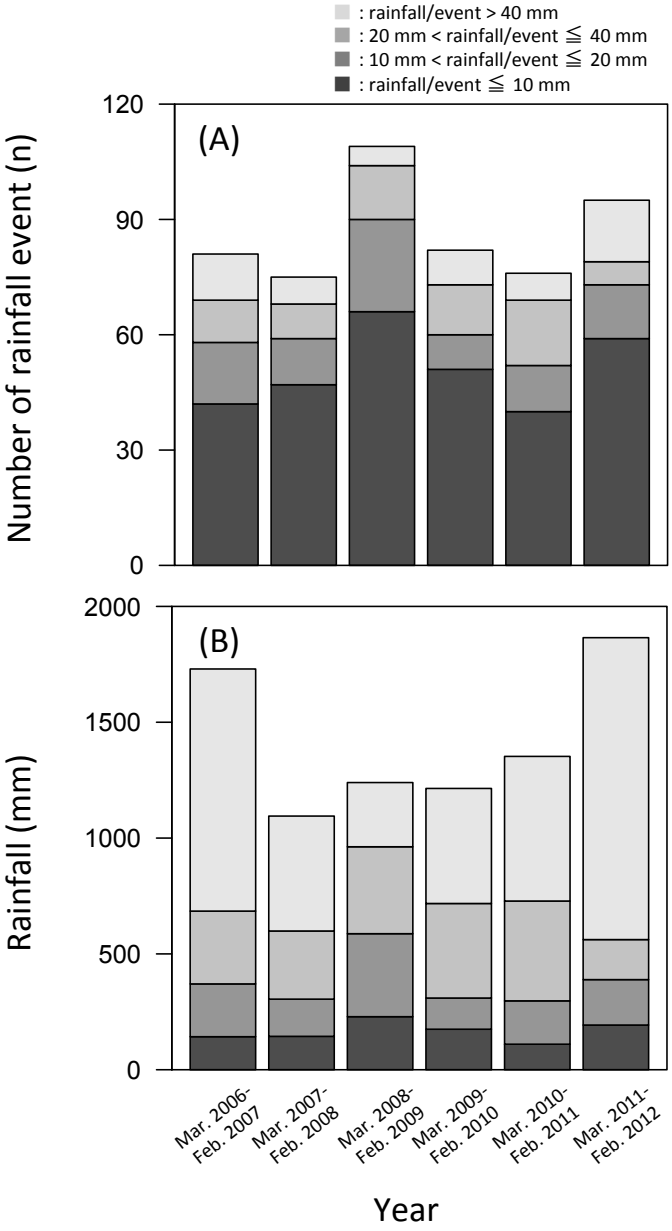

Fig. 2.4 (A) Number of rain events and (B) Total amount of annual rainfall between Mar. 2006 and Feb. 2012. It should be noted that hydrological year and annual statistic values were defined and calculated period from March and next February. It is classified using specific rainfall depth. ■ show cumulative rainfall when the rain event is ≤ 10 mm, ■ show cumulative rainfall when 10 mm < rain event ≤ 20 mm, ■ show cumulative rainfall when 20 mm < rain event ≤ 40 mm and ■ show cumulative rainfall when the rain event is >40 mm.

2.3.3 Data quality control and accuracy of eddy flux measurement

To remove the noise due to rainfall, over range output of USA-1 and LI7500 and unstationality data, quality control was conducted. The total number of flux measurement in this study period (Jan. 2006 - July, 2012) was 51829 except data missing period due to the electric missing troubles and machine broken troubles. The number of daily time (R_n > 30 W m^{-2}) data was 23816 (45.95 %). Rainy time (before 3hours and after 12 hours from rainfall event time) data was removed. The total number of no rainfall time data was 20361 (39.28 %). The total number of after applied spike filter (over range of USA-1 and LI7500) and stationality filter (stationality < 30%) was 20191 (38.69 %) and 10866 (20.97 %), respectively. In this study, effect of tower shadowing was also examined (Fig. 2.5 A and B). The turbulence intensity in boundary layer depends on the stability of atmosphere, the roughness length and the vertical height. The standard deviation of horizontal (σ_u: m s^{-1}) and vertical (σ_w: m s^{-1}) turbulence intensity is proportional to intensity of friction velocity (u^*: m s^{-1}) under the near-neutral condition (Kondo, 1994). Under the near-neutral condition ($|z/L| < 0.05$), the mean σ_u/u^* was 2.63 with range between 2.03 and 2.81. However mean σ_u/u^* range between 0 ° and 270 ° wind direction (no tower shadowing angle) was 2.21. The mean σ_w/u^* was 1.10 with range betwen 1.01 and 1.21. The difference between tower shadowing angle and no tower shadowing angle of σ_u/u^* was insignificant. According to Bradley (1980), σ_u/u^* and σ_w/u^* above forest canopy were 2.2 and 1.2, respectively. Kondo (1994) also reported that σ_u/u^* and σ_w/u^* in forest were 2.7 and 1.2, respectively. Compared to these previous studies, the values of σ_u/u^* and σ_w/u^* in this site were in range of previous studies. However, σ_u/u^* of tower shadowing angle (270 ° - 360 °) was slightly larger relative to σ_u/u^* of no tower shadowing angle. σ_u/u^* and σ_w/u^* characterize whether or not the turbulence is well developed and/or some typical effect of the nonhomogeneous terrain (Foken and Wichura, 1996). It should be noted that there was a little hill about 500 m distance and northwest side from the tower. Therefore, it was considered that the horizontal wind direction from 270 ° to 360 ° was affected by the tower shadowing and nonhomogeneous terrain. Therefore, the data of wind direction from 270 ° to 360 ° was removed. 8703 (16.79 %) eddy flux data was used in analysis in this study.

Spectral analyses of the fluctuations in atmosphere T_a, CO_2 and H_2O associated with turbulent transport provide a useful tool for assessing the reliability of flux easements (Kaimal et al., 1972). For after quality controlled dataset, spectral and co-spectrum analyses were conducted. Under ideal circumstances the shapes of the co-spectrum should be similar (Ohtaki, 1985). Typical temporal deviation of x-axis velocity (x; m s^{-1}), y-axis velocity (y; m s^{-1}), vertical velocity (z; m s^{-1}), temperature (t; °C), CO_2 concentration (mmol m^{-3}) and H_2O concentration (mmol m^{-3}) were shown in Fig. 2.6 (A). Using the time series data, spectrum

Table 2.3 Number of rainfall events in each rainfall intensity

Period	2006-2007	2007-2008	2008-2009	2009-2010	2010-2011	2011-2012	Average (n)	S.D. (n)
rianfall <10 mm	40.0	49.0	65.0	50.0	44.0	56.0	50.7	8.9
10 mm ≦ rianfall <20 mm	16.0	14.0	22.0	9.0	13.0	13.0	14.5	4.3
20 mm ≦ rianfall <40 mm	11.0	9.0	14.0	15.0	15.0	6.0	11.7	3.7
rianfall ≧ 40 mm	12.0	7.0	5.0	10.0	6.0	16.0	9.3	4.2
Total	79.0	79.0	106.0	84.0	78.0	91.0	86.2	10.9

Table 2.4 Percentage of number of rainfall events in each rainfall intensity

Period	2006-2007	2007-2008	2008-2009	2009-2010	2010-2011	2011-2012	Average
rianfall <10 mm	50.6%	62.0%	61.3%	59.5%	56.4%	61.5%	58.6%
10 mm ≦ rianfall <20 mm	20.3%	17.7%	20.8%	10.7%	16.7%	14.3%	16.7%
20 mm ≦ rianfall <40 mm	13.9%	11.4%	13.2%	17.9%	19.2%	6.6%	13.7%
rianfall ≧ 40 mm	15.2%	8.9%	4.7%	11.9%	7.7%	17.6%	11.0%

Table 2.5 Rainfall in each rainfall intensity

Period	2006-2007	2007-2008	2008-2009	2009-2010	2010-2011	2011-2012	Average (mm)	S.D. (mm)
rianfall <10 mm	133.0	146.3	226.8	172.3	121.4	190.3	165.0	39.5
10 mm ≦ rianfall <20 mm	227.9	193.5	325.4	134.6	197.2	186.0	210.8	63.8
20 mm ≦ rianfall <40 mm	314.3	294.2	375.2	454.7	384.3	172.8	332.6	96.7
rianfall ≧ 40 mm	1045.2	496.1	277.2	544.8	576.1	1303.3	707.1	385.4
Total	1720.4	1130.0	1204.7	1306.5	1278.9	1852.4	1415.5	296.8

Table 2.6 Percentage of rainfall in each rainfall intensity

Period	2006-2007	2007-2008	2008-2009	2009-2010	2010-2011	2011-2012	Average
rianfall <10 mm	7.7%	12.9%	18.8%	13.2%	9.5%	10.3%	12.1%
10 mm ≦ rianfall <20 mm	13.2%	17.1%	27.0%	10.3%	15.4%	10.0%	15.5%
20 mm ≦ rianfall <40 mm	18.3%	26.0%	31.1%	34.8%	30.0%	9.3%	24.9%
rianfall ≧ 40 mm	60.8%	43.9%	23.0%	41.7%	45.0%	70.4%	47.5%

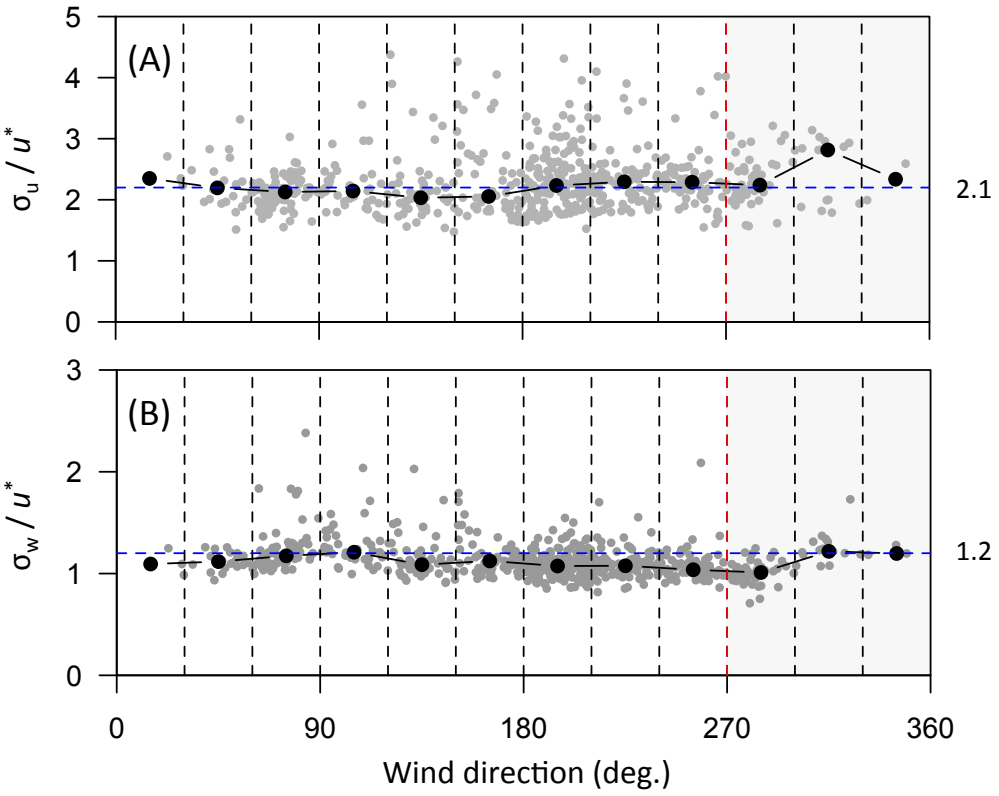

Fig. 2.5 (A) The relationship between wind direction and σ_u / u^* under near-neutral condition $|z/L| < 0.05$, (B) the relationship between wind direction and σ_w / u_* under near-neutral condition $|z/L| < 0.05$. The wind direction between 270 - 360 ˚ was tower shadowing. Blue dotted line in (A) and (B) represents 2.1 and 1.2 line (Bradley, 1980).

(A)

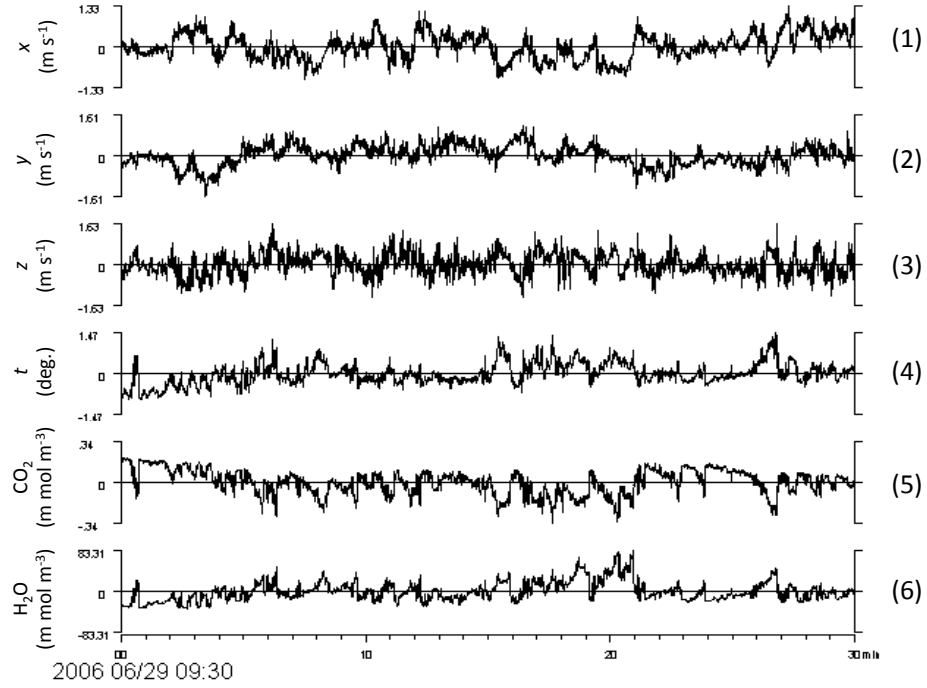

(B)

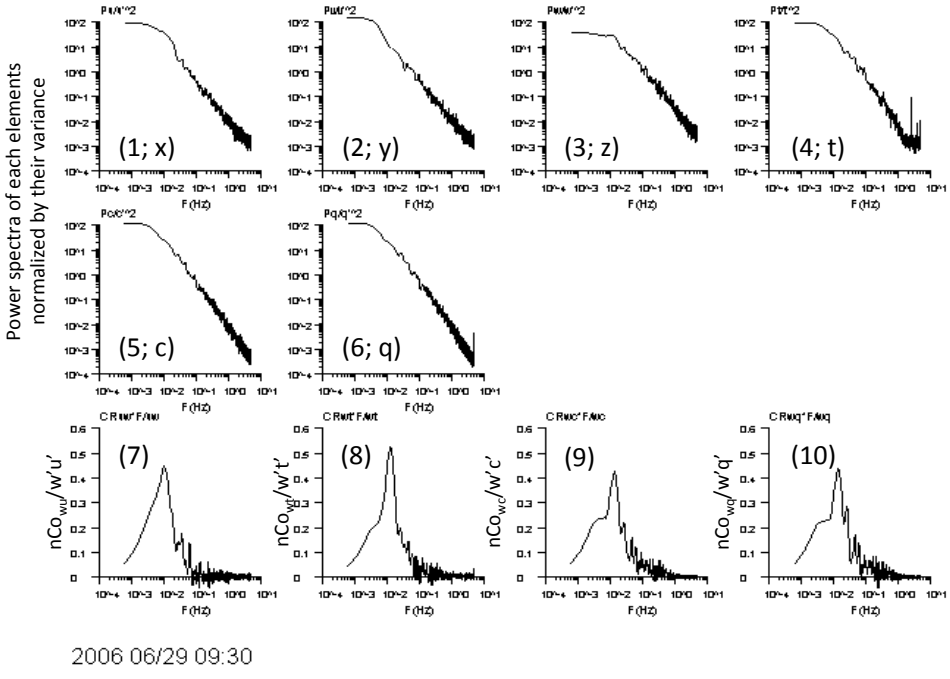

Fig.2.6 The temporal deviation of x-axis velocity (*x*; m s^{-1}), y-axis velocity (*y*; m s^{-1}), vertical velocity (*z*; m s^{-1}), temperature (*t*; ˚C), CO2 concentration (mmol m^{-3}) and H2O concentration (mmol m^{-3}) (A) and notarized spectrum of *x*, *y*, *z*, *t*, *c* and *q* and co- spectrum of vertical velocity (*w*) and horizontal velocity (*u*), *c*, *t*, and *q* (B).

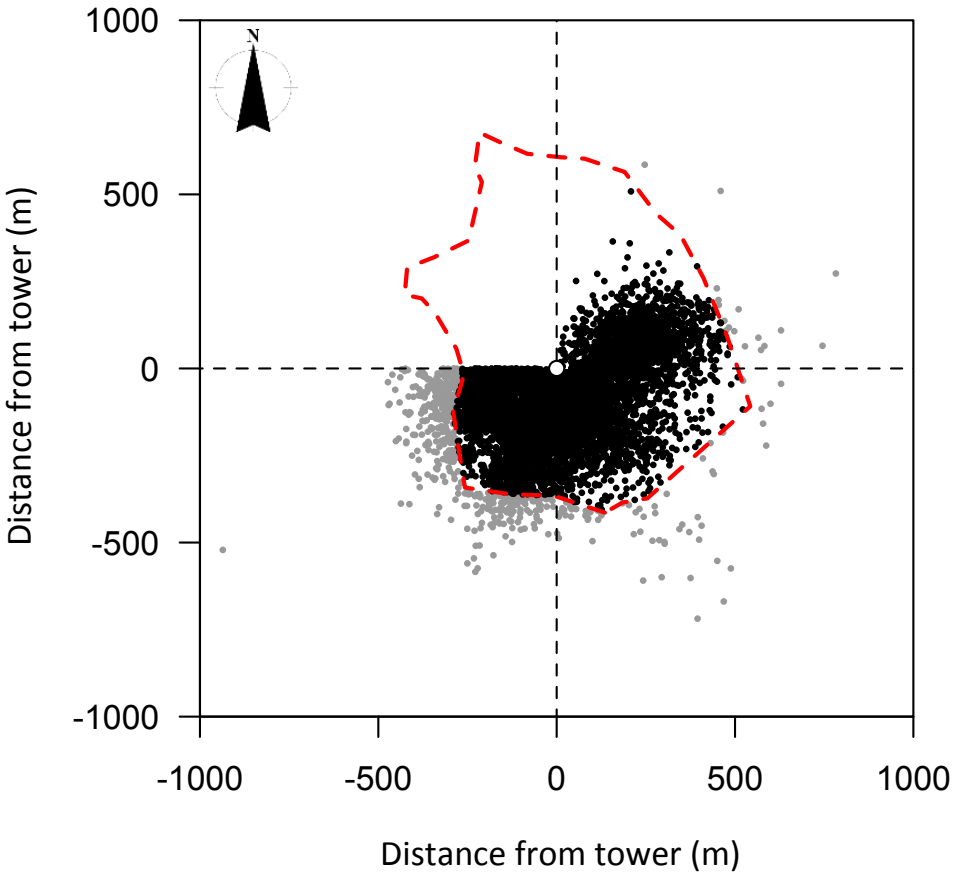

Fig. 2.7 Integration relative source intensity over 80 % from some point to tower. Black and gray dots represent source point in the site boundary and out of site boundary. Dotted red line represent site boundary line. Data that was located range from 270 ˚ to 360 ˚ wind direction were already removed.

and co-spectrum were calculated. Power spectrum of x, y, z, t, c and q were shown in Fig. 2.6 (B 1- 6). Each normalized spectrum converged to a - 2 / 3 line at the high frequencies. This result corresponded to the previous studies (e.g. Baldocchi and Meyers, 1991; Toda et al., 2002). The co-spectrum of vertical velocity (w) and horizontal velocity (u), c, t, and q were shown in Fig. 2.6 (B 7- 10). Each co-spectrum also converged to a - 4/3 line at high-frequencies. This result corresponded ideal shape in high-inertial range (Kaimal et al., 1994). These result showed that each variable of flux easements is measured appropriately in this study site.

Footprint analysis (Lloyd, 1995) also examined. Fig. 2.7 showed that the representative fetch length in daytime (80 % integration relative source intensity from some point to tower). Among the after quality control data (n = 8703), 7037 data sets (80.86 %) were plotted inside the boundary line of this study site. It was considered that the source of observed eddy flux at tower was almost within the range of site boundary line.

2.3.4 Energy balance closure

The relationship between available energy (R_n - G) and sum of observed sensible heat (H_{obs}) and observed latent heat (LE_{obs}) fluxes was shown in Fig. 2.8. Data number (n), regression slope and regression coefficient were 8703, 0.673 and 0.635, respectively. The regression line of within site boundary line data (n = 7037) was 0.690 (R^2 = 0.711) and slightly larger. The difference of energy balance ratio between after quality controlled all data and within site boundary line data was insignificant (data not shown). The energy imbalance in this site was 31 - 33 %. The energy balance is often not closed using the eddy covariance technique (Mahrt, 1998; Gu et al., 1999; Twine et al., 2000). According to Wilson et al. (2002), the primary reasons usually suspected for the energy imbalance: (1) systematic errors associated with the sampling mismatch between the flux footprint and the sensors measuring other components of the energy balance, (2) a systematic instrument bias, (3) neglected energy sinks, (4) low and high frequency loss of turbulent fluxes, and (5) horizontal and/or vertical advection of heat and water vapor. According to Takanashi et al. (2010), energy balance was improved using the data whose fetch lengths were within the boundary. However, it was limited that the effect of fetch length to improve energy balance closure in this study. Based on Wilson et al.'s (2002) summary of energy balance closure across 50 site-years in FLUXNET, the averaged energy balance closure in the world was 0.79 ± 0.01 with ranging from 0.53 to 0.99. Energy balance closure in this study was within the range reported by Wilson et al. (2002). Fig. 2.9 (A) showed that the relationship between friction velocity (u^*; m s^{-1}) and imbalance ratio (IBR = (H_{obs} + LE_{obs}) / (R_n - G)). IBR was smaller and was more depend on u^* when $u^* < 0.2$ (m s^{-1}) although IBR was increasing with

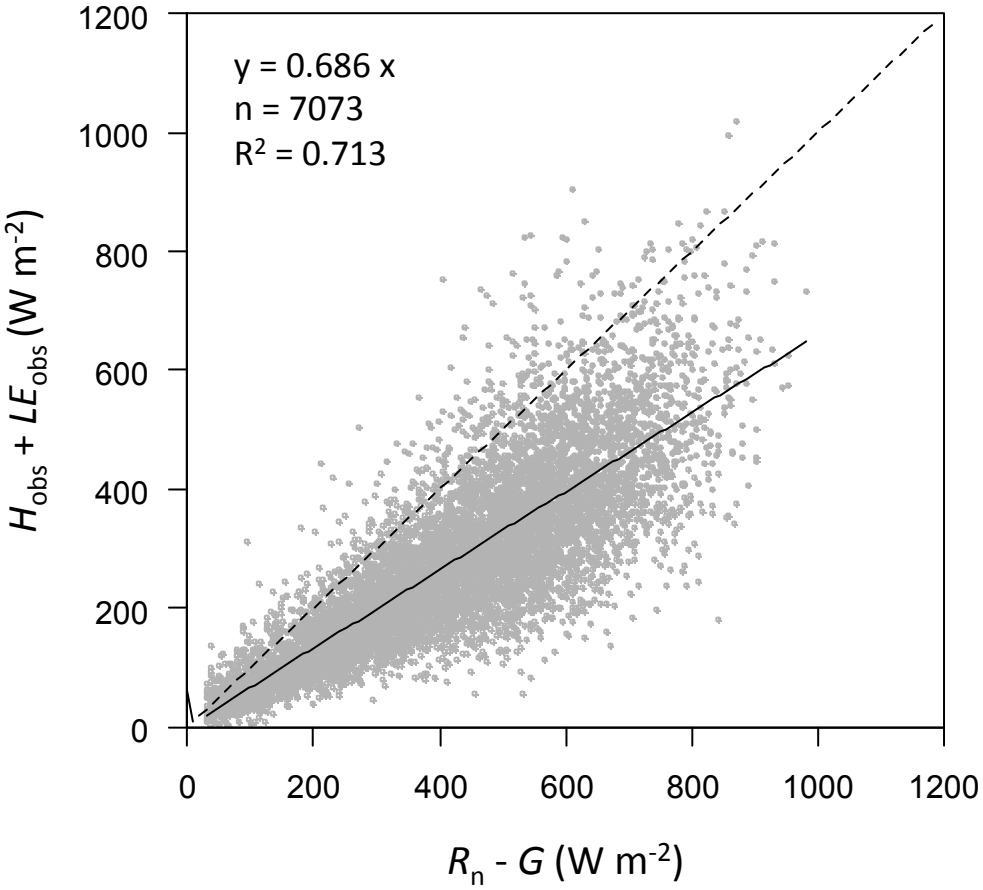

Fig.2.8 Relationship between available energy (R_n - G) and sum of observed sensible heat (H_{obs}) and latent heat (LE_{obs}) fluxes.

Table 2.7 Number of total eddy flux measurement data and number of after quality control data.

	Data number	Daily data	After	Spike fillter	Stationality test fillter	Non tower shadowing
	(n)	(Rs > 50 W m^{-2})	remove rainfall time	(spile <180 n. $30min^{-1}$)	(stationality < 30%)	(0 ˚ - 270 ˚)
Number (n)	51829	23816	20361	20191	10866	8703
Percent (%)	100.00%	45.95%	39.28%	38.96%	20.97%	16.79%

Table 2.8 Results of eddy flux imbalance data in each season and year. JFM is January, February and March. AMJ is April, May and June. JAS is July, August and September. OND is October, November and December, respectively.

Year	JFM		AMJ		JAS		OND		Annual	
	Mean	S.D.	Mean	S.D.	Mean	S.D.	Mean	S.D.	Mean	S.D.
2006	0.708	0.257	0.832	0.256	0.635	0.203	0.575	0.172	0.677	0.240
2008	0.667	0.217	0.757	0.234	0.704	0.213	0.664	0.175	0.700	0.211
2010	0.610	0.200	0.646	0.181	0.628	0.184	-	-	0.630	0.187
2012	0.601	0.172	0.599	0.171	0.579	0.164	-	-	0.592	0.169

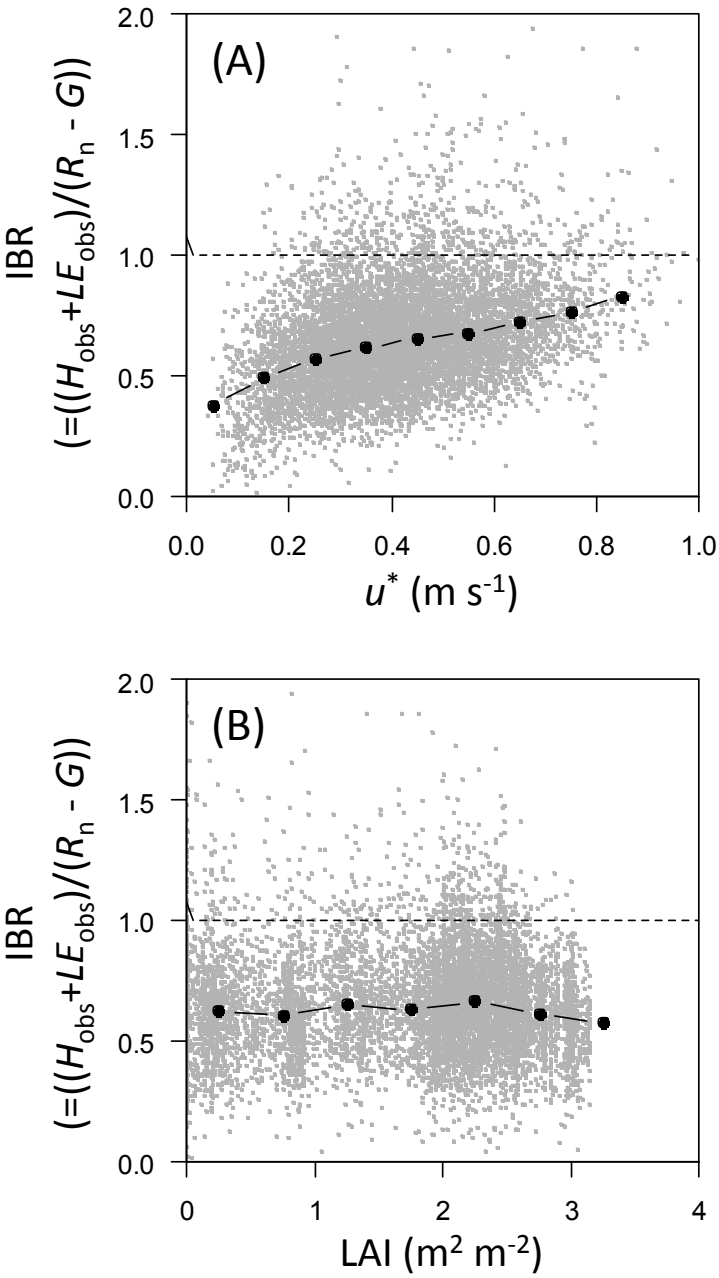

Fig.2.9 Relationship between u^*, LAI and energy imbalance. (A) Relationship between u^* and imbalance ratio (IBR=$((H_{obs}+LE_{obs})/(R_n - G))$, (B) Relationship between leaf area index (LAI) and IBR.

increasing u^* in linearly when $u^* > 0.2$ (m s^{-1}). This tendency was as same as the previous study (e.g. Wilson et al., 2002) due to the effect of turbulent mixing improvement. In this study, the seasonal and inter annual variation of energy balance closure was also examined. Fig. 2.9 (B) showed the relationship between LAI and IBR. In each LAI levels, IBR showed insignificant difference. The effect that was difference of season and year was also examined (Table 2.8). However, IBR did not have bias in specific LAI, season of wet and dry, and observed year. Based on these findings, it was considered that, although energy imbalance occurred, eddy flux measurement was conducted as appropriately and sufficient data for analysis the seasonal and interannual variation of heat, water and carbon flux between forest and atmosphere was observed in this study.

Based on the study of imbalance correction (Twine et al., 2000), observed H and LE were corrected using the ratio of energy balance expressed as:

$$\mathrm{H} = \mathrm{H_{obs}} \frac{R_\mathrm{n} - G}{\mathrm{H_{obs}} + \mathrm{LE_{obs}}} \tag{2.19}$$

$$\mathrm{LE} = \mathrm{LE_{obs}} \frac{R_\mathrm{n} - G}{\mathrm{H_{obs}} + \mathrm{LE_{obs}}} \tag{2.20}$$

Here, H_{obs} and LE_{obs} were observed and before corrected sensible and latent heat flux. H and LE were after corrected sensible and latent heat flux.

According to Twine et al. (2000), it was pointed out that energy imbalance affected to F_c. Dealing of F_c was noted in chapter 5.

2.3.5 Seasonal and interannual variation of eddy flux measurement

Fig. 2.10 showed a temporal variation of H and LE with micrometeorology variables and LAI. Clearly seasonal variation of H and LE was observed. LE was more prominent than H during the wet season, whereas in the dry season, the latter was the major form of energy emitted to the atmosphere. The reduction in LE in the dry season, when available net radiation did not greatly decrease may have resulted from a lack of available water for evapotranspiration within the forest ecosystem due to a prolonged dry period. Such a reduction in LE in the dry season has not been reported for evergreen forest sites in mainland Southeast Asia. Tanaka et al. (2003) reported that at an upland evergreen forest site in Thailand, evapotranspiration in the hot dry season was considerably higher than during the wet season. Nobuhiro et al. (2009) also showed that at a lowland evergreen forest

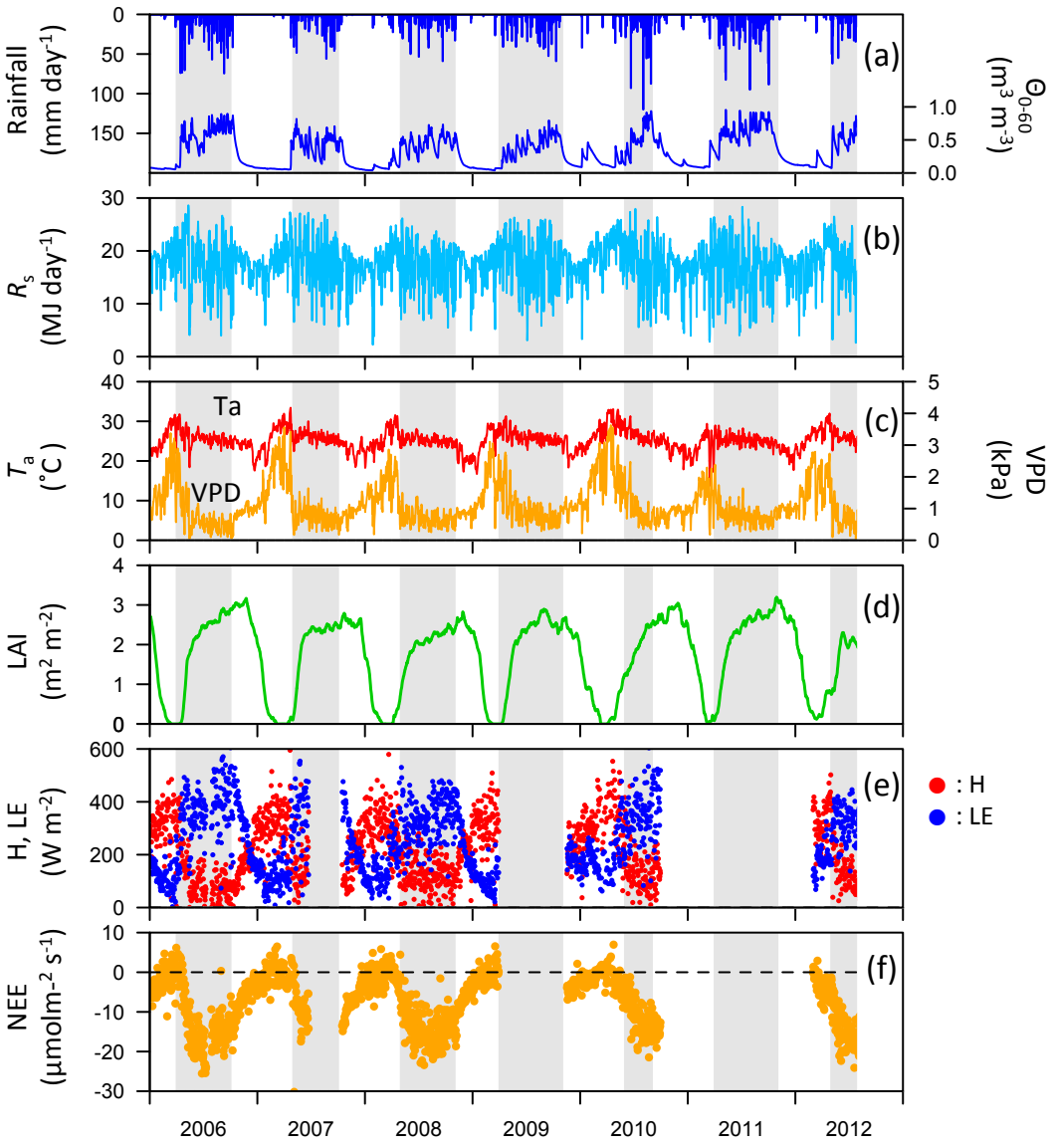

Fig.2.10 Temporal variations in (a) Rainfall and soil water contents ($\Theta_{0\text{-}60}$) (b) downward short-wave radiation (R_s), (c) temperature (T_a), and vapor pressure deficit (VPD), (d) leaf area index (LAI), (e) Mid-day (10:00-15:00) averaged sensible heat flux (H) and latent heat flux (LE), (f) Mid-day (10:00-15:00) averaged net ecosystem exchanges (NEE) in the period from January 2006 to August 2012.

site in Cambodia, evapotranspiration in the hot dry season was higher than in the wet season. The seasonality in energy partitioning observed here also differs from typical tropical rain forests in SE Asia (Kumagai et al., 2004; Takanashi et al., 2010), where seasonal patterns in LE are often ambiguous. Due to the effects of Asian monsoons, differences in the seasonal variation of H and LE were influenced by differences in vegetation type between deciduous and evergreen forests. In contrast, the Amazon region, which experiences less than 1700 mm of annual precipitation and a longer dry season, exhibited clear evidence of reduced evaporation in the dry season. (e.g., Vourlitis et al., 2008; da Rocha et al., 2009). For example, at a Eucalyptus plantation in Brazil, more than 80% of available energy was utilized in evaporation in the summer (wet season), and 74% of the available energy was directed to sensible flux in the winter (dry season) (Cabral et al., 2010). Such a clear seasonal contrast in the pattern of energy partitioning is often less pronounced in tropical rain forests in the Amazon (Carswell et al., 2002; Malhi et al., 2002; Hutyra et al., 2007) and in SE Asia, as these sites are located close to the equator and the Intertropical Convergence Zone. As noted above, clear energy partitioning is not often observed at boreal or temperate deciduous forest sites (e.g., Greco and Baldocchi, 1996; Wilson and Baldocchi, 2000; Pejam et al., 2006) because in the winter (corresponding to the dry season at this site), these sites receive much lower net radiation compared to the summer months (the wet season at this site). Occasional increases in LE occurred during the hot dry season, when teak trees were almost leafless (Fig. 2.9 d). These increases may have been caused by soil evaporation from the moist ground, as the above-mentioned rainfall events prior to the beginning of leaf-out were followed by the eventual increases in LE. Another possible explanation for the increases of LE involves transpiration by understory plants, such as shrubs and bamboos, which are patchily distributed at this site. Some of these plants had leaves throughout the dry season, and the energy available to them may have been sufficient because of the absence of light interception by teak leaves. The temporal variation of NEE was noted and discussed in chapter 5.

2.4 Conclusion

In this chapter, temporal variation of meteorological variables and LAI was examined. Clear seasonality of rainfall was observed. Temperature, VPD and $\Theta_{0\text{-}60}$ had a clear senility corresponded with seasonality of rainfall. R_s showed a seasonal variation caused by the changes of solar elevation. Mean annual air temperature and vapor pressure deficit were 25.2 ˚C and 11.2 hPa, respectively, and also showed clear seasonality. VPD increased in the late dry season in response to the increase in Ta, and showed maximum value in the late dry season. Then, VPD decreased in the beginning of the wet season following to the decrease in

Ta, and kept the lowest value during the wet season. Based on these findings, the season of this site can be separated into cool dry season, hot dry season and wet season, respectively. LAI increased rapidly with onset of wet season following to the increase $\Theta_{0\text{-}60}$ and decreased with end of wet season. Mean maximum LAI value was 3.0 ± 0.2 (m^2 m^{-2}) during from 2006 to 2011 and interannual variation of maximum LAI was insignificant. The mean growing season length (GSL) from 2006 to 2011, defined as the period LAI greater than 0.2 (m^2 m^{-2}), was 310 ± 16.8 (days) and growing season length was corresponded to timing of onset and offset of wet season.

The difference the number of annual rainfall event was mainly caused by the number of small rainfall event (≤ 10mm) although the difference annual rainfall was mainly caused the amount of heavy rainfall event (> 40mm) because about half of rainfall was supplied by the heavy intensity rainfall event (> 40 mm). The characteristic of rainfall in this site was simile to that of tropical rainforest in Borneo, Malaysia.

To remove the noise due to rainfall, over range output of USA-1 and LI7500 and unstationality data, quality control was conducted. After quality control, 8703 (16.79 %) eddy flux data was used in analysis in this study. For after quality controlled dataset, spectral and co-spectrum analyses were conducted. Each power spectrum decreased through the sub-inertial range between 0.01 Hz to 1 Hz with - 2/3 slope and each co-spectrum represented that large eddies with frequency less than 0.1 Hz dominant fluxes. These results showed that each variable of flux easements is measured appropriately in this study site. Footprint analysis also examined. Among the after quality control data (n = 8703), 7037 data sets (80.86 %) were plotted inside the boundary line of this study site. It was considered that the source of observed eddy flux at tower was almost within the range of site boundary line.

The relationship $(R_n - G)$ and sum of H and LE was examined. As a results, regression slope and regression coefficient were 0.673 and 0.635, respectively (n = 8703). The regression line of within site boundary line data (n = 7037) was 0.690 (R^2 = 0.71) and slightly larger. The difference of energy balance ratio between after quality controlled all data and within site boundary line data was insignificant. The energy imbalance in this site was 31 - 33 % although energy balance closure in this study was within the range reported by Wilson et al. (2002). IBR was smaller and was more depend on u^* when u^* < 0.2 (m s^{-1}) although IBR was increasing with increasing u^* in linearly when u^* > 0.2 (m s^{-1}). This tendency was as same as the previous study (e.g. Wilson et al., 2002) due to the effect of turbulent mixing improvement. In this study, the seasonal and inter annual variation of energy balance closure was also examined. In each LAI levels, IBR showed insignificant difference. IBR did not have bias in specific LAI, season of wet and dry, and observed year. Based on these

findings, it was considered that, although energy imbalance occurred, eddy flux measurement was conducted as appropriately and sufficient data for analysis the seasonal and interannual variation of heat, water and carbon flux between forest and atmosphere was observed in this study.

Clearly seasonal variation of H and LE was observed. LE was more prominent than H during the wet season, whereas in the dry season, the latter was the major form of energy emitted to the atmosphere. Occasional increases in LE occurred during the hot dry season, when teak trees were almost leafless. These increases may have been caused by soil evaporation from the moist ground, as the above-mentioned rainfall events prior to the beginning of leaf-out were followed by the eventual increases in LE. Another possible explanation for the increases of LE involves transpiration by understory plants, such as shrubs and bamboos, which are patchily distributed at this site. Based on these findings in this chapter, the ratio of sensible and latent heat flux showed largely seasonal changes due to the seasonality of rainfall with following the seasonal variation of LAI.

References

Arneth, A., Kelliher, F. M., Bauer, G., Hollinger, D. Y., Byers, J. N., Hunt, J. E., McSeveny, T. M., et al. (1996). Environmental regulation of xylem sap flow and total conductance of Larix gmelinii trees in eastern Siberia. *Tree physiology*, *16*(1_2), 247–255.

Baldocchi, D., Meyers, P., Division, D., & Ridge, O. (1991). Trace Gas Exchange Above the Floor of a Deciduous Forest 1 . Evaporation and CO_2 Efflux ha -l to about 3 Mg ha -l between, *96*, 7271–7285.

Baldocchi, D., Hincks, B., & Meyers, T. (1988). Measuring biosphere-atmosphere exchanges of biologically related gases with micrometeorological methods. *Ecology*, *69*(5), 1331–1340.

Bradley, E. (1980). An experimental study of the profiles of wind speed, shearing stress and turbulence at the crest of a large hill. *Quarterly Journal of the Royal Meteorological …*, 101–123.

Cabral, O. M. R., Rocha, H. R., Gash, J. H. C., Ligo, M. a. V., Freitas, H. C., & Tatsch, J. D. (2010). The energy and water balance of a Eucalyptus plantation in southeast Brazil. *Journal of Hydrology*, *388*(3-4), 208–216. doi:10.1016/j.jhydrol.2010.04.041

Carswell, F. E., Costa, A. L., Palheta, M., Malhi, Y., Meir, P., Costa, J. de P. R., Ruivo, M. de L., et al. (2002). Seasonality in CO_2 and H_2O flux at an eastern Amazonian rain forest. *Journal of Geophysical Research*, *107*(D20), 8076. doi:10.1029/2000JD000284

Dantec, Â. Le, Dufre, E., & Saugier, B. (2000). Interannual and spatial variation in maximum leaf area index of temperate deciduous stands. *Forest Ecology and Management*, *134*, 71–81.

Davis, K. J., Bakwin, P. S., Yi, C., Berger, B. W., Zhao, C., Teclaw, R. M., & Isebrands, J. G. (2003). The annual cycles of CO_2 and H_2O exchange over a northern mixed forest as observed from a very tall tower. *Global Change Biology*, *9*(9), 1278–1293. doi:10.1046/j.1365-2486.2003.00672.x

Foken, T., & Wichura, B. (1996). Tools for quality assessment of surface-based flux measurements. *Agricultural and Forest Meteorology*, *78*(1-2), 83–105. doi:10.1016/0168-1923(95)02248-1

Greco, S., & Baldocchi, D. (1996). Seasonal variations of CO_2 and water vapour exchange rates over a temperate deciduous forest. *Global Change Biology*, *2*(3), 183–197. doi:10.1111/j.1365-2486.1996.tb00071.x

Gu, J., Smith, E. A., & Merritt, J. D. (1999). Testing energy balance closure with GOES-retrieved net radiation and in situ measured eddy correlation fluxes in BOREAS. *Journal of Geophysical Research: Atmospheres*, *104*(D22), 27881–27893. doi:10.1029/1999JD900390

Hino, M. (1977). Basic theory in spectral analysis [in Japanease] (pp. 9–48). Tokyo, Japan: Asakura Book.

Hutyra, L. R., Munger, J. W., Saleska, S. R., Gottlieb, E., Daube, B. C., Dunn, A. L., Amaral, D. F., et al. (2007). Seasonal controls on the exchange of carbon and water in an Amazonian rain forest. *Journal of Geophysical Research*, *112*(G3), 1–16. doi:10.1029/2006JG000365

Kaimal, J. C., Wyngaard, J. C., Izumi, Y., & Coté, O. R. (1972). Spectral characteristics of surface-layer turbulence. *Quarterly Journal of the Royal Meteorological Society*, *98*(417), 563–589. doi:10.1002/qj.49709841707

Kondo, J. (1994). *Meteorology in water regime – water and energy balance on land surface [in Japanese]* (p. - 348 pp). Tokyo, Japan: Asakura shoten.

Kumagai, T., Saitoh, T. M., Sato, Y., Morooka, T., Manfroi, O. J., Kuraji, K., & Suzuki, M. (2004). Transpiration, canopy conductance and the decoupling coefficient of a lowland mixed dipterocarp forest in Sarawak, Borneo: dry spell effects. *Journal of Hydrology*, *287*(1-4), 237–251. doi:10.1016/j.jhydrol.2003.10.002

Lee, X., William Massman, & Law, B. (2004). *Handbook of Micrometeorology: A Guide for Surface Flux Measurement and Analysis.* (p. 250p). Kluwer, Dordrecht: Springer.

Lloyd, C. R. (1995). The effect of heterogeneous terrain on micrometeorological flux measurements: a case study from HAPEX-Sahel. *Agricultural and Forest Meteorology*, *73*(3–4), 209–216. doi: 10.1016/0168-1923(94)05075-H

Ohtaki, E. (1985). On the similarity in atmospheric fluctuations of carbon dioxide, water vapor and temperature over vegetated fields. Boundary-Layer Meteorology, 32(1), 25–37. doi:10.1007/BF00120712

Pejam, M. R., Arain, M. A., & McCaughey, J. H. (2006). Energy and water vapour exchanges over a mixedwood boreal forest in Ontario, Canada. *Hydrological Processes*, *20*(17), 3709–3724. doi:10.1002/hyp.6384

Mahrt, L. (1998). Flux Sampling Errors for Aircraft and Towers. *Journal of Atmospheric and Oceanic Technology*, *15*(2), 416–429. doi:10.1175/1520-0426(1998)015<0416:FSEFAA>2.0.CO;2

Malhi, Y., Pegoraro, E., Nobre, A. D., Pereira, M. G. P., Grace, J., Culf, A. D., & Clement, R. (2002). Energy and water dynamics of a central Amazonian rain forest. *Journal of Geophysical Research*, *107*(D20), 1–17. doi:10.1029/2001JD000623

Nobuhiro, T. (2009). Evapotranspiration Characteristics of a Lowland Dry Evergreen Forest in Central Cambodia Examined Using a Multilayer Model. *Journal of Water Resource and Protection*, *01*(05), 325–335. doi:10.4236/jwarp.2009.15039

Da Rocha, H. R., Goulden, M. L., Miller, S. D., Menton, M. C., Pinto, L. D. V. O., De Freitas, H. C., & e Silva Figueira, A. M. (2004). Seasonality of water and heat fluxes over a tropical forest in eastern Amazonia. *Ecological Applications*, *14*(sp4), 22–32.

Schuepp, P. H., Leclerc, M. Y., MacPherson, J. I., & Desjardins, R. L. (1990). Footprint prediction of scalar fluxes from analytical solutions of the diffusion equation. *Boundary-Layer Meteorology*, *50*(1-4), 355–373. doi:10.1007/BF00120530

Tanaka, K., Takizawa, H., Tanaka, N., Kosaka, I., Yoshifuji, N., Tantasirin, C., Piman, S., et al. (2003). Transpiration peak over a hill evergreen forest in northern Thailand in the late dry season: Assessing the seasonal changes in evapotranspiration using a multilayer model. *J. Geophys. Res.*, *108*(D17), 4533. doi:10.1029/2002JD003028

Tanaka, N., Kume, T., Yoshifuji, N., Tanaka, K., Takizawa, H., Shiraki, K., Tantasirin, C., et al. (2008). A review of evapotranspiration estimates from tropical forests in Thailand and adjacent regions. *Agricultural and Forest Meteorology*, *148*(5), 807–819. doi:10.1016/j.agrformet.2008.01.011

Takanashi, S., Kosugi, Y., Ohkubo, S., Matsuo, N., Tani, M., & Nik, A. R. (2010). Water and heat fluxes above a lowland dipterocarp forest in Peninsular Malaysia. *Hydrological Processes*, *24*(4), 472–480. doi:10.1002/hyp.7499

Twine, T. E., Kustas, W. P., Norman, J. M., Cook, D. R., Houser, P. R., Meyers, T. P., Prueger, J. H., et al. (2000). Correcting eddy-covariance flux underestimates over a grassland. *Agricultural and Forest Meteorology*, *103*(3), 279–300. doi:10.1016/S0168-1923(00)00123-4

Toda, M., Nishida, K., Ohte, N., Tani, M., Mushiake, K. (2002). Observations of Energy Fluxes and Evapotranspiration over Terrestrial Complex Land Covers in the Tropical Monsoon Environment. Journal of the Meteorological Society of Japan. Ser. II, 80(3), 465–484.

Yoshifuji, N., Kumagai, T., Tanaka, K., Tanaka, N., Komatsu, H., Suzuki, M., & Tantasirin, C. (2006). Inter-annual variation in growing season length of a tropical seasonal forest in northern Thailand. *Forest Ecology and Management*, *229*(1-3), 333–339. doi:10.1016/j.foreco.2006.04.013

Yoshifuji, N., Komatsu, H., Kumagai, T., Tanaka, N., Tantasirin, C., & Suzuki, M. (2011). Interannual variation in transpiration onset and its predictive indicator for a tropical deciduous forest in northern Thailand based on 8-year sap-flow records. *Ecohydrology*, *4*(2), 225–235. doi:10.1002/eco.219

Vourlitis George, De Souza Nogueira, J., De Almeida Lobo, F., Sendall, K. M., De Paulo, S. R., Antunes Dias, C. A., Pinto, O. B., et al. (2008). Energy balance and canopy conductance of a tropical semi-deciduous forest of the southern Amazon Basin. *Water Resources Research*, *44*(3), 1–14. doi:10.1029/2006WR005526

Webb, E. K., Pearman, G. I., & Leuning, R. (1980). Correction of flux measurements for density effects due to heat and water vapour transfer. *Quarterly Journal of the Royal Meteorological Society*, *106*(447), 85–100. doi:10.1002/qj.49710644707

Wilson, K. B., & Baldocchi, D. D. (2000). Seasonal and interannual variability of energy fluxes over a broadleaved temperate deciduous forest in North America. *Agricultural and Forest Meteorology*, *100*(1), 1–18. doi:10.1016/S0168-1923(99)00088-X

Wilson, K., Goldstein, A., Falge, E., Aubinet, M., Baldocchi, D., Berbigier, P., Bernhofer, C., et al. (2002). Energy balance closure at FLUXNET sites. *Agricultural and Forest Meteorology*, *113*(1-4), 223–243. doi:10.1016/S0168-1923(02)00109-0

Chapter 3

Seasonal and inter-annual variation of stomatal conductance and its controlling factors at a tropical deciduous forest in Northern Thailand

3.1. Introduction

Recent studies suggest that phenological and physiological changes in the tropical monsoon forests are followed by the inter-annual variation in rainfall (Yoshifuji et al., 2006 and 2011). These responses may, in turn, influence energy partitioning and land surface evapotranspiration. To know the response of parameters like a stomatal conductance which effect transpiration to phenological and physiological changes is to understand the characteristic of transpiration in tropical deciduous forests. In the Penman–Monteith equation (Monteith, 1965), land-surface regulation of evapotranspiration is determined mainly by surface conductance (G_s) and aerodynamic conductance (G_a). Latent heat flux (LE) was regulated by G_a relative to G_a in a forest due to the large surface roughness. G_s was easily calculable from LE which measured by eddy covariance method. Sometimes G_s was similar to canopy conductance (G_c) in an evergreen forest with large LAI. To make a reasonable approximation (Raupach and Fininigan, 1988; Raupach, 1994), G_c can be regarded as the parallel sum of the stomatal conductance (g_s) of individual leaves (Kelliher, 1995). However, G_s differ from G_c in fundamentally because LE from eddy covariance contained not only canopy transpiration but also soil evaporation in deciduous forest. Therefore, after separating transpiration and soil evaporation, it was necessary to clarify the g_s which was the most important element to regulate LE, and its controlling factors.

The value of maximum conductance (g_{smax}) which determined under very favorable conditions (e.g. non-limitation of light and water availability and optimum temperature, Dai, Edwards & Ku 1992) was a one of the most important and useful parameter to represent a magnitude of g_s. However g_{smax} cannot be measured because it occurs near water vapor saturation where measurements of g_s and vapor pressure deficit (VPD) suffer large relative

errors (Arneth et al. 1996), and due to the field measurements, low VPD often occurs when irradiance is low (Martin et al. 1997). So, the value of g_{smax} must be extrapolated from the data using a function describe the response of g_{s} and VPD (e.g. Martin et al., 1997, Lloyd 1991). To solve the problem of extrapolating to g_{smax}, $f(\mathrm{VPD})$ in Oren's function (modified from Lohammar's function) is often used; $g_{\mathrm{s}} = g_{\mathrm{sref}} - m \ln(\mathrm{VPD})$. The parameter g_{sref} is reference conductance at VPD = 1 kPa, which conveniently occurs within the range in VPD of most data set. The values of g_{sref} and m were decided using a boundary line analysis (Ewers et al., 2005). The resulting boundary line analysis provides the best estimate of hydraulic limitation to water flux in trees because the boundary line occurs during conditions that lead to the highest g_{s} at any given VPD. These are the most appropriate conditions in which to analysis for seasonal and interannual variability on g_{s} and sensitivity of g_{s} to VPD. Across a large range of species, and even environmental conditions within species, m is 0.6 g_{sref} (Oren et al., 1999b; Ewers et al., 2001; Gunderson et al., 2002; Addington et al., 2004). The 0.6 proportionality between m and g_{sref} results from the regulation of minimum leaf water potential to prevent excessive xylem capitation as describing by Oren et al. (1999b). Therefore, a deviation from the 0.6 proportionality is considered as an index of phonological and physiological changes of leaves.

Objective in this chapter was to reveal the characteristic of seasonal and interannual variation of transpiration, surface, canopy and stomatal conductance and its controlling factor. To this objective, soil evaporation was modeled using the latent heat flux in dry (leaf-less) season to divide the latent heat flux into canopy transpiration and soil evaporation. In this chapter, the response of g_{sref} and m/g_{sref} to phonological and physiological changes was also examined.

3.2. Material and methods

The details of site descriptions, meteorological measurements, eddy covariance method and monitoring of LAI were shown in chapter 2. Material and method in this chapter mainly described the calculation of surface conductance and how separate canopy conductance from surface conductance. The determination of g_{sref} and m was also described in this chapter.

3.2.1 Calculation of surface, canopy and stomatal conductance and aero dynamic conductance

To evaluate the response of surface conductance (G_{s}; mmol m^{-2} s^{-1}) to environmental driving variables, the actual G_{s} was calculated using the actual data of canopy transpiration (LE;

W m^{-2}) from the inverted Penman-Monteith equation (Dolman et al., 1991) as

$$G_s^{-1} = \left[\left(\frac{\Delta}{\gamma}\beta - 1\right) G_a^{-1} + \frac{\rho c_p \mathrm{VPD}}{\mathrm{LE}\gamma}\right] \frac{P}{RT_a} \quad (3.1)$$

where LE is the latent heat flux (Wm^{-2}), Δ is the ratio of charge of saturation water vapor pressure with temperature (Pa K^{-1}), γ is the psychometric constant (Pa K^{-1}), β is the Bowen ratio (H/LE), Ga is the aero dynamic conductance, ρ a is the density of dry air (kg m^{-3}), C_p is the specific heat of air at a constant pressure (J kg^{-1} K^{-1}), VPD is the vapor pressure deficit above the canopy (Pa), P is an atmospheric pressure (Pa), R is a gas constant (8.314 Pa m^3 mol^{-1} K^{-1}).

G_a was estimated using the measured friction velocity (u^*; m s^{-1}), from

$$G_a = \frac{u^{*2}}{u} \quad (3.2)$$

where u is the wind speed above the canopy measured by sonic anemometer (USA-1) at 28m (m s^{-1}). From eddy covariance measurements, the surface conductance (G_s) was obtained, which is differ from canopy conductance (G_c) because G_s includes the effect of soil evaporation (Raupach 1995). In this study, G_c was calculated from G_s according to Keliher et al. (1995). After that stomatal conductance (g_s) was calculated from G_c and LAI.

The available energy $(R_n - G)$ can be described the sum of contributions from the canopy (A_c) and the soil (A_s):

$$R_n - G = A_c + A_s \quad (3.3)$$

According to Keliher et al (1995), the energy available at a soil surface A_s can be estimated as:

$$A_s = \tau(R_n - G) \quad (3.4)$$

$$\tau = exp(-c_A \mathrm{LAI}) \quad (3.5)$$

where LAI is the leaf area index of plant canopy (m^2 m^{-2}), τ is the term of available energy transmitted downwards at LAI. The coefficient c_A is 0.8 (Denmead, 1976). In principle, A_s was decided by the radiative transfer with in the canopy. It should be noted that the

estimation of A_s in Keliher et al. (1995) (Eq. 3.4 and3.5) implicitly assuming that there was a linear relationship between A_s and canopy light transmittance that was assumed as Beer-Lambert Law.

Consequently, the energy available at canopy A_c was can be estimated as:

$$A_c = (1 - \tau)(R_n - G) \qquad \text{for} \qquad (LAI > 0) \tag{3.6}$$

Total latent heat flux (observed LE above canopy: W m^{-2}) is also expressed the sum of contributions from the canopy transpiration (LE_c: W m^{-2}) and the soil evaporation (LE_s: W m^{-2}).

$$LE = LE_c + LE_s \tag{3.7}$$

To assess how G_s differ from G_c because of the contribution of soil evaporation, it was assumed that the soil evaporation (LE_s) occurs at the equilibrium rate with soil water regulation function (Demead amd Mcllroy, 1970; Priestley and Taylor, 1972).

$$LE_s = 1.26 \frac{\Delta A_s}{(\Delta+\gamma)} [1 + d_m \log(\theta_{10})] \tag{3.8}$$

$$LE_s = 1.26 \frac{\Delta A_s}{(\Delta+\gamma)} [1 + d_m \log(\Theta_{0-60})] \tag{3.9}$$

where, θ_{10} (m^3 m^{-3}) and Θ_{0-60} were the relative extractable water in the 10 cm and 0 - 60 cm soil layer (details in chapter 2). d_m is a parameter to decide a performance of water regulation. Equilibrium rate equation is plausible estimate for soil evaporation in conditions of adequate soil water supply, when soil evaporation is determined meteorologically rather than by the diffusion of soil water in the soil. Therefore, equilibrium rate function was converted to equilibrium rate function with soil water regulation function. Model parameter d_m was decided during leaf-less season (LAI = 0, $\tau = 1$ and $A_s = (R_n - G)$) because it is thought that source of LE in leaf-less season was mostly assumed as LE_s. In this study, the difference of between Eq. 3.8 and Eq. 3.9 was also examined because it was not known the how much soil layer did contribute to soil evaporation in leaf-less season.

The canopy contribution can be described with the Penman-Monteith equation, using the single-layer of big-leaf approximation:

$$A_c = (R_n - G) - A_s \quad (3.10)$$

$$LE_c = \frac{\Delta A_c + \rho c_p VPD G_a}{\Delta + \gamma\left(1 + {}^{G_a}/_{G_c}\right)} \quad (3.11)$$

Combining Eqs. (3.5), (3.6), (3.7), (3.8),(3.9) and invert the Penman-Monteith Eq (3.11) gives an expression for G_c.

$${G_c}^{-1} = \left\{\left[\frac{\Delta}{\gamma}\left(\frac{A_c}{LE - LE_s} - 1\right) - 1\right] {G_a}^{-1} + \frac{\rho c_p VPD}{\gamma(LE - LE_s)}\right\} \frac{P}{RT_a} \quad (3.12)$$

Stomatal conductance (g_s) was calculated following equation:

$$g_s = \frac{G_c}{LAI} \quad (3.13)$$

In this chapter, for easy to compere the value, the molar flux unit (mmol m^{-2} s^{-1}) was used as for the unit of G_s, G_c and g_s, because of, the molar flux unit for the value of g_{sref} and m (detail description are described in 3.2.2) are often used in the related researches (e.g. Oren et al., 1999b) in the field of plan physiology.

3.2.2 Determination of g_{sref} and m

To estimate hydraulic limitation to transpiration, to extract parameters from equation of relationship between g_s and VPD proposed by Oren et al. (1999b).

$$g_s = g_{sref} - m \ln(VPD) \quad (3.14)$$

where g_s is a reference conductance at VPD = 1 kPa and m is the sensitivity of the g_s response to ln VPD or the slope of g_s versus ln VPD$(-dg_s/d\ln VPD)$. To decide both parameters, boundary line analysis (Ewers et al., 2005) was applied. By partitioning a data into categories of soil moisture, light, and temperature, and performing a boundary line analysis on gs versus VPD within each category, the data can be reduced to the parameters describing the relationship between g_s and VPD (Chambers et al. 1985; Pezeshki & Hinckley 1988; Schafer et al. 2000; Ewers et al. 2001; Ewers et al. 2005). When a boundary analysis is made on a data set, it allows analysis of the best physiological response (in this case highest g_s) under the measured conditions (Martin et al. 1997). The resulting boundary line provides the best estimate of hydraulic limitation to water flux in trees

because the boundary line occurs during conditions that lead to the highest g_s at any given VPD. These are the most appropriate conditions in which to analyses for seasonal and inter-annual variability on g_{sref} and m. A more complete description of the analysis is available in Ewers et al. (2005).

3.3 Results

3.3.1 Estimation of soil evaporation

To assess the soil evaporation, depth of soil layer (in Eq. 3.8 and 3.9) and model parameter d were examined during the period in leaf-less season (LAI = 0). Hereby, As in Eq. 3.8 and 3.9 was $(R_n - G)$, because in Eq. 3.5 is 1. The parameter value was decided to minimize the root mean square error (RMSE) between the observed and calculated values of LE in leaf-less season. As shown in Fig. 3.1, that the relationship between latent heat flux (LE) and calculated latent heat flux (LE_{est}) in leaf-less season (LAI = 0). The coefficient of determination (R^2) and RSME in Eq. 3.8 were 0.66 and 100.3, respectively. On the other hands, R^2 and RSME in Eq. 3.9 were 0.86 and 58.6, respectively. The calculated values in each equation showed good agreement with LE although R^2 and RSME of Eq. 3.9 was better than that of Eq. 3.8. The difference between Eq 3.8 and Eq. 3.9 was variable. The Eq 3.9 was controlled by the soil water content in 0 - 60 cm although Eq 3.8 was controlled by the just only soil water content 0 - 10 cm. As a reason which Eq. 3.9 was better than Eq 3.8, it was considered that LE in leaf-less season was affected not only the just soil surface water content but also the transpiration from understory vegetation which was controlled by the relative deep soil water content. As the author had already mentioned in section 2.3.5, there were understory plants, such as shrubs and bamboos, which are patchily distributed at this site. Therefore, it was reasonable to use the Eq 3.9 as a soil evaporation model in this site. Typical temporal variation period from before and after rainfall event in leaf-less season in March 2008 also showed in Fig. 3.2. Both LE and LE_{est} (calculated by Eq. 3.9) were low in before the rainfall event although both LE_{obs} and LE_{est} after rainfall event increased corresponding to increase of soil water content. Consequently, it was considered that soil evaporation model (Eq. 3.9) and model parameter d were sufficiently accurate to estimate soil evaporation.

3.3.2 Seasonal and interannual variation of G_s G_c and g_s

Seasonal and interannual variation of mid-day (10:00-15:00) averaged G_s and G_c were observed (Fig. 3.3 A). G_s began to increase from 1 -2 month before starting wet season. The

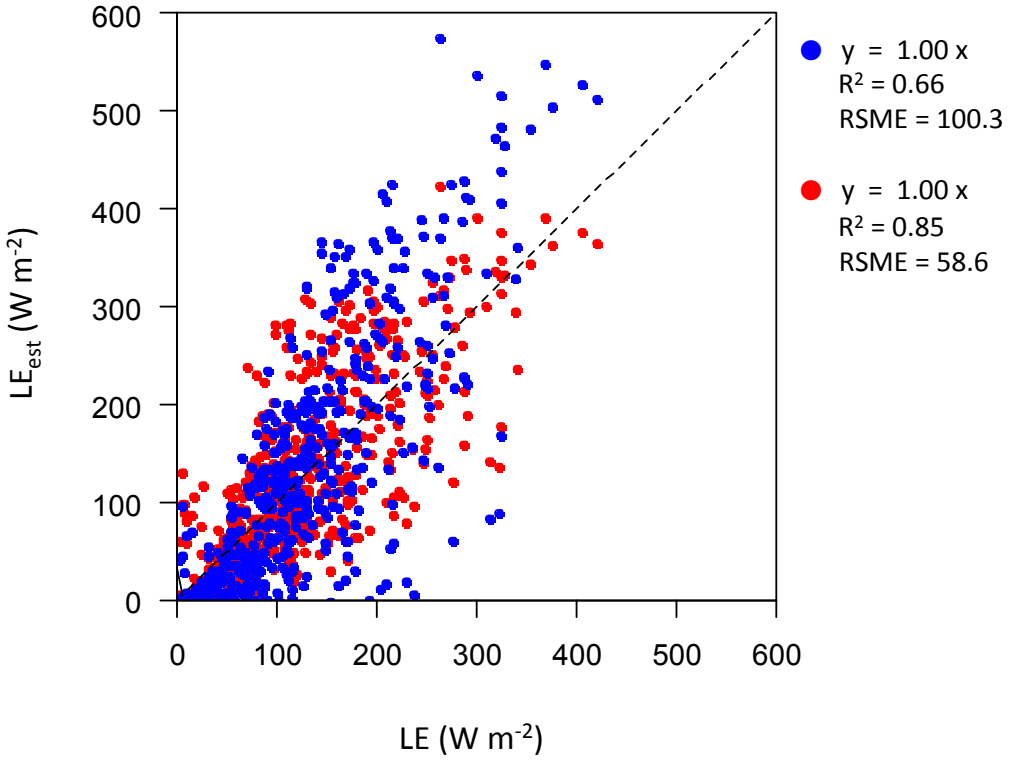

Fig. 3.1 Relationship between latent heat flux (LE) and modeled latent heat flux (LE_{est}) in leaf-less season (LAI = 0). Blue dots represents the calculated latent heat flux (LE_{est}) by Eq.3.8 with d_m = 0.371. Red dots represents the calculated latent heat flux (LE_{est}) by Eq.3.9 with d_m = 0.295.

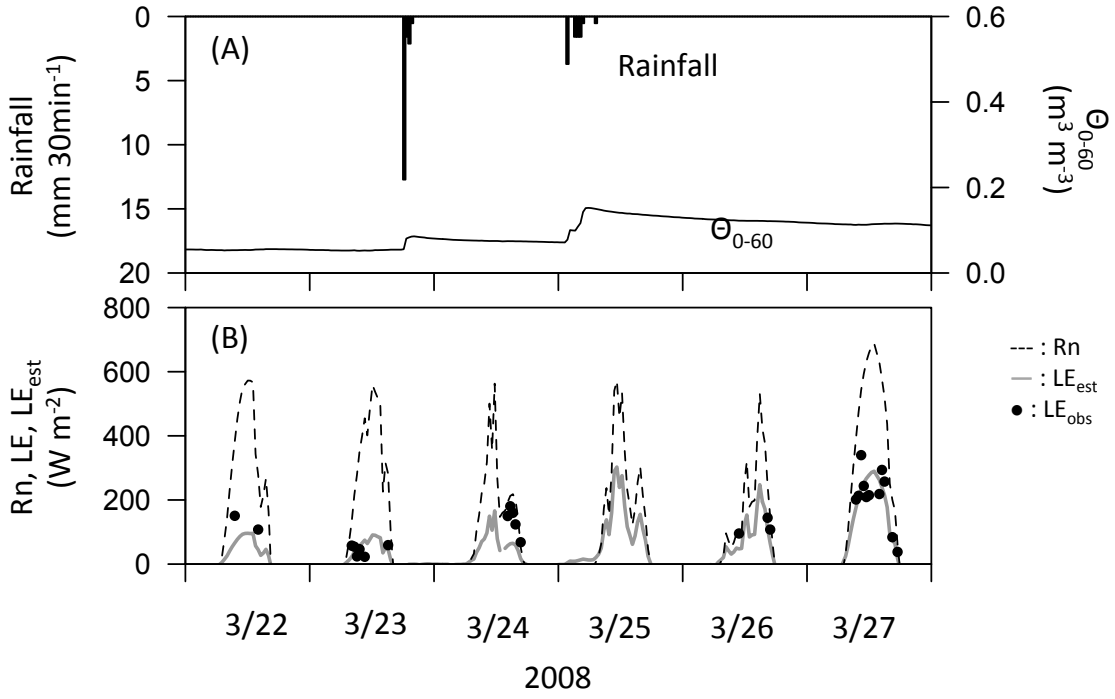

Fig. 3.2 Typical temporal variation period from before and after rainfall event in leaf-less season in March 2008. Measured time series of rainfall, soil water content ($\Theta_{0\text{-}60}$) (A), net radiation (R_n), latent heat flux (LE_{obs}) and modeled latent heat flux (LE_{est}) (B). Bar and solid line in (A) represent rainfall and $\Theta_{0\text{-}60}$. Dash line, gray solid line and solid dot in (B) represent R_n, LE_{est} and LE_{obs}, respectively.

increase of G_c started simultaneously with start of leaf-out. Ever after the increase in LAI finished, G_c increased a little until the end of wet season. After that G_c begun to decrease rapidly. The value of G_s was observed even after G_c was not observed in dry season. Seasonal and inter annual variation of mid-day (10:00-15:00) averaged g_s was showed in Fig.3.3 (B). The value of g_s was calculated from G_c / LAI using Eq. (3.10). The value of g_s began to increase from leaf-out to end of wet season. After wet season, g_s began to decrease rapidly. Averaged G_s, G_c and g_s in mid-growing season (August-October) showed a significant difference ($p < 0.01$; ANOVA), and 2006 were significant larger ($p < 0.001$; Tukey test) than that of 2008 and 2010 (Table 3.1) in spite of indifferent maximum LAI (Table 2.2).

The relationship between LAI and g_s are showed in Fig.3.4 pink, gray and light blue dots showed every 30-min g_s data in leaf-out (March-July), mid-growing (August-October) and leaf-senescence season (November-February), respectively. Red, black and blue dots showed median of g_s in each LAI levels from 1.5 to 3.5. The value of g_s was increasing with increasing of LAI. g_s in mid-growing season was the highest in a year. g_s in leaf-out season was higher than that of leaf senescence season despite of the same LAI level.

3.3.3 Seasonal changes of response stomatal conductance to VPD

To know the relationship between g_{sref} and m, g_{sref} and m was calculated in monthly data set. As shown in Fig. 3.5, the relationship between monthly g_{sref} and m was almost plotted near 1:0.6 line (Oren et a., 1999b) although data in mid-growing season tended to be plotted below the line. It was interesting to note that the relationship between g_{sref} and m was influenced by not the interannual changes but the seasonal changes.

To know the effect of seasonal changes to magnitude of g_s and response of g_s to VPD, g_{sref} and m was calculated among the three years. Fig.3.5 shows the relationship between VPD and g_s in leaf-out (A), mid-growing (B) and leaf-senescence season (C), respectively. Averaged g_{sref} in leaf-out mid-growing and leaf-senescence season were 273.6, 339.4 and 168.1 mmol m^2 s^{-1}, respectively (Table 3.2). The value of g_{sref} was significant higher in the growing season than in that of leaf-senescence season ($p < 0.01$; Tukey test). But insignificant differences of g_{sref} were observed in between leaf-out and mid-growing season ($p = 0.06$; Tukey test) and between leaf-out and leaf-senescence season ($p = 0.20$; Tukey test). Seasonal changes of m/g_{sref} was also examined. Averaged m/g_{sref} of leaf-out season, mid-growing season and leaf-senescence season were 0.58, 0.46 and 0.64, respectively (Table 3.2). The significant seasonal difference of m/g_{sref} was observed (ANOVA, $p < 0.05$).

To clarify the controlling factor to decide a magnitude of g_s, the response of g_{sref} to controlling factors was examined. The relationship between $\Theta_{0\text{-}60}$ and g_{sref} are shown in Fig.

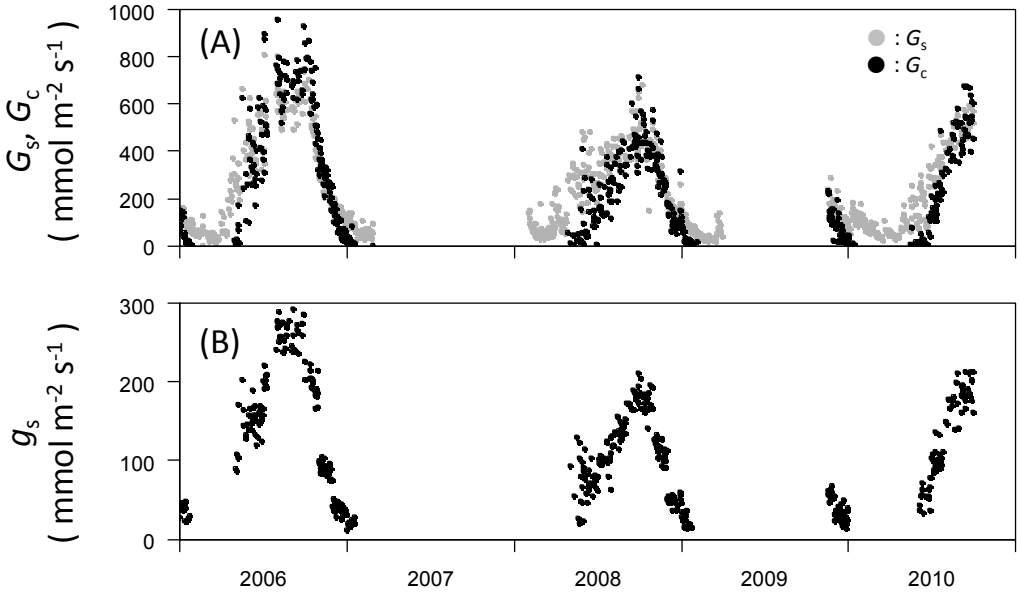

Fig. 3.3 Temporal variation of midday averaged surface conductance (G_s), canopy conductance (G_c) and stomatal conductance (g_s). Gray and black dots in (A) represent G_s and G_c, respectively.

Table 3.1 Averaged surface conductance (G_s), canopy conductance (G_c) and stomatal conductance (g_s) in mid-growing season

	2006		2008		2010	
	Mean	S.D.	Mean	S.D.	Mean	S.D.
G_s (mmmol m^{-2} s^{-1})	838.7	242.0	635.9	162.8	736.4	184.0
G_c (mmmol m^{-2} s^{-1})	660.5	220.8	379.6	164.1	473.0	199.3
g_s (mmmol m^{-2} s^{-1})	237.2	81.8	165.9	68.8	187.3	76.1

3.7 (A). The clear relationship between $\Theta_{0\text{-}60}$ and g_{sref} was observed (R^2 = 0.79). On the other hands, the relationship between LAI and g_{sref} was not clear (R^2 = 0.27, Fig. 3.7 B).

3.4 Discussion

In this chapter, to calculate the stomatal conductance, the soil evaporation was modeled using the latent heat flux in dry (leaf-less) season to divide the latent heat flux into canopy transpiration and soil evaporation. To assess the soil evaporation, two soil evaporation models which were different about variable to regulate evaporation using a soil water contents were examined. The results of two models showed good agreement with observed value although R^2 and RSME of deep soil layer were better than that of surface soil layer. It was able to be considered that LE in leaf-less season was affected not only the soil surface water content but also deep soil water content, due to the effect of understory vegetation, such as shrubs and bamboos. Using a soil water regulation function, the relationship between observed LE and calculated LE and temporal variation of observed LE and calculated LE showed good agreements, and this implied that the accuracy of this soil evaporation model and its parameter d.

The values of G_{s}, G_{c} and g_{s} were measured during 3 growing season. At first, the author discussed interannual variation of g_{s}. Averaged G_{s}, G_{c} and g_{s} in mid-growing season (August-October) in 2006 were significant larger ($p < 0.001$; Tukey test) than that of 2008 and 2010 (Table 3.1). Therefore, it was able to be considered that interannual variation of G_{s}, G_{c} and g_{s} were made by not interannual variation of maximum LAI but the interannual variation of environmental factors.

The seconds, the author discussed seasonal changes of g_{s}. As mentioned above (section 3.3.2), the relationship between LAI and g_{s} showed hysteresis which related to seasonal changes (Fig.3.4). The values of g_{s} in leaf-out and mid-growing season were higher than that of leaf senescence season despite of the same LAI level. This result supports a possibility that seasonality of g_{s} was affected by not only environmental factors but also physiological changes like a maturing and aging of teak leaves.

To know the effect of seasonal physiological changes like a maturing and aging of teak leaves and environmental variables, seasonal changes of g_{sref} and m were examined. g_{sref} is a reference conductance at VPD = 1 kPa and m was the sensitivity of the g_{s} response to ln VPD or the slope of g_{s} versus ln VPD ($-g_{\mathrm{s}}\, \mathrm{d}g_{\mathrm{s}}/\mathrm{d}\ln\mathrm{VPD}$) (e.g. Oren et al., 1999b; Ewers et al., 2005). Across a wide range of isohydric species, and environmental conditions within those species, m was 0.6 g_{sref} (Oren et al. 1999a and 1999b, Ewers et al. 2001b, Oren et al. 2001, Wullschleger et al. 2002, Addington et al. 2004, Ewers et al. 2005).

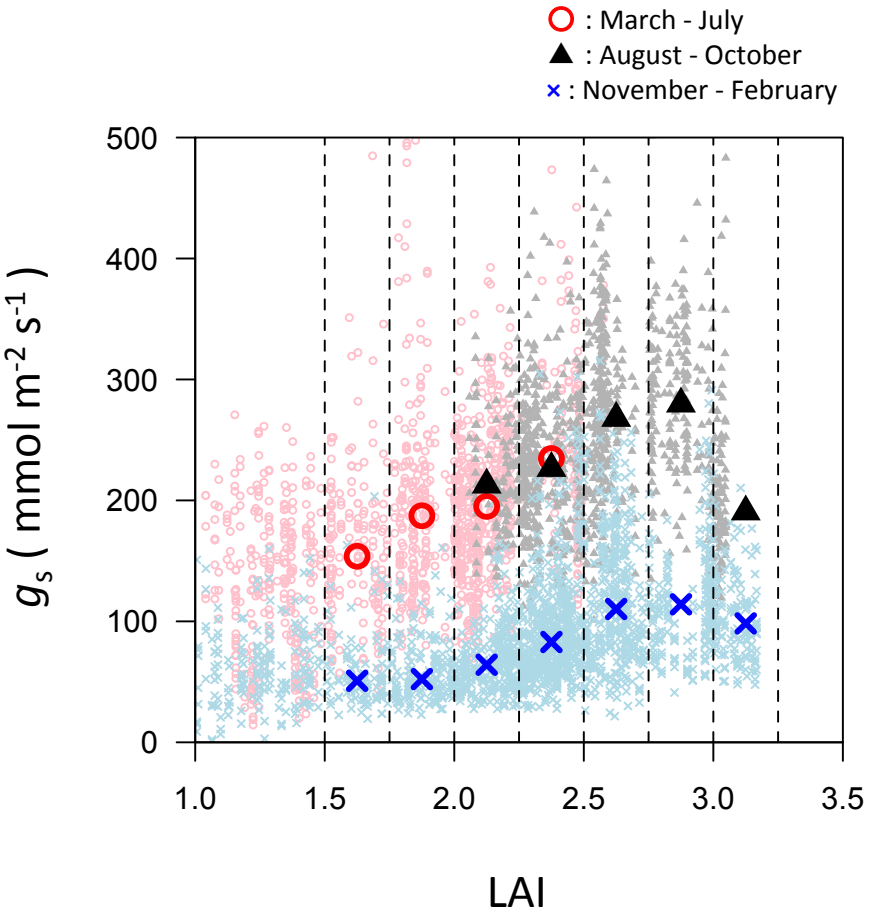

Fig.3.4 Relationship between leaf area index (LAI) and stomatal conductance (g_s). Small circle, triangle and cross represents period from March to July, from August to Octover and from November to next year's February, respectively. Large sings represents median of each LAI levels from 1.5 to 3.25 at 0.25 interval.

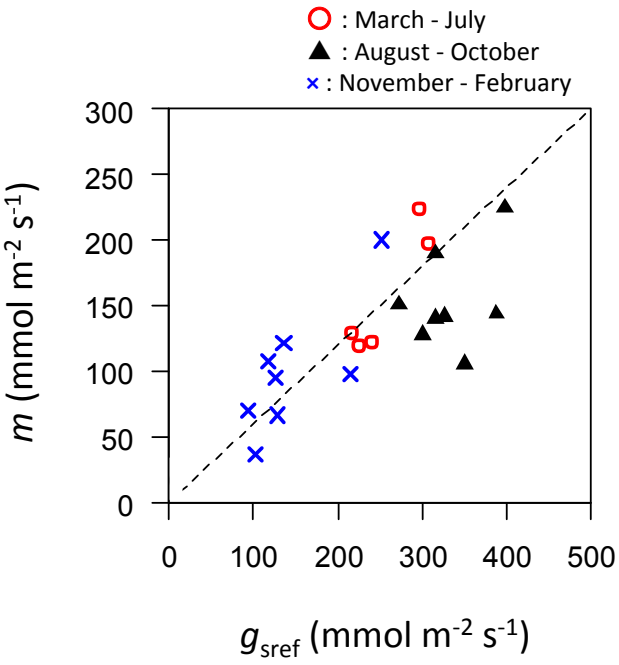

Fig.3.5 Relationship between reference stomatal conductance (g_{sref}) and sensitive value in Oren's model (m). Circle, triangle and cross represents period from March to July, from August to Octover and from November to next year's February, respectively.

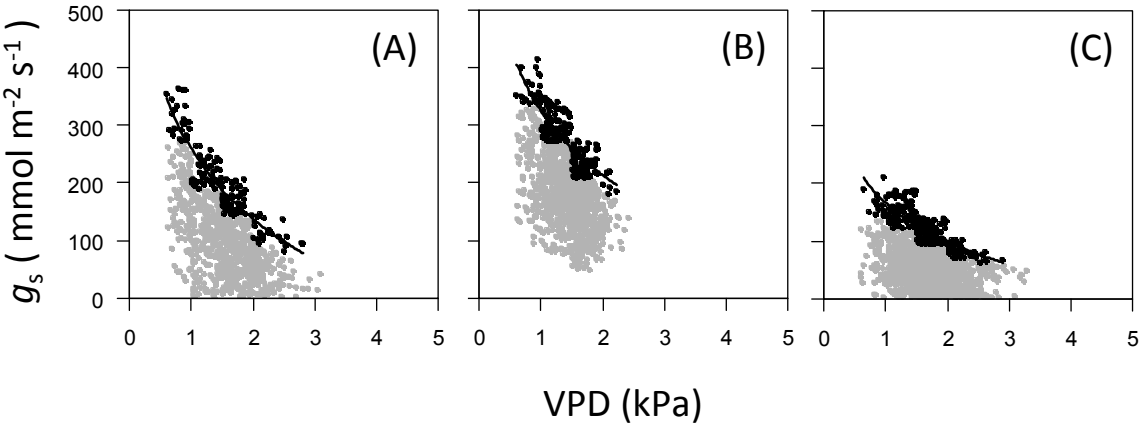

Fig.3.6 Relationship between vapor pressure deficit (VPD) and stomatal conductance (*gs*).
(A), (B) and (C) represent period from March to July, from August to Octover and from November to next year's February, respectively. Black dots represent outer value boundary line analysis . Solid lines represent regression line to boundary value.

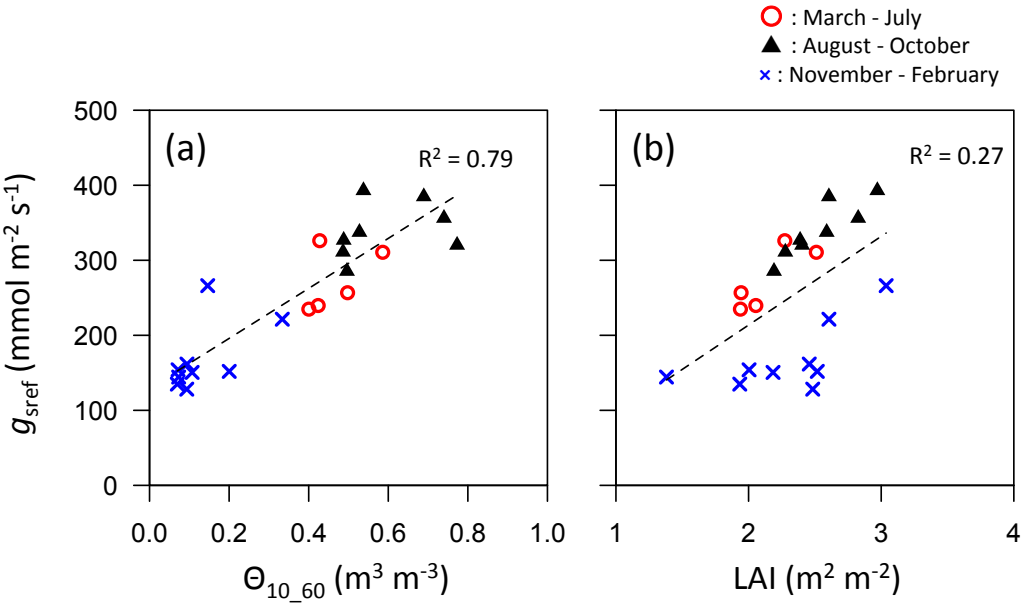

Fig.3.7 Response of reference stomatal conductance (g_{sref}) to soil moisture condition (Θ_{10_60})(A) and LAI (B). Circle, triangle and cross represents period from March to July, from August to Octover and from November to next year's February, respectively.

Table 3.2. Mean reference conductance (g_{sref}), sensitivity of stomatal conductance (m) and m / g_{sref} for the three season.

	g_{sref}		m		m / g_{sref}	
	Mean	S.D.	Mean	S.D.	Mean	S.D.
Leaf-out season	273.62	42.02	161.38	42.70	0.58	0.08
Mid-growing season	339.39	36.78	154.87	30.98	0.46	0.10
Leaf-senecence season	168.14	45.45	107.76	43.56	0.64	0.16
	***		*		**	

The significance of individual parameters are indicated by asterisks (P > 0.05; *, P < 0.05; **, P < 0.01; ***, P < 0.001; ****).

The 0.6 proportionality between m and g_{sref} results from the regulation of minimum leaf water potential to prevent excessive xylem cavitation. Therefore as VPD increases, the sensitivity of stomatal closure was larger, when the proportionality between m and g_{sref} was larger than 0.6. On the other hands, stomatal closure was insensitive when the proportionality between m and g_{sref} smaller than 0.6. As shown in Fig. 3.5, the relationship between g_{sref} and m was almost plotted near 1:0.6 line (Oren et a., 1999b) although data in mid-growing season tended to be plotted below the line. This tendency implies that stomatal sensitivity to VPD in mid-growing season was more insensitive relative to that of other season due to the relative high soil water content (Fig. 2.3).

As mentioned above, g_{sref} was varied through a year although m and m/g_s which represent a sensitivity of g_s to VPD was rather stable. Therefore, the author examined the factors to affect the value of g_{sref}. In this study, the relationship between $\Theta_{0\text{-}60}$ and g_{sref} are shown in Fig. 3.7 (A). Significant relationship between $\Theta_{0\text{-}60}$ and g_{sref} was observed (R^2 = 0.79). On the other hands, the significant relationship between LAI and g_{sref} was not observed (R^2 = 0.27, Fig. 3.7 B). About the relationship between g_s and soil moisture, Loranty et al. (2008) showed that insignificant relationship between g_{sref} and soil water content was observed in Aspen stand. Traver et al. (2010) also showed soil moisture does not attempt to explain how soil moisture deficit limits transpiration. In general, saturated soils are common and result in well-known declines in transpiration and stomatal conductance in species that poorly respond to anaerobic conditions in northern temperate and boreal forest (Kozlowski 1984; Zhang & Davies 1987; Else et al. 1996). This tendency appeared in Southeast Asian tropical rainforest. According to Kumagai et al., 2004, the responses of stomatal conductance would have been little influenced by a soil moisture condition due to a little seasonal variation in rainfall although stomatal conductance was rarely influenced during the short-term and unpredictable dry spells. On the other hands, the effect of soil moisture to g_s was significant in tropical semi-deciduous forest with seasonal variation in rainfall. According to Vourlitis et al. (2008), the seasonality canopy conductance was correlated with the variation of soil moisture in the Central Amazonian rainforest. In fact, Dickinson et al. (1991) reported that the magnitude of stomatal conductance in the wet season differ from in that of dry seasons at Amazonian rainforest. The results of this study showed that soil moisture played important role as a stomatal conductance controlling factor at a tropical deciduous forest in northern Thailand because this site located under the strong solar radiation, high temperature and heavy seasonality of rainfall, due to the Asian monsoon climate. This study also found that the tendency of the relationship between g_{sref} and LAI in mid-growing season and leaf-senescence season (Fig. 3.7 B). According to Kitajima et al. (2002), seasonal changes of LAI was determined by not only seasonality of

meteorological variables but also seasonal changes of the leaf mas per area, nitrogen contents in leaves in tropical pioneer tree species in Panama. This result implies that the effect of physiological changes like a maturing and aging of teak leaves (allocation and reallocation of nitrogen) affected to the relationship between g_{sref} and LAI, especially in mid-growing season and leaf-senescence season, respectively. In addition, seasonality of LAI was strongly influenced by the seasonal changes of soil moisture contents in this study site (Yoshifuji et al., 2006; Yoshifuji et al, 2011). Based on these findings, the effect of physiological changes of leaves to stomatal conductance was mostly explained by the seasonal variation of soil moisture contents.

3.5 Conclusion

In this chapter, seasonal and intreanual variation of G_{s}, G_{c} and g_{s} and its controlling factors were examined. To evaluate g_{s} observed LE was decomposed into transpiration from teak and soil evaporation using developed soil evaporation model and LAI. The seasonal and interannual variation of G_{s}, G_{c} and g_{s} were estimated and the averaged g_{s} in mid-growing season showed a interannual variation despite the maximum LAI was almost constant in every year. The value of g_{s} was increasing with increasing of LAI. The value of g_{s} in mid-growing season was the highest in a year and g_{s} in leaf-out season was higher than that of leaf senescence season despite of the same LAI level. The relationship between monthly g_{sref} and m was almost plotted near Oren's line although data in mid-growing season tended to be plotted below the line The value of g_{sref} was significant higher in the growing season than other season. But insignificant difference of m/g_{sref} was observed throughout a year. To clarify the controlling factor to decide a magnitude of g_{s}, the response of g_{sref} to controlling factors was examined. The seasonality of g_{sref} mainly correlated with soil water contents. On the other hand, the tendency of the relationship between LAI and g_{sref} was also observed. As results, it was implied that the effect of physiological changes like a maturing and aging of teak leaves (allocation and reallocation of nitrogen) affected to the relationship between g_{sref} and LAI in mid-growing season and leaf-senescence season, respectively. In addition, seasonality of LAI was strongly influenced by the seasonal changes of soil moisture contents in this study site

References

Arneth, A., Kelliher, F. M., Bauer, G., Hollinger, D. Y., Byers, J. N., Hunt, J. E., McSeveny, T. M., et al. (1996). Environmental regulation of xylem sap flow and total conductance of Larix gmelinii trees in eastern Siberia. *Tree physiology*, *16*(1_2), 247–255.

Addington, R. N., Mitchell, R. J., Oren, R., & Donovan, L. a. (2004). Stomatal sensitivity to vapor pressure deficit and its relationship to hydraulic conductance in Pinus palustris. *Tree physiology*, *24*(5), 561–9.

Chambers, J., Hinckley, T., & Cox, G. (1985). Boundary-line analysis and models of leaf conductance for four oak-hickory forest species. *Forest …*, *31*(2), 437–450.

Dai, Z., Edwards, G. E., & Ku, M. S. (1992). Control of Photosynthesis and Stomatal Conductance in Ricinus communis L. (Castor Bean) by Leaf to Air Vapor Pressure Deficit. *Plant physiology*, *99*(4), 1426–34.

Denmead, O.T., 1976. Temperate cereals. In: J.L. Monteith (Editor), Vegetation and the Atmosphere, 2. Case Studies. Academic Press, London, pp. 1-31

Denmead, O. T., & McIlroy, I. C. (1970). Measurements of non-potential evaporation from wheat. *Agricultural Meteorology*, *7*(1970), 285–302. doi:10.1016/0002-1571(70)90024-5

Dickinson, R. E., Henderson-Sellers, A., Rosenzweig, C., & Sellers, P. J. (1991). Evapotranspiration models with canopy resistance for use in climate models, a review. *Agricultural and Forest Meteorology*, *54*(2-4), 373–388. doi:10.1016/0168-1923(91)90014-H

Dolman, A. J., Gash, J. H. C., Roberts, J., & Shuttleworth, W. J. (1991). Stomatal and surface conductance of tropical rainforest. *Agricultural and Forest Meteorology*, *54*(2-4), 303–318. doi:10.1016/0168-1923(91)90011-E

Else, M.A., Tiekstra, A.E., Croker, S.J., Davies, W.J. & Jackson, M.B. (1996) Stomatal closure in flooded tomato plants involves abscisic acid and a chemically unidentified antitranspirant in xylem sap. Plant Physiology, 112,239– 247.

Ewers, B. E., Oren, R., Phillips, N., Strömgren, M., & Linder, S. (2001). Mean canopy stomatal conductance responses to water and nutrient availabilities in Picea abies and Pinus taeda. *Tree physiology*, *21*(12-13), 841–50.

Ewers, B. E., Mackay, D. S., & Samanta, S. (2007). Interannual consistency in canopy stomatal conductance control of leaf water potential across seven tree species. *Tree physiology*, *27*(1), 11–24.

Ewers, B.E., Oren, R. & Sperry, J.S. (2000) Influence of nutrient versus water supply on hydraulic architecture and water balance in Pinus taeda. PlantCell &Environment, 23, 1055–1066.

Ewers, B.E., Gower, S.T., Bond-Lamberty, B. & Wang, C.K. (2005) Effects of stand age and tree species on canopy transpiration and average stomatal conductance of boreal forests. Plant, Cell andEnvironment, 28,660.

Gunderson, C. A., Sholtis, J. D., Wullschleger, S. D., Tissue, D. T., Hanson, P. J., & Norby, R. J. (2002). Environmental and stomatal control of photosynthetic enhancement in the canopy of a sweetgum (Liquidambar styraciflua L.) plantation during 3 years of CO_2 enrichment. *Plant, Cell and Environment*, *25*(3), 379–393. doi:10.1046/j.0016-8025.2001.00816.x

Kelliher, F., & Leuning, R. (1995). Maximum conductances for evaporation from global vegetation types. *Agricultural and Forest …*, *73*(1), 1–16. doi:10.1016/0168-1923(94)02178-M

Kitajima, K., Mulkey, S. S., Samaniego, M., & Joseph Wright, S. (2002). Decline of photosynthetic capacity with leaf age and position in two tropical pioneer tree species. *American journal of botany*, *89*(12), 1925–32. doi:10.3732/ajb.89.12.1925

Kozlowski, T.T. (1984) Flooding and Plant Growth. AcademicPress, New York, p. 356.

Kumagai, T., Saitoh, T. M., Sato, Y., Morooka, T., Manfroi, O. J., Kuraji, K., & Suzuki, M. (2004). Transpiration, canopy conductance and the decoupling coefficient of a lowland mixed dipterocarp forest in Sarawak, Borneo: dry spell effects. *Journal of Hydrology*, *287*(1-4), 237–251. doi:10.1016/j.jhydrol.2003.10.002

Lloyd, J. (1991). Modelling stomatal responses to environment in Macadamia integrifolia. *Functional Plant Biology*, (1977).

Loranty, M. M., Mackay, D. S., Ewers, B. E., Traver, E., & Kruger, E. L. (2010). Contribution of competition for light to within-species variability in stomatal conductance. *Water Resources Research*, *46*(5), 1–18. doi:10.1029/2009WR008125

Mackay, D.S., Ahl, D.E., Ewers, B.E., Gower, S.T., Burrows, S.N., Samanta, S.&Davis, K.J. (2002) Effects of aggregated classifications of forest compo- sition on estimates of evapotranspiration in a northern Wisconsin forest. GlobalChangeBiology, 8, 1253–1265.

Mackay, D.S., Ewers, B.E., Cook, B.D. & Davis, K.J. (2007) Environmental drivers of evapotranspiration in a shrub wetland and an upland forest in NorthernWisconsin. Water Resources Research, 43,W03442; doi: 10.1029/ 2006WR005149.

Martin, T. a., Brown, K. J., Cermák, J., Ceulemans, R., Kucera, J., Meinzer, F. C., Rombold, J. S., et al. (1997). Crown conductance and tree and stand transpiration in a second-growth <I>Abies amabilis</I> forest. *Canadian Journal of Forest Research*, *27*(6), 797–808. doi:10.1139/cjfr-27-6-797

Monteith, J. L. (1965), Evaporation and the environment, in Proceedings of the 19th Symposium of the Society for Experimental Biology, Cambridge Univ. Press, New York.

Oren, R., Phillips, N., Ewers, B. E., Pataki, D. E., & Megonigal, J. P. (1999a). Sap-flux-scaled transpiration responses to light, vapor pressure deficit, and leaf area reduction in a flooded Taxodium distichum forest. Tree Physiology, 19(6), 337–347. doi:10.1093/treephys/19.6.337

Oren, R., Sperry, J. S., Katul, G. G., Pataki, D. E., Ewers, B. E., Phillips, N., & Schäfer, K. V. R. (1999b). Survey and synthesis of intra- and interspecific variation in stomatal sensitivity to vapour pressure deficit. *Plant, Cell & Environment*, *22*(12), 1515–1526. doi:10.1046/j.1365-3040.1999.00513.x

Pezeshki, S. R., & Hinckley, T. M. (1988). Water relations characteristics of Alnusrubra and Populustrichocarpa: responses to field drought. *Canadian Journal of Forest Research*, *18*(9), 1159–1166. doi:10.1139/x88-178

Priestley, C. H. B., & Physics, R. J. T. A. (1972). On the Assessment of Surface Heat Flux and Evaporation Using Large-Scale Parameters. *Monthly Weather Review*, (February), 81–92. doi: 10.1175/1520-0493(1972)100<0081:OTAOSH>2.3.CO;2

Raupach, M. (1995). Vegetation-atmosphere interaction and surface conductance at leaf, canopy and regional scales. *Agricultural and Forest Meteorology*, *1923*(94). doi:org/10.1016/0168-1923(94)05071-D

Raupach, M., & Finnigan, J. (1988). "Single-Layer Models of Evaporation From Plant Canopies Are Incorrect but Useful, Whereas Multilayer Models Are Correct but Useless": Discuss. *Australian Journal of Plant Physiology*, *15*(6), 705. doi:10.1071/PP9880705

Samanta, S., Clayton,M.K., Mackey,D.S., Kruger, E.L.&Ewers, B.E. (2008) Quantitative comparison of canopy conductance models using a Baysian approach. Water Resources Research; 44, W09431, DOI: 10.1029/ 2007WR006761.

Schafer, K. V. R., Oren, R., & Tenhunen, J. D. (2000). The effect of tree height on crown level stomatal conductance. *Plant, Cell and Environment*, *23*(4), 365–375. doi:10.1046/j.1365-3040.2000.00553.x

Tanaka, K., Tantasirin, C., & Suzuki, M. (2011). Interannual variation in leaf expansion and outbreak of a teak defoliator at a teak stand in northern Thailand. *Ecological applications : a publication of the Ecological Society of America*, *21*(5), 1792–801.

Traver, E., Ewers, B. E., Mackay, D. S., & Loranty, M. M. (2010). Tree transpiration varies spatially in response to atmospheric but not edaphic conditions. *Functional Ecology*, *24*(2), 273–282. doi:10.1111/j.1365-2435.2009.01657.x

Vourlitis George, De Souza Nogueira, J., De Almeida Lobo, F., Sendall, K. M., De Paulo, S. R., Antunes Dias, C. A., Pinto, O. B., et al. (2008). Energy balance and canopy conductance of a tropical semi-deciduous forest of the southern Amazon Basin. Water Resources Research, 44(3), 1–14. doi:10.1029/2006WR005526

Wullschleger, S. D., Gunderson, C. A., Hanson, P. J., Wilson, K. B., & Norby, R. J. (2002). Sensitivity of stomatal and canopy conductance to elevated CO_2 concentration - interacting variables and perspectives of scale. New Phytologist, 153(3), 485–496. doi:10.1046/j.0028-646X.2001.00333.x

Yoshifuji, N., Kumagai, T., Tanaka, K., Tanaka, N., Komatsu, H., Suzuki, M., & Tantasirin, C. (2006). Inter-annual variation in growing season length of a tropical seasonal forest in northern Thailand. *Forest Ecology and Management*, *229*(1-3), 333–339. doi:10.1016/j.foreco.2006.04.013

Yoshifuji, N., Komatsu, H., Kumagai, T., Tanaka, N., Tantasirin, C., & Suzuki, M. (2011). Interannual variation in transpiration onset and its predictive indicator for a tropical deciduous forest in northern Thailand based on 8-year sap-flow records. *Ecohydrology*, *4*(2), 225–235. doi:10.1002/eco.219

Zhang, J.&Davies, W.J. (1987)ABAin roots and leaves of flooded pea plants. Journal of ExperimentalBotany, 38, 649–659.

Chapter 4

Modeling of stomatal conductance and estimation of evapotranspiration at tropical deciduous forest in Northern Thailand

4.1 Introduction

In tropical ecosystem water cycling, evapotranspiration (ET) as the sum of transpiration (E_{tc}), soil evaporation (E_{ts}) and interception (EI) is a hydrologic component of major importance in determining the water budget of forest areas due to the significant volumes involved (e.g., Calder et al., 1986; Shuttleworth, 1988; Malhi et al., 2002). Some studies conducted in temperate forests showed that forest ET had large interannual variations and that soil drought resulting from seasonal and interannual rainfall variations could be factors determining interannual ET variations, which reduced ET due to limitations on transpiration (Wilson and Baldocchi, 2000; Lafleur et al., 2005; Granier et al., 2007). The value of ET also showed interannual variation resulting from growing season length (GSL) in temperate deciduous forest (White et a., 1999). In some cases, annual ET increased with increasing rainfall due to more frequent occurrence of rainfall interception (e.g., Loescher et al., 2005). Therefore, it could be considered as seasonal and interannual variation of ET was made by not only the environmental factors but also phenological and physiological affect.

In tropical deciduous forest under the Asian monsoon influence had a large interannual variation of GSL and transpiration period was observed due to the inter-seasonal variation of rainfall. And, interannual variation of GSL in tropical deciduous forest was large relative to that of temperate deciduous forest (Yoshifuji et al., 2006 and 2011). And, high radiant energy is available throughout the year in tropical deciduous forests. These previous findings, it was able to be considered that the ET in tropical deciduous forest strongly correlated to GSL and had a large interannual variation.

The eddy covariance method is a widely used technique for assessing ET, and has advanced understanding of ecosystem water balance processes in short-time scale (e.g.,

Fisher et al., 2009; Giambelluca et al., 2009; Li et al., 2010). Although, the range which can apply the eddy covariance method was restricted due to the technical problem (e.g. effect of rainfall and wind profile condition). And continuous observation by eddy covariance is difficult due to the hard operation (e.g. electric supply, maintenance and machine correction). Therefore, it was needed that the estimation of long-time scale ET using a model. In general, ET has been simplified modeled as functions of rainfall and potential evaporation (Zhang et al., 2001; Komatsu et al., 2008). Although to know the effect of seasonal and interannual variation of rainfall and GSL, it was needed that the complex model which employs more process-based formulations including the Penman - Monteith equation likes a big-leaf model. As mentioned in chapter 3, soil evaporation (E_{ts}) was one of the important elements of ET in deciduous forest. Therefore, E_{ts} also should be calculated in a big-leaf model.

This chapter was undertaken to quantify six-year ET at a teak plantation in northern Thailand based on the micrometeorology measurements and a big-leaf model that was used for estimate ET. In the big-leaf model, transpiration from dry canopy (E_{tc}), during the fully-leafed period, was calculated from Penman - Monteith that contained Jarvis-type stomatal conductance model. Interception (EI) from wet canopy was calculated from simplified Rutter's model. Soil evaporation (E_{ts}) during leaf-less period was calculated from improved Priestley and Taylor model (in Chapter 3). Evapotranspiration during leaf-out and leaf-fall period was calculated from sum of E_{tc} and E_{ts}. Contribution ratio of E_{tc} and E_{ts} was calculate from LAI.

The model was validated by observed LE under dry canopy conditions derived from eddy covariance techniques and observed rainfall interception. The model was applied to the six-year continuous 10-min meteorological measurements above the canopy. It was examined that seasonal and interannual variations in EI, E_{tc}, E_{ts} and ET for six-year. The estimates were compared with those observed in previous studies conducted in other tropical seasonal/monsoon forests to provide a global context for ET characterized at this site.

4.2 Material and methods

The details of site descriptions, meteorological measurements, eddy covariance method and monitoring of LAI were shown in chapter 2. In this section, detail of model description and application were explained.

4.2.1 Calculation of aero dynamic resistance

In this chapter, aero dynamic resistance (R_{aest}) was estimated by Eq(4.1) using wind speed which was measured by cup-anemometer. A cup-anemometer (AC750, Makino Instruments, Tokyo, Japan) were installed on the tower at 39 m height. Wind speed was calculated using cumulative pulses from the cup-anemometers every 10 min (CR10X, Campbell Scientific).

$$R_{\mathrm{aest}} = \left(\ln\frac{z-d}{z_0}\right)^2 \left(\frac{1}{\kappa^2 U_z}\right) \tag{4.1}$$

Here, z is the reference height (39 m), z_0 is the roughness length (m), d is the zero plane displacement (m), κ is the von Karman's constant (= 0.41) and U_z is the wind speed at z (m s^{-1}). According to Matsumoto et al. (2008), the value of d and z_0 were calculated to minimize the root mean square error (RMSE) between the observed aero dynamic resistance ($R_{\mathrm{aobs}} = 1/G_a$; Eq. 3.2) and R_{aest} under near-neutral conditions, $|z/L| \leq 0.05$.

4.2.2 Jarvis type stomatal conductance model

In this section, model used in this study to simulate the stomatal conductance at the leaf scale is described. In this study, the effect of phonological and physiological changes (maturing and aging of leaves) was ignored because m/g_{sref} which was considered as an index of phonological and physiological changes was rather stable throughout a year (section 3.4 in Chapter 3). Therefore, based on an improved version of the model proposed by Jarvis (1976), stomatal conductance can be described as the form of multiplication of each individual function of solar radiation, vapor pressure deficit, soil moisture and air temperature as follow,

$$g_s = g_{\mathrm{smax}} f(R_s) f(\mathrm{VPD}) f(\Theta_{0-60}) f(T_a) \tag{4.2}$$

where g_{smax} is the maximum stomatal conductance (m s^{-1}) and $f(R_s)$, $f(\mathrm{VPD})$ $f(\Theta_{0-60})$, and $f(T_a)$ are the functions of the solar radiation (R_s, W m^{-2}), vapour pressure deficit (VPD, kPa), air temperature (T_a, ˚C) and soil water content (Θ_{0-60}, m^3 m^{-3}), respectively. $f(R_s)$ represents the relationship between R_s and g_s. Since the stomatal opening induced by light is related to photosynthesis. Fractional equation which often used for the simple light-photosynthesis curve is used as follow,

$$f(R_s) = \frac{R_s(Q_{\max}+k_1)}{Q_{\max}(R_s+k_1)} \tag{4.3}$$

$f(\mathrm{VPD})$ represents the relationship between VPD and g_s. Several have been used in the past including: $e^{-p\,\mathrm{VPD}}$ (Martin et al. 1997), p / VPD, and $p\,\mathrm{VPD}^{-1/2}$ (Lloyd 1991), $1 - p_1\,\mathrm{VPD} + p_2\,\mathrm{VPD}^2$ (Shuttleworth 1989), $(1 + p\,\mathrm{VPD})^{-1}$ (Granier and Loustau 1994; Loustau et al. 1996), where p, p_1 and p_2 were empirical parameters. In this study according to Lohammar et al. (1980), the relationship between VPD and g_s was express as follow because the author had already examined the fitness of this function to calculate g_{sref} and m in chapter 3.

$$f(\mathrm{VPD}) = 1 - m \ln(\mathrm{VPD}) \tag{4.4}$$

$f(\Theta_{0-60})$ represents the relationship between Θ_{0-60} and g_s. The function which was modified from Oren and Pataki (2001) was express as follow,

$$f(\Theta_{0-60}) = 1 + k_2 \ln(\Theta_{0-60}) \tag{4.5}$$

$f(T_a)$ represents the relationship between T_a and g_s. Though the function derived by Sharpe and De Michele (1977) to represent the thermodynamic reaction controlled by enzymes seems more suitable to represent this relationship, the procedure of parameter optimization is more difficult with function. Thus the function proposed by Jarvis (1976) was used.

$$f(T_a) = \left(\frac{T - T_{\min}}{T_{\mathrm{opt}} - T_{\min}}\right)\left(\frac{T_{\max} - T}{T_{\max} - T_{\mathrm{opt}}}\right)^{\left[(T_{\max} - T_{\mathrm{opt}})/(T_{\mathrm{opt}} - T_{\min})\right]} \tag{4.6}$$

Among the parameters in Eq (4.3 - 6), g_{smax}, $Q_{\max}$, k_1, m, k_2, T_{opt}, $T_{\max}$ and $T_{\min}$ were the fitting parameters.

4.2.3 Selection of optimum stomatal conductance model

In this study, the parameters value were calculated to minimize the root mean square error (RMSE) between the observed and predicted values of g_s under the constraint that the function line did not fit to a lower position than the upper boundary of the scatter of observed g_s values. Nelder-Mead method in statistical software R was used as a nonlinear least-squares technique for the parameter fitting.

In order to choose optimum model and paramours, it was tested that comparison between observed g_s and simulated g_s using the model at L1, L2, L3 and L4. In each model levels,

RSME and R^2 were compered.

$$\text{L1}: g_s = g_{smax} f(R_s) \quad (4.7)$$

$$\text{L2}: g_s = g_{smax} f(R_s) f(\text{VPD}) \quad (4.8)$$

$$\text{L3}: g_s = g_{smax} f(R_s) f(\text{VPD}) f(\Theta_{0-60}) \quad (4.9)$$

$$\text{L4}: g_s = g_{smax} f(R_s) f(\text{VPD}) f(\Theta_{0-60}) f(T_a) \quad (4.10)$$

L1 was assumed stomatal opening was mainly controlled by the photosynthesis. L2 was used in tropical rainforest where soil moisture was constant throughout a year (Kume et al., 2011). L3 was assumed the condition that soil moisture had a seasonal variation but temperature was constant throughout a year. And L4 was one of the most common types of Jarvis-type conductance model (e.g. Matsumoto et al. 2008).

4.2.4 Description of Big-leaf model and its application

The big-leaf model used in this study was formulated based on the Penman–Monteith equation (e.g., Monteith and Unsworth, 1990). Interception from canopy (E_i) and from trunks (E_{it}) was calculated using simplified Rutter's model (Rutter et al., 1975) was used.

The canopy and trunks were assumed to have canopy water storage capacity (S_c) and trunks water storage capacity (S_t), and current canopy water storage (s_c) and trunk water storage (s_t) were charged by rainfall (P) and discharged by rainfall interception (E_i), throughfall (T_f), and stemflow (S_f). Canopy water balance was calculated as follows:

$$\frac{ds_c}{dt} = \int [(1 - p_t)P - E_i - T_f] dt \quad (4.11)$$

$$\frac{ds_t}{dt} = \int (p_t P - E_i - S_f) dt \quad (4.12)$$

Here, p_t was stemflow partitioning coefficient in Rutter's original model. T_f and S_f, calculated as over-flow from the canopy water storage capacity, were neglected because it was conceivable that model calculation interval in this model was 10min and shorter than other interception model study (Rutter et al., 1975; Gash and Morton, 1978; Kume et al., 2011). The value of p_t and St were set on 0.035 and 0.15mm, respectively (Tanaka, private

communication). The examination of model parameter p_t and s_t were discussed in section 4.4.3 (in this chapter).

Evaporation from wet surface (E_p, mm), transpiration from dry canopy (E_{pt}, mm) and soil evaporation (E_{ps}, mm) were defined as follows:

$$E_p = \frac{\Delta(R_n - G) + \rho c_p \mathrm{VPD}/R_a}{(\Delta+\gamma)\lambda} \quad (4.13)$$

$$E_{pt} = \frac{\Delta(R_n - G)[1-\exp(-c_A \mathrm{LAI})] + \rho c_p \mathrm{VPD}/R_a}{\Delta+\gamma(1+R_c/R_a)} \quad (4.14)$$

$$E_{ps} = 1.26\frac{\Delta(R_n - G)\exp(-c_A \mathrm{LAI})}{(\Delta+\gamma)}[1 + d\log(\Theta_{0-60})] \quad (4.15)$$

where, Δ was the slope of the saturation vapor pressure function (hPa K^{-1}), R_n was net radiation (W m^{-2}), c_A (= 0.8) was model parameter constant (detail in section 3.2.1, Chapter 3). LAI was leafarea index (m^2 m^{-2}). G is soil heat flux (W m^{-2}), ρ is air density (kg m^{-3}), c_p is the specific heat of air (J kg^{-1} K^{-1}), VPD is the vapor pressure deficit of air (hPa), R_a is the aerodynamic resistance for heat and water from vegetation (s m^{-1}), γ is the psychomotor constant (hPa K^{-1}), and λ is the latent heat of water vaporization (J g^{-1}) and R_c (= $1/G_c$ = $1/(g_s \mathrm{LAI})$) is the canopy resistance (s m^{-1}) calculated from stomatal conductance model (detail in section 4.2.2 in Chapter 3).

In this study, S_c was defined as function of LAI. S_c was calculated as follow:

$$S_c = S_{cmax}\mathrm{LAI} \quad (4.16)$$

Model parameter S_{cmax} was examined. S_{cmax} was calculated as to minimize the residual between observed interception and estimated interception.

The big-leaf was calculated in four dry and wet canopy condition as follow:

When, $S_c = s_c$ and $S_t = s_t$ then both expressed as millimeters of water, evaporation from the wet canopy (E_i) and wet trunk (E_{it}) were calculated from simplified Rutter's model (Rutter et al., 1975) as follows:

$$E_i = (1 - p_t)E_p \quad (4.17)$$

$$E_{it} = p_t E_p \quad (4.18)$$

$$E_{ts} = 0 \quad (4.19)$$

$$E_{tc} = 0 \quad (4.20)$$

Then, dry canopy transpiration (E_{tc}) and soil evaporation (E_{ts}) were set 0 because, all available energy was used for evaporation.

When the canopy and trunks were partially dry ($0 < s_c < S_c$) and ($0 < s_t < S_t$), E_i, E_{it}, E_{tc} and E_{ts} were calculated as follows:

$$E_i = (1 - p_t)E_p\,(s_c + s_t)/(S_c + S_t) \quad (4.21)$$

$$E_{it} = p_t E_p\,(s_c + s_t)/(S_c + S_t) \quad (4.22)$$

$$E_{ts} = E_{pt}[1 - (s_c + s_t)/(S_c + S_t)] \quad (4.23)$$

$$E_{tc} = E_{ps}[1 - (s_c + s_t)/(S_c + S_t)] \quad (4.24)$$

When the trunk was partially dry ($S_c = 0$) and ($0 < s_t < S_t$), E_i, E_{it}, E_{tc} and E_{ts} were calculated as follows:

$$E_i = 0 \quad (4.25)$$

$$E_{it} = E_p\,s_t/S_t \quad (4.26)$$

$$E_{ts} = E_{pt}(1 - s_t/S_t) \quad (4.27)$$

$$E_{tc} = E_{ps}(1 - s_t/S_t) \quad (4.28)$$

When the dry canopy and trunk condition ($S_c = 0$) and ($S_t = 0$), E_i, E_{it}, E_{tc} and E_{ts} were calculated as follows:

$$E_i = 0 \quad (4.29)$$

$$E_{it} = 0 \quad (4.30)$$

$$E_{ts} = E_{pt} \quad (4.31)$$

$$E_{tc} = E_{ps} \quad (4.32)$$

Finally, total evaporation (ET) was expressed as follows:

$$ET = E_i + E_{it} + E_{tc} + E_{ts} \quad (4.33)$$

4.3 Results

4.3.1 Calculation of aerodynamic resistance

To calculate aerodynamic resistance the values of roughness length (d) and zero plane

displacement (z_0) were estimated from the friction velocity, which was determined using the sonic anemometer under near-neutral condition, $|z/L| < 0.05$. Fig. 4.1 shows relationship between observed R_a and estimated R_a, R_a was aero dynamic resistance (s^{-1} m). d and z_0 that were calculated using all data were 20.73 and 1.93, respectively. To know the effect of LAI to d and z_0, in this study d and z_0 were calculated range from $0 < LAI \leq 1$, $1 < LAI \leq 2$, $2 < LAI \leq 3$ and $LAI > 3$, respectively. As shown in Table 4.1, the effect of LAI to change d and z_0 is not clear. In this study, d and z_0 set at 20.71 m and 1.93 m in every LAI levels, respectively.

4.3.2 Evaluation of stomatal conductance model

The parameter values to minimize the root mean square error (RMSE) between the observed and predicted values of g_s under the constraint that the function line did not fit to a lower position than the upper boundary of the scatter of observed g_s values. In this study, the agreements of four levels models (L1, L2, L3 and L4) were examined. Fig. 4.2 and Table. 4.2 showed the relationship between g_s and environmental variables with fitted function lines and the fitted parameter values, respectively. The optimum parameter sets and R^2 and RSME in Table 4.2. In L1 that is function of R_s, RSME and R^2 were 0.00321 and 0.072, respectively. In L2 that is function of R_s and VPD, RSME and R^2 were 0.00263, 0.381, respectively. In L3 that is function of R_s, VPD and Θ_{0-60}, RSME and R^2 were 0.00143, 0.834, respectively. In L4 that is function of R_s, VPD and Θ_{0-60} and T_a, RSME and R^2 were 0.00149 and 0.816, respectively. The agreement of L4 was better than L1 and L2 but it was worse than L3. The L3 model showed the best agreement among L1 to L4. To avoid the over fitting problem, L3 that is a function of R_s, VPD and Θ_{0-60} was selected as a best fitting model. The value of gsmax was estimated as 0.014 (m s^{-1}). As shown in Fig. 4.3, the model value of g_s that was calculated by L3 showed a good agreement with observed g_s throughout a observed period. Fig. 4.4 showed the relationship between observed LE and modeled LE that was sum of E_{tc} and E_{ts} during dry canopy condition ($s_c = 0$ and $s_t = 0$). The regression coefficient and correlation coefficient were 1.04 and 0.84, respectively. Modeled valued is a slightly larger than observed value. Fig. 4.5 showed temporal variation of observed LE and modeled LE during dry canopy. Modeled LE represents a good agreement to observed LE throughout the observed periods. The error in specific season and year were not detected.

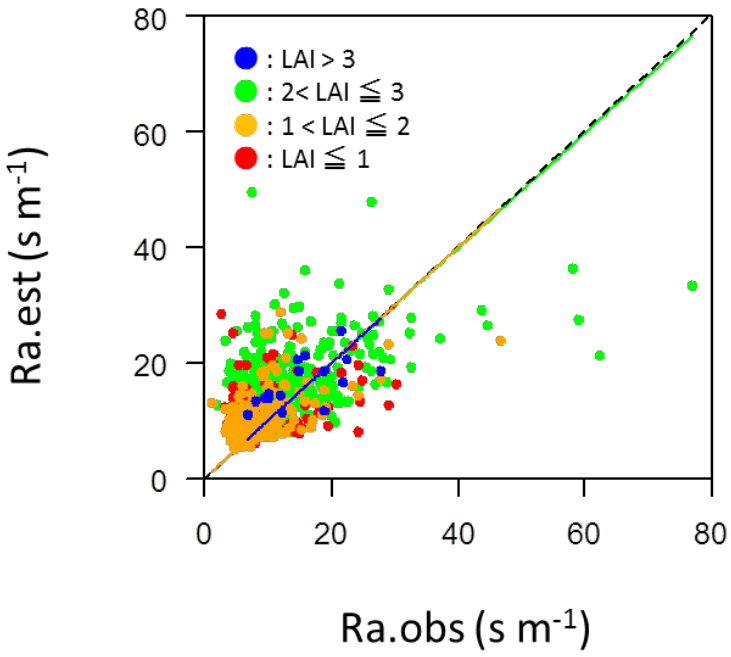

Fig. 4.1 Relationship between observed aerodynamic resistance (Ra.obs) and estimated aerodynamic resistance (Ra.est). Blue , green and red dots represent LAI > 3, 2 < LAI ≦ 3 and LAI < 1, respectively.

Table. 4.1 List of zero-plane displacement (d) and roughness length (z0) in each (LAI) levels.

	d	z0
LAI <1	20.87	1.85
1≦LAI 2	20.85	2.31
2≦LAI 3	19.66	1.98
LAI>3	20.64	2.02
ALL	20.73	1.93

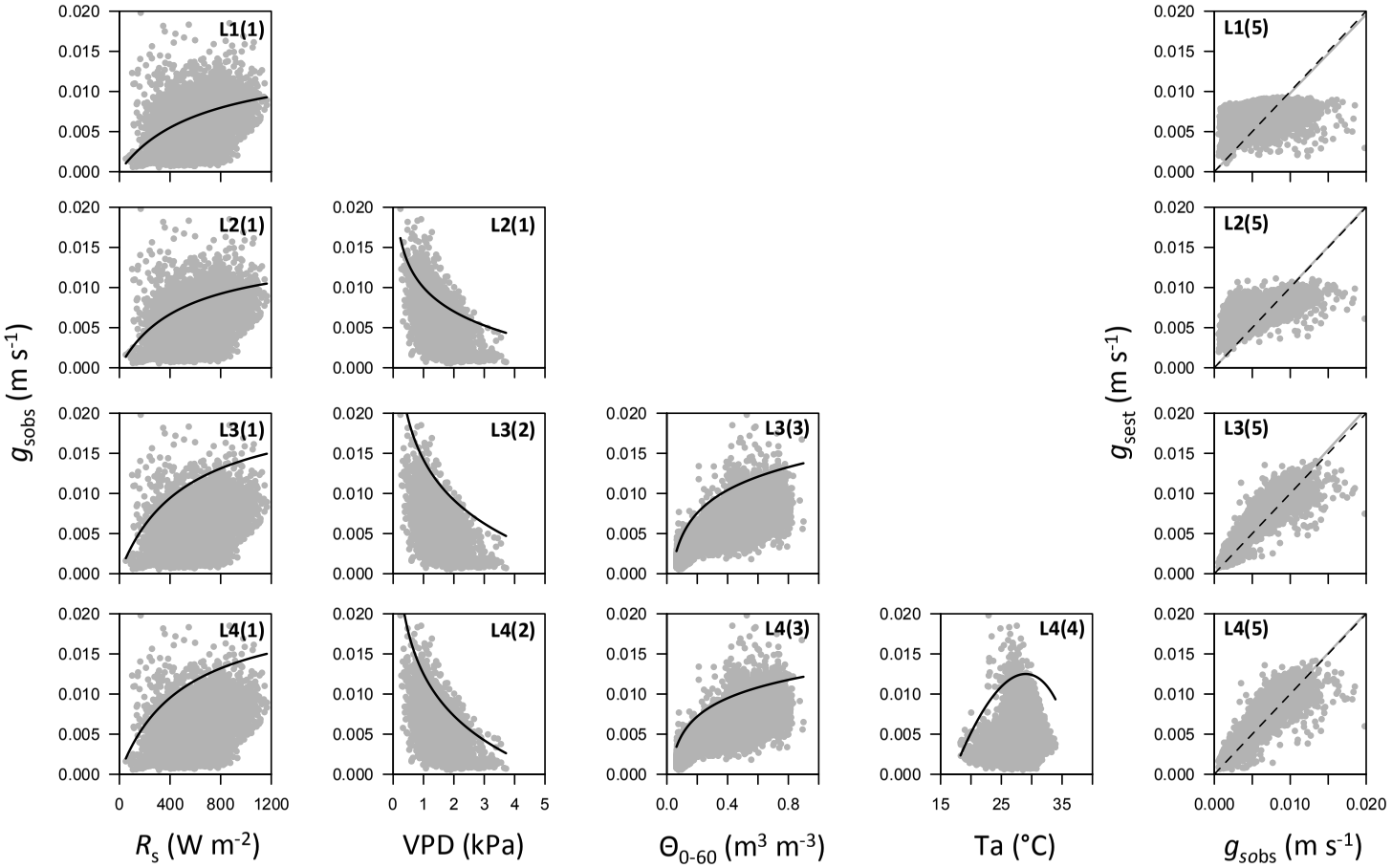

Fig. 4.2 Relationship between stomatal conductance (g_s, ms^{-1}) and environmental variables, and the model fitting function. R_s is the solar radiation (W m^{-2}), VPD is the vapor pressure deficit (kPa), $\Theta_{0\text{-}60}$ is the soil moisture content (m^3 m^{-3}), T_a is the air temperature(°C).

4.3.3 Estimation of canopy water storage capacity

Based on the throughfall and stemflow measurements, interception has been measured from 2001 at this site. However, due to the data quality and missing data, data that can be used for the analysis of interception was restricted. According to Tanaka (private communication), annual rainfall interception during 2006 (period from January to December) was 106.2 mm. Optimum S_{cmax} in Eq. 4.16 was calculated to minimize the residual between observed interception (= 106.2 mm) and modeled interception. Fig. 4.5 showed the relationship between S_{cmax} and annual interception in 2006. Modeled EI was increasing with increases of S_{cmax}. Optimum S_{cmax} that was to minimize the residual between observed interception (= 106.2) and modeled interception (EI) was estimated 0.26 mm (Table 4.3).

4.3.4 Evapotranspiration estimates

Annual component of evapotranspiration (ET) that was transpiration from canopy (E_{tc}), soil evaporation (E_{ts}), interception from canopy (E_{i}) and interception from trunks (E_{it}) were estimated using big-leaf model. The estimated values showed in Table 4.4. As shown in Fig. 4.7, clear seasonal change of ET was observed. E_{tc} was calculated as very low and/or zero following the seasonal change of LAI. On the other hands, E_{ts} was more prominent in dry (leaf-less) season. The averaged E_{ts} in dry season was approximately ~ 1 mm day^{-1} although it exceeded over 2 ~ 3 mm day^{-1} in after rainfall event in dry season (e.g., dry season from 2009 to 2010).

The relationship between annual rainfall (P_G) and interception components was shown in Fig. 4.6. The annual value of EI, E_{i} and E_{it} increased with increasing annual rainfall and the mean interception rates of EI, E_{i} and E_{it} to rainfall were 7.5 %, 6.2 % and 1.3 %, respectively. The relationship between P_{G} and ET was shown in Fig. 4.7. Annual ET has a linear relationship to rainfall in 4 years (2007, 2008, 2009, 2010) which annual rainfall less than 1500 mm, and this relationship was in not clear in 2 years (2006, 2011) which annual rainfall over than 1500 mm. But, in roughly, annual ET was increasing with increases of rainfall. The mean ratio ET to P_{G} was 81.6 % with range from 64.2 % to 92.7%.

4.4 Discussion

4.4.1 Validation of aerodynamic resistance

In this study, d and z_0 were set in 20.71 m and 1.93 m throughout the every LAI levels.

Table. 4.2 Optimized parameter values, RSME and R^2 in the model at each level

Model	g_{smax}	Q_{max}	k_1	m	k_2	T_{opt}	T_{max}	T_{min}	RMSE	R^2
$g_s = g_{smax} f(R_s)$	0.009	1209.1	656.9	-	-	-	-	-	0.00321	0.072
$g_s = g_{smax} f(R_s)\, f(\mathrm{VPD})$	0.010	1026.3	447.5	0.43	-	-	-	-	0.00263	0.381
$g_s = g_{smax} f(R_s)\, f(\mathrm{VPD}) f(\Theta_{0\text{-}60})$	0.014	993.2	514.0	0.51	0.29	-	-	-	0.00143	0.834
$g_s = g_{smax} f(R_s)\, f(\mathrm{VPD}) f(\Theta_{0\text{-}60}) f(T_a)$	0.013	699.6	501.1	0.50	0.27	29	37	17	0.00149	0.816

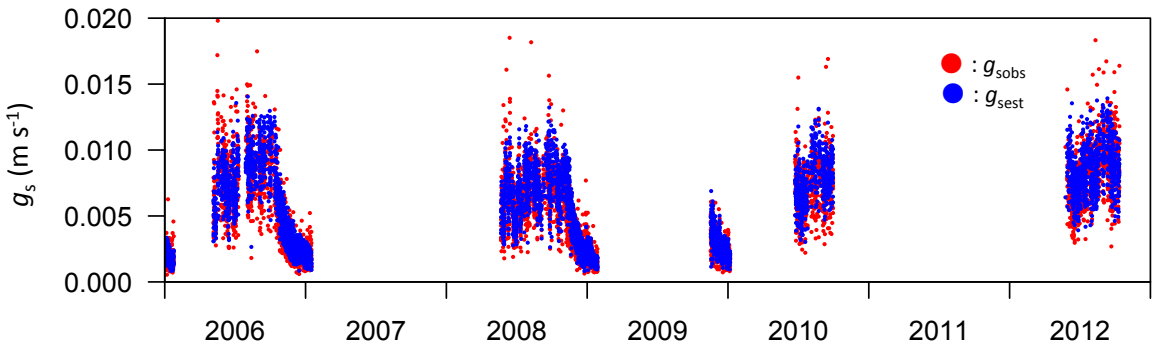

Fig. 4.3 Temporal variation of observed stomatal conductance (g_{sobs}, m s^{-1}) and modeled stomatal conductance (g_{sest}, m s^{-1}). Red and blue dots represent g_{sobs} and g_{sest}, respectively.

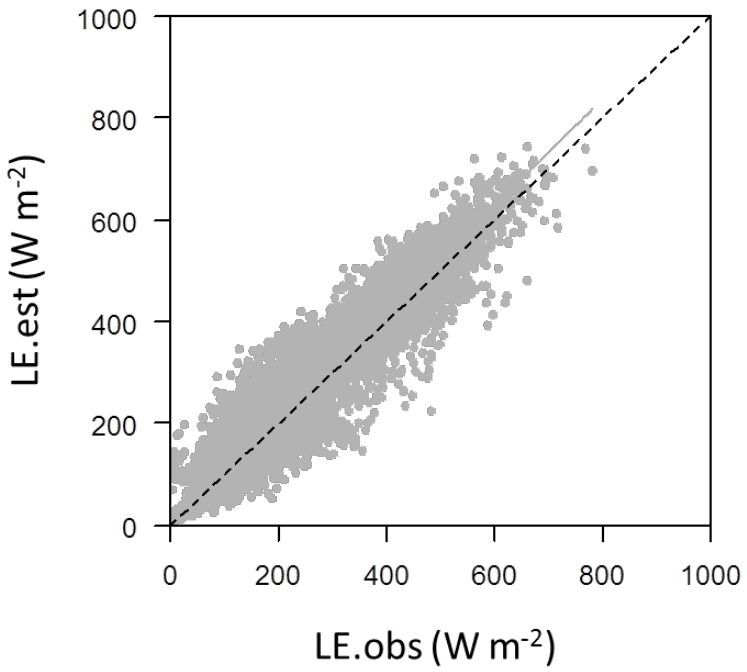

Fig. 4.4 Relationship between observed latent heat flux from dry canopy (LE.obs, W m^{-2}) and sum of modeled transpiration from canopy and evaporation from soil surface and understory vegetation (LE.est, W m^{-2}). Regression coefficient was 1.04. Correlation coefficient (R^2) was 0.86.

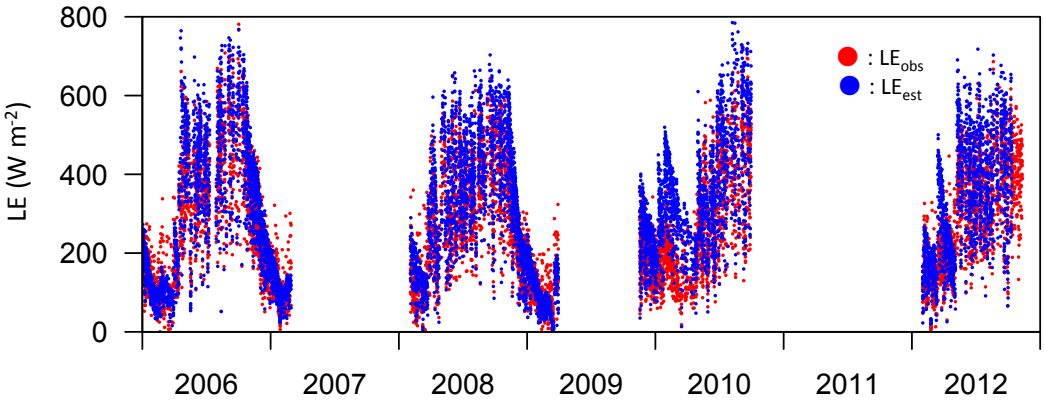

Fig. 4.5 Temporal variation of observed latent heat flux from dry canopy (LE_{obs}, m s^{-1}) and sum of modeled transpiration from canopy and evaporation from soil surface and understory vegetation (LE_{est}, W m^{-2}). Red and blue dots represent LE_{obs} and LE_{est}, respectively.

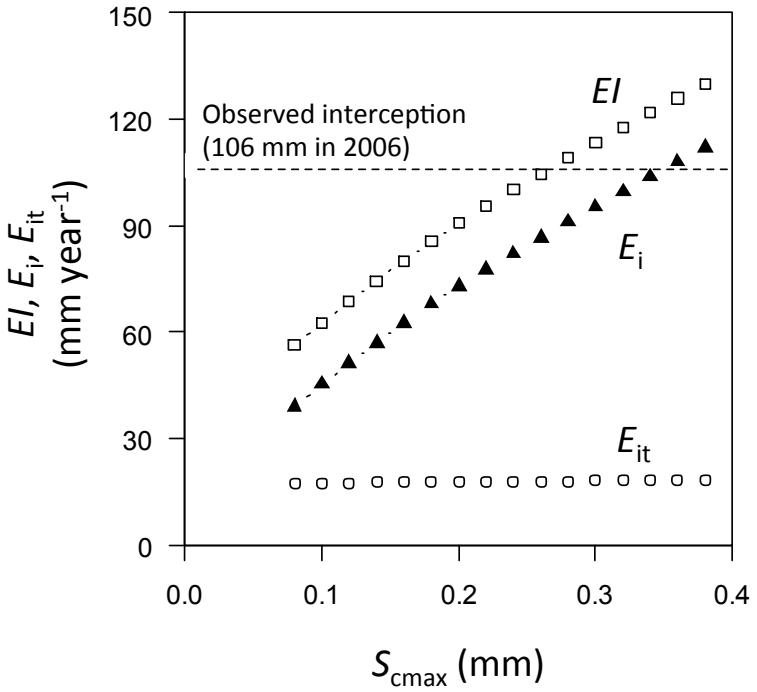

Fig. 4.6 Relationship between maximum canopy water storage capacity (S_{cmax}, mm LAI^{-1}) and evaporation components in 2006. E_i is the evaporation from canopy (solid triangle). E_{it} is the evaporation from trunks (open circle). *EI* is the sum of E_i and E_{it} (open square). Doted line represents the observed interception value in 2006 (102.3 mm).

Table. 4.3 Relationship between Rutter model parameter S_{cmax} and interception from trunks (E_{it}), interception from canopy (E_i) and total interception ($EI = E_{it} + E_i$) in 2006.

S_{cmax} (mm)	0.08	0.10	0.12	0.14	0.16	0.18	0.20	0.22	0.24	0.26	0.28	0.30	0.32	0.34	0.36	0.38
E_{it} (mm)	17.9	17.9	17.9	17.9	17.9	17.9	17.9	17.9	17.9	**17.9**	17.9	17.9	17.9	17.9	17.9	17.9
E_i (mm)	38.9	45.2	51.2	56.9	62.5	67.9	72.9	77.6	82.1	**86.6**	91.0	95.4	99.6	103.8	107.9	111.9
EI (mm)	56.8	63.1	69.0	74.8	80.3	85.7	90.8	95.5	100.0	**104.5**	108.9	113.2	117.5	121.7	125.8	129.8

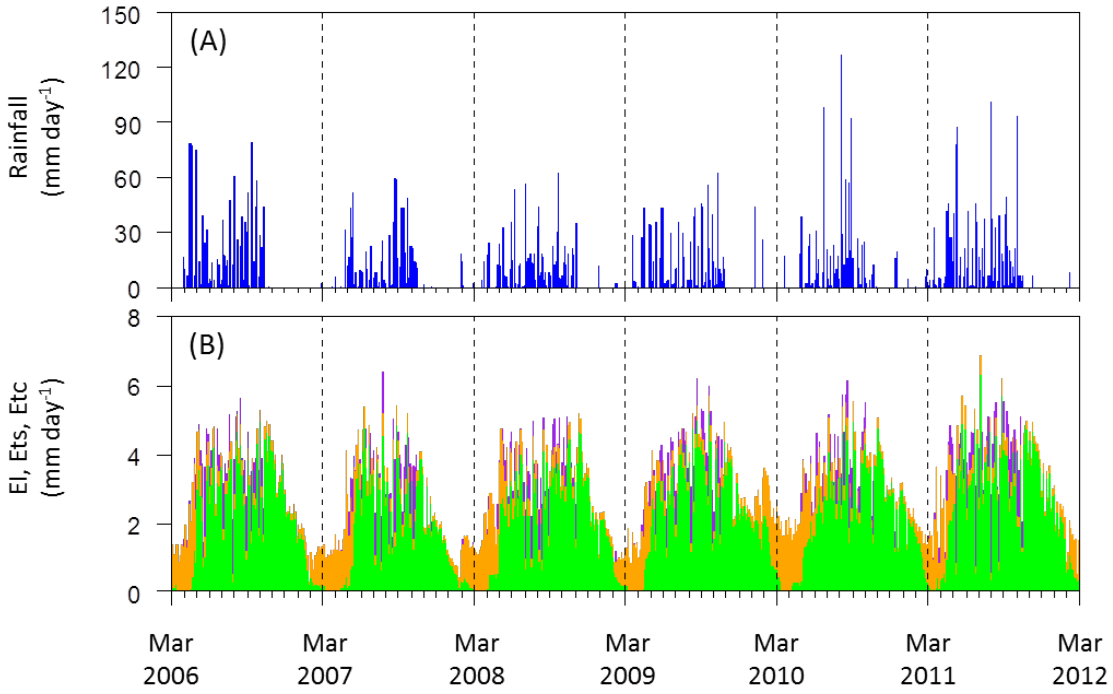

Fig.4.7 Temporal variation of rainfall (P_G) (A) and interception (EI), evapotranspiration form soil and understory vegetation (Ets) and transpiration from canopy (Etc) (B). Purple, orange and green bar in (B) represent EI, Ets and Etc, respectively.

Table. 4.4 Water table at a teak plantation in Northern Thailand during six-year period from March 2006 to February 2012.

Period	2006-2007	2007-2008	2008-2009	2009-2010	2010-2011	2011-2012	Average	S.D.	CV (%)
P_G (mm)	1720.4	1130	1204.7	1306.5	1278.9	1852.4	1415.5	296.8	21.0
ET (mm)	1104.4	1017.6	1102.7	1211.5	1170.1	1321.3	1154.6	105.1	9.1
E_{tc} (mm)	773.7	675.9	738.2	850.6	782.2	932.4	792.1	89.4	11.3
E_{ts} (mm)	230.7	252.8	256	262.4	289.7	247.8	256.6	19.5	7.6
EI (mm)	100.0	88.9	108.5	98.5	98.2	141.1	105.9	18.4	17.3
E_i (mm)	82.1	72.8	88.9	82.1	81.4	117.2	87.4	15.5	17.7
E_{it} (mm)	17.9	16.0	19.6	16.4	16.9	23.9	18.5	3.0	16.0
Growing season length (day)	297	285	315	318	312	333	310	16.8	5.4

* P_G and ET represents annual rainfall and evapotranspiration, respectively. E_{tc}, E_{ts} and *EI* represents canopy transpiration, soil evaporation and interception, respectively. E_i and E_{it} represents canopy interception and trunks interception, respectively. GSL represents growing season length.

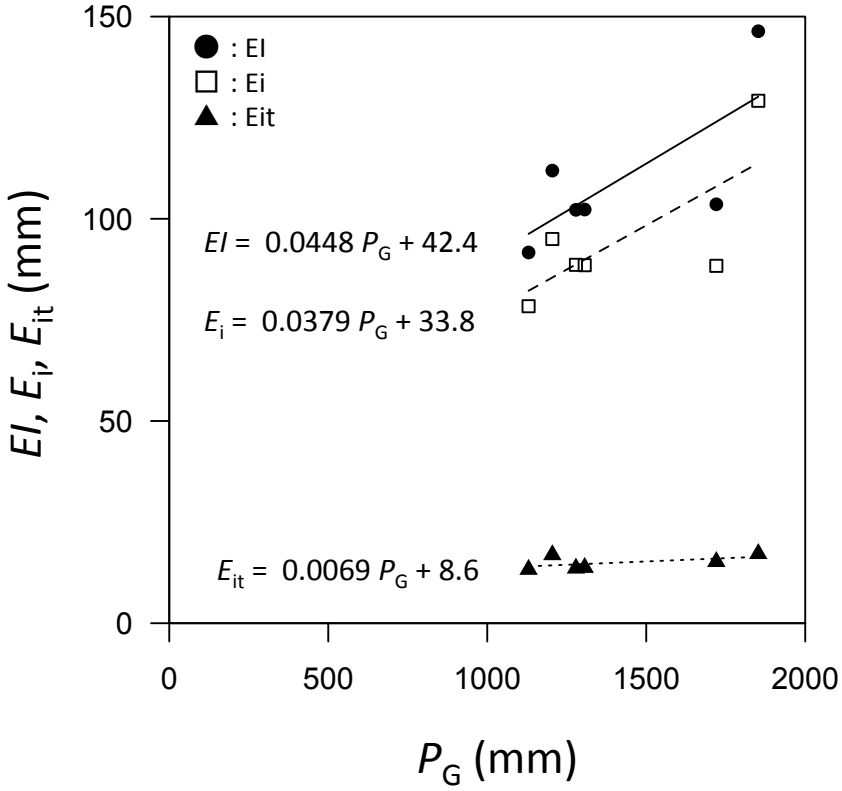

Fig. 4.8 Relationship between annual rainfall (P_G) and interception (EI), interception from canopy (E_i) and interception from trunks (E_{it}). Solid circle, open square and solid triangle represent EI, E_i and E_{it} respectively.

Sato et al. (2009) examined the effect of LAI changed to d and z_0. They calculated d and z_0 using a wind profile data that measured by cup-anemometers in neutral condition. They were not able to detect the clear different of d and z_0 between leaf-less and leafy (canopy-closed) season. A calculation method of d and z_0 in this study was different from Sato et al. (2009) although the result was same. Schmid et al. (2000) also reported indistinct seasonality of d and z_0 in temperate deciduous forest in US. They proposed the possibility that thickness of roughness sub-layer for constant d and z_0 although they did not mention about crucial influence for indistinct seasonality of d and z_0. According to Hattori (1985), d/h and z_0/h range from 0.61 to 0.92 and from 0.02 to 0.14, respectively. Using Hattori's function, d and z_0 in this site range from 13.42 m to 20.24 m and from 0.44 m to 3.08 m (h = 22 m in this site), respectively. The value of d and z_0 in this study that ranged in Hattori's value justified estimated d and z_0 in this study although the exact effect of LAI to d and z0 awaits future studies.

4.4.2 Stomatal conductance model and dry canopy transpiration

In this thesis, Jarvis-type conductance model was used for estimated stomatal conductance. The modeling of stomatal conductance was conducted using micro meteorological variables because daily and seasonal changes of stomatal conductance mainly depended on the solar radiation and vapor pressure deficit and seasonality of soil moisture condition. The agreements of L3 and L4 that considered the regulation of soil water content have been greatly improved rather than L1 and L2 that no regulation of soil water content. According to Kume et al. (2011), Jarvis-type surface conductance model that was just regulated by the solar radiation and vapor pressure defect showed good agreement with observed surface conductance in tropical rainforest in Borneo, Malaysia. As compared with Kume et al al. (2011), the effect of controlling stomatal conductance by the soil moisture condition in tropical monsoon forest was more important than that of tropical rainforest. On the other hands, results of L4 that is a function of solar radiation, vapor pressure deficit, soil moisture condition and temperature showed that the possibility of over-fitting. It was well known that stomatal conductance is sensitive to variations in environmental parameters especially temperature in temperate and boreal forest (e.g., Neilson and Jarvis, 1975; Stewart, 1988; Matsumoto et al., 2008). Kosugi (1995) showed that the effect temperature regulation in Jarvis-type conductance greatly improved the predicted value in temperate forest in Japan. However, the effect of temperature regulation (L4) was considered as over-fitting rather than improvement predicts value in the high temperature environment through the year under the tropical climate condition, like in this study site.

As shown in Table 4.2, the value of g_s was estimated at 0.014 m s^{-1}. The value of gsmax

was approximately convertible to G_s max using Eq. 3.12. In this study, G_{smax} was approximately 0.042 m s^{-1} with range from 0.039 m s^{-1} to 0.045 m s^{-1}. Kelliher et al. (1995) reported that G_{smax} was range from 0.005 m s^{-1} to 0.033 m s^{-1} using data measured in temperate, boreal and tropical forest, respectively. Matsumoto et al. (2008) also reported that G_{smax} was range from 0.016 m s^{-1} to 0.037 m s^{-1} within temperate and boreal forest. Compere to these previous studies, the value of G_{smax} in this site was characterized as large G_{smax} relative to other forest type.

4.4.3 Estimation of interception

The value of total interception (EI), canopy interception (E_i) and trunks interception (E_{it}) were 7.5 %, 6.2 % and 1.3 % of annual rainfall, respectively. First, E_i that was determined by S_{cmax} was examined because E_i occupied the large portion of EI. Acording to Herwitz (1985), Scmax is approximately 0.1 mm LAI^{-1} in tropical broadleaf species. Aston (1979) reported the average value of S_{cmax} was 0.1 mm LAI^{-1} with range from 0.02 mm LAI^{-1} to 0.15 mm LAI^{-1} among small trees of six eucalypt species in Australia. Pitman (1989) and Kondo et al. (1992) reported that S_{cmax} = 0.15 mm LAI^{-1} for broadleaved forest and 0.2 mm LAI^{-1} for coniferous forest stands, respectively. Deguchi et al. (2006) concluded that S_{cmax} = ~ 0.3 mm LAI^{-1} in their deciduous forest study stands in Japan. Carlyle-Moses and Price (2007) found S_{cmax} = 0.5 mm LAI^{-1} in Pine - Oak forest in north-eastern Mexico. Many previous studies reported about S_{cmax}. Compered to these studies, S_{cmax} in this site (= 0.26 mm LAI^{-1}) was very close to the results at deciduous forest in Japan. It was considered that S_{cmax} has large site dependence due to a stand age and structure, and S_{cmax} in this study was suitable because S_{cmax} in this study was validated by a precise filed observation data. The parameter p_t that decide a proportion of rainfall to stems and trunks, and S_t that the trunk storage capacity, were often derived from regression of measured stemflow against gross rainfall (e.g. Gash, 1979; Bruijnzeel and Wiersum, 1987). In this study, p_t and S_t were estimated based on stemflow and gross rainfall measurements conducted by Tanaka (private communication). There were some studies of examining p_t and S_t based on the stemflow measurements. For example, p_t and S_t were 0.015 and 0.03 mm (Pine, New Zeeland, Perce and Rowe, 1981), 0.016 and 0.014 mm (Scots Pine, UK, Gash, 1979),0.04 and 0.125 mm (Oak, UK, Thompson, 1972), 0.036 and 0.15 mm (undisturbed Amazonian rainforest, Lloyd et al., 1988) and 0.026 and 0.185 mm (Tropical spaces, Kenya, Jackson, 2000), respectively. Compare to above studies, p_t and S_t in this study were close to the result in undisturbed Amazonian rainforest. However, as Zhang et al. (2006) had already pointed p_t and S_t were fairly insensitive parameters because p_t was quite small.

If the Rutter model parameters were suitable, interception (7.5 %) in this study was

smaller than other study site. For example, interception rate in temperate Japanese forest sites was range from 18 % to 24 % (Suzuki, 1980; Toba and Ohta, 2005). Mulder et al (1985) also reported that interception rate in Dutch was range from 20 % to 50 %. Scatena (1990) reported that intercepting rate was over 50 % in tropical rainforest in Puerto Rico. Kuraji and Tanaka (2003) summarized that interception rate was range from 10 % to 20 %, with annual rainfall 200 - 3500 mm whether for climate and forest types. Compared to these studies, interception rate in this site was relatively small. It can be considered that intensity of rainfall, number of rainfall events and stand structure as a reason of small interception in this study. About intensity of rainfall, in general, interception rate is getting smaller with increasing of rainfall intensity. Manfroi et al. (2006) showed that intercepting rate was over 70 % in single storm rainfall under 5 mm but interception rate was under 10 % in single storm rainfall over 20 mm in Borneo. As shown in Chapter 2, heavy rainfall event (over 20 mm) in this site occupied 54.2 - 79.7 % every year, and number of rainfall events was less than that of tropical rainforest in Borneo and Puerto Rico. Therefore, it considered that heavy rainfall and less rainfall events made small interception at this site. Further, Manfroi et al. (2006) also showed that the relationship between basal area and interception at tropical rainforest in Borneo. They showed that decreasing of basal area from 145 to 42 m^2 ha^{-1} decreased interception rate from 25 to 3.5 %. It was possible that small interception in this site has validity of enough as a real value because basal area in this site was 17.8 m^2 ha^{-1} in November 2005(Tanaka, private communication).

4.4.4 Estimation evapotranspiration

Six-year averaged P_G and ET in this site were 1415.5 mm and 1154.6 mm, respectively. The author compared ET in this site with other 8 tropical seasonal and/or monsoon forests with annual rainfall of 1000 ~ 1500 mm (Table. 4.5). In the typical seasonal and/or monsoon forests, averaged P_G and ET were 1355 mm and 1058 mm, respectively. The value of averaged ET ratio (= ET/P_G) in the region was 0.79, respectively. On the other hands, ET ratio in this site was 0.82. According to Kume et al. (2012), Most ET ratio in the tropical forest that includes both seasonal and/or monsoon forests and various types of rainforest ranged between 0.3 and 0.9. Compare with various tropical forests, the value of evapotranspiration in this site was characterized by a relatively close to annual rainfall. At the evergreen forest in the seasonal and/or monsoon forests, Zhiheng et al. (2010) reported that P_G and ET were 1322mm and 1029 mm in tropical seasonal forest in southeast China. Nobuhiro et al., 2009 also reported that P_G and ET were 1500 mm and 1140 mm tropical seasonal forest in Cambodia. Both forest types were evergreen forest. Compare with those

evergreen forests, ET in this site was relatively larger despite 2- 3 months leaf-less season in this site. For this season, it was considered that relative large g_{smax} (= 0.014 m s^{-1}) in this site made a large transpiration during growing season. The value of canopy scale maximum conductance in this site was approximately 0.042 m s^{-1}. Therefore, it was considered that large stomatal conductance made a large transpiration rate that exceeded over 4 mm day^{-1} during growing season (Fig. 4.7). This transpiration rate was larger than that of tropical rainforest (= 2.9 - 3.5 mm day^{-1}) in Borneo (Kumagai et al., 2004).

Komatsu et al. (2012) proposed that a simple evapotranspiration using potential evaporation (revision and based Zhang's model; Zhang et al., 2001). The ET calculated from Komatsu' model was 1088 ± 87 (S.D.) mm and the estimated valued in this study was in the range in error of Komatsu's model. This implies that the estimated valued in this study can be considered to be reasonable values relative to global and regional P_G and climate.

4.4.5 Interannual variability of evapotranspiration

There have been many previous studies examining the sensitivity of ET to temporal variations in P_G (Koster and Suarez, 1999; Yang et al., 2007; Potter and Zhang, 2009), because such examinations are critical for predicting changes in the terrestrial water cycle corresponding to possible changes in precipitation. The sensitivity of ET to P_G relates the sensitivity of annual runoff to temporal variations in P_G, because annual runoff primarily approximates to P_G minus ET (Koster and Suarez, 1999; Arora, 2002). When ET is sensitive to P_G, the change in P_G is mainly reflected in a change in ET, and the annual runoff and/or discharge is therefore insensitive to temporal variations in P_G. When ET is insensitive to P_G, the change in P_G is not reflected in a change in ET, and the annual runoff is therefore sensitive to temporal variations in P_G. The relationship of the sensitivity with ET/P_G shown in Fig. 10 of Komatsu et al. (2012) is expected from the results of several previous studies. Koster and Suarez (1999) and Arora (2002), conducting simulations using climate and/or hydrological models, have already pointed out the relationships of the aridity index (E_0/P_G) with ET/P_G and with the sensitivity of ET to temporal variations in P_G, implying a relationship of the sensitivity with ET/P_G. In case of this study, there is a possibility that ET was influenced by the P_G as well as growing season length (GSL), because interannual variation of GSL in a tropical deciduous forest was larger than that of temperate deciduous forest (Yoshifuji et al., 2011). Therefore, the impact of GSL on ET was evaluated as follow.

First, the author conducted linier regression analysis on the relationship between the value of P_G and ET in this study site and compered to the difference in impact of P_G to ET

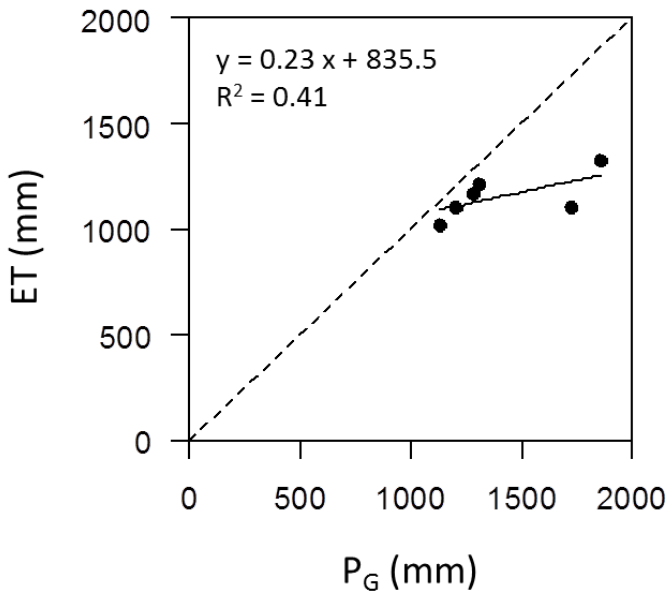

Fig. 4.9 Relationship between rainfall (P_G) and evapotranspiration (ET).

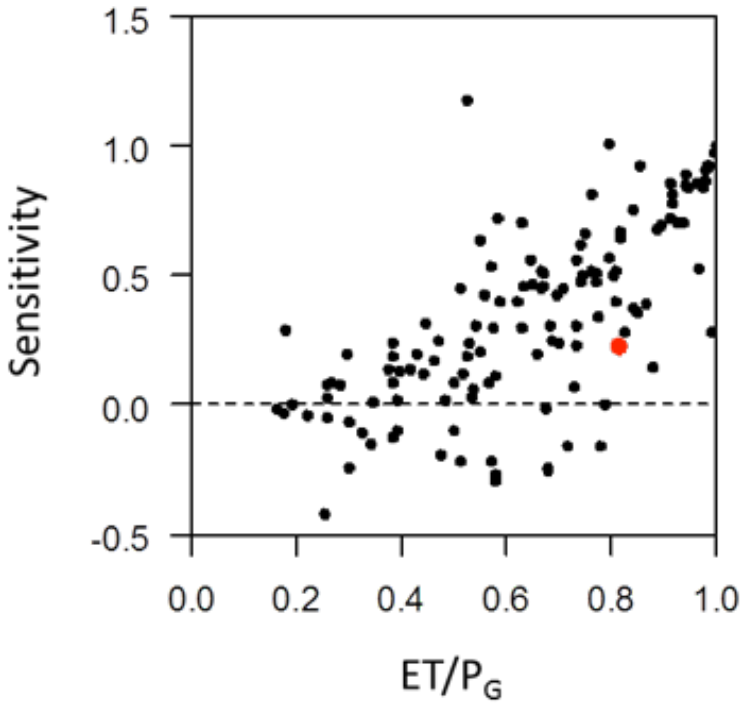

Fig. 4.10 Relationship of the sensitivity of annual evapotranspiration (ET) to annual precipitation (P_G) with ET/ P_G. The red dot shows the results this study site. The black circles indicate observed data. ET/ P_G for the observed data were calculated using the mean ET and P_G values for the measurement period from Komatsu et al. (2012).

among results of other sites. The results of linier regression analysis as follow (Table 4.5),

$$ET = 0.23P_G + 835.52\ (R^2 = 0.41) \quad (4.34)$$

According to Komatsu et al. (2012), the value of regression coefficient (slope) means that the sensitivity of forest ET to temporal variations in P_G. The value of sensitivity increased exponentially with increasing of ET/P_G regardless of magnitude of P_G and difference of vegetation types like evergreen and/or deciduous. And, the value of sensitivity was strongly influence by the P_G when ET/P_G closed to 1 (Fig.10, Komatsu et al. 2012). The value of sensitivity and ET/P_G in this site was 0.23 and 0.82, respectively. On the other hands, the value of sensitivity that was measured by the world (data from Komatsu et al., 2012) was 0.52 ± 0.16 (S.D.) for a same range ($0.80 < ET/P_G < 0.85$). The value of sensitivity in this site was smaller than the world average. This means that the impact of P_G to ET was smaller than other forests where the amount of evapotranspiration will be about 80 % to rainfall. Here, the author tries to reveal how GSL influence on ET, and which factor more influence on interanual variation of ET. It is able to break P_G and GSL into six-years averages (P_{Gave} and GSLave) and six-years deviation (ΔP_G and ΔGSL), respectively, as follow;

$$P_G = P_{Gave} + \Delta P_G \quad (4.35)$$

$$GSL = GSL_{ave} + \Delta GSL \quad (4.36)$$

Fig. 4.11 showed that the response of annual ET to difference from mean of annual P_G (a) and GSL (b), respectively. The x-axis in Fig. 4.11 (a) and (b) residents ΔP_G and ΔGSL in Eq. 4.37 and 4.38, respectively. The relationship between ΔP_G and ET was not clear (Fig. 4.11 a, $R^2 = 0.41$).

This result refracting the Eq. 4.34, and relatively low impact of fluctuation of ΔP_G to ET. On the other hands, the clear relationship between ΔGSL to ET (Fig. 4.11 b, $R^2 = 0.80$) is observed.

This result means that GSL also influences interannual variation of ET. Therefore to know the impact of P_G and GSL to ET, the author conducted multiple regression analysis of ET against P_G and GSL.

$$ET = 0.10P_G + 4.96GSL - 526.06$$
$$= 0.10(P_{Gave} + \Delta P_G) + 4.96(GSL_{ave} + \Delta GSL) - 526.06$$

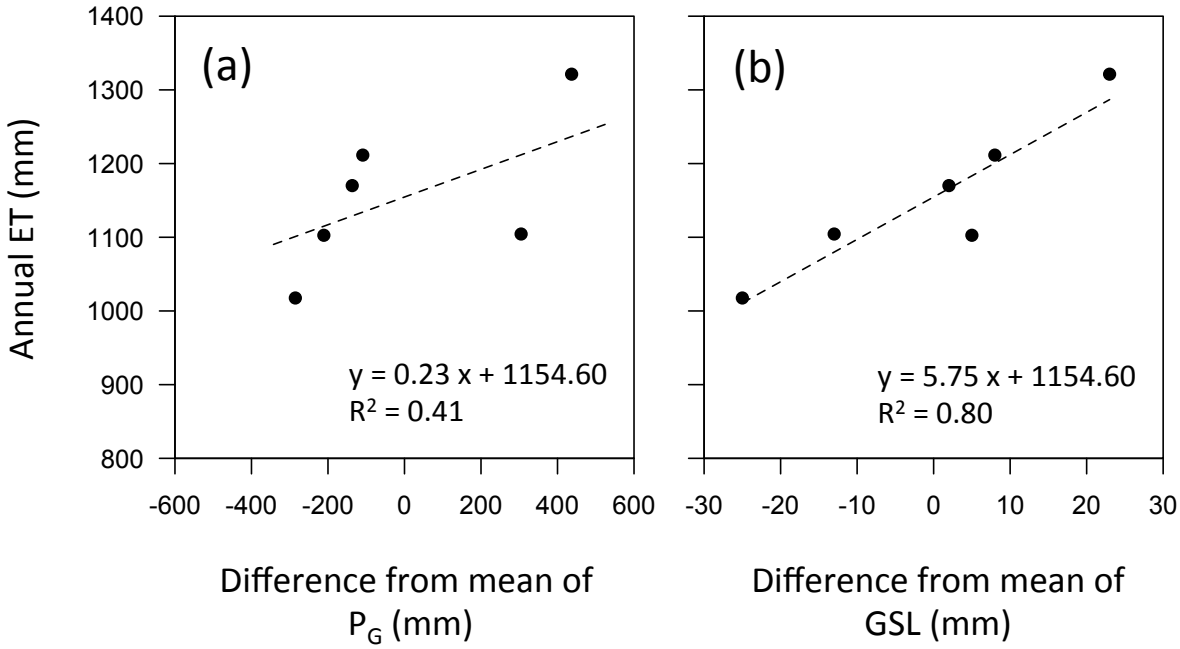

Fig. 4.11 The response of annual evapotranspiration (ET) to difference from mean of annual rainfall (P_G)(a) and difference from mean of annual growing season length (GSL)(b), respectively.

Table. 4.5 List of regression equation and coefficient of determination

Variables	Equation	R^2
P_G	ET = 0.23 ΔP_G + 1154.60	0.41
GSL	ET = 5.75 ΔGSL + 1154.60	0.82
P_G, GSL	ET = 0.10 ΔP_G + 4.96 ΔGSL + 1154.60	0.90

Equation was simplified as follow;

$$ET = 0.10\Delta P_G + 4.96\Delta GSL + 1154.60 \quad (4.37)$$

Consequently, the value of constant term of Eq. 4.37 was six-year averaged evapotranspiration (ET_{ave} = 1154.6 mm). And the results of multiple regression analysis of ET against P_G and GSL can be understood as the value of ET was decided by the sum of fluctuation of ΔP_G, ΔGSL and ET_{ave}.

To detect the quantitative impact of interannual variability of ΔP_G and ΔGSL to ET in this site, α'(mm) and β'(mm) were defined as follow;

$$\alpha' = \alpha\sigma(\Delta P_G) = 30.55 \text{ mm} \quad (4.38)$$

$$\beta' = \beta\sigma(\Delta GSL) = 83.45 \text{ mm} \quad (4.39)$$

α and β in Eq 4.40 and Eq 4.41 were regression coefficient of the multiple regression analysis (Eq. 3.36). $\alpha\sigma(\Delta P_G)$ and $\beta\sigma(\Delta GSL)$ were standard deviation of ΔP_G and ΔGSL, respectively. In other words, α' and β' means that the fluctuation of ΔP_G and ΔGSL to ET when each variables change 1σ. The value of α' and β' that were calculated from Table 4.4 and Table 4.5 were 30.05 mm (Eq. 4.38) and 83.45 mm (Eq. 4.39), respectively. This result showed that impact of fluctuation of ΔGSL to ET was larger than that of ΔP_G in a tropical deciduous forest when each variables change 1σ.

4.5 Conclusion

To evaluate the seasonal and interannual variation evapotranspiration and its elements at a teal plantation in Northern Thailand, this chapter conducted modeling of stomatal conductance and six-year estimation of evapotranspiration based on the big-leaf model that successfully reproduced ET, E_{ts}, E_{tc} and EI at this study site (Fig.4.2, Fig. 4.3 and Fig. 4.5). The values of roughness length (z_0) and zero plane displacement (d) were estimated as 20.73 m and 1.93 m, respectively and the influence of seasonal change of LAI to d and z_0 were not clear. To calculate big-leaf model's canopy conductance, Jarvi-type stomatal conductance model was chosen. The parameter values of Jarvis conductance model to minimize the root mean square error (RMSE) between the observed and predicted values of g_s under the

constraint that the function line did not fit to a lower position than the upper boundary of the scatter of observed gs values. The model function of R_s, VPD and Θ_{0-60} was selected as a best fitting model. The relationship between observed LE and modeled LE that was sum of canopy transpiration and soil evaporation during dry canopy showed good agreement. The accuracy of soil evaporation was already examined in chapter 3. In this study, Rutter type interception model parameter was also examined. Based on the through-fall and stemflow measurements, annual summed interception during 2006 (period from January to December) was 106.2 mm (Tanaka, private communication). Optimum S_{cmax} that canopy storage capacity was calculated as to minimize the residual between observed interception (= 106.2 mm) and modeled interception and optimum S_{cmax} that was to minimize the residual between observed interception and modeled interception was estimated 0.26 mm (Table 4.3). According to Tanaka (private communication), p_t and St were set on 0.036 and 0.15mm, respectively. As a result of big-leaf model calculation, 6-year averaged ET, E_{ts}, E_{tc} and EI were 1154.6 mm, 792.1 mm, 256.6 mm, and 105.9 mm, respectively. The result of interception of this study, EI, canopy interception (E_i) and trunks interception (E_{it}) were 7.5 %, 6.2 % and 1.3 % of annual rainfall, respectively. Compared to previous studies, it was shown that the interception rate in this site was relatively small. It can be considered that heavy rainfall, less rainfall events and small basal area made small interception as a reason of small interception in this study.

In this study site, the value of annual ET was changed with P_G and GSL, respectively. The mean and standard deviation of P_G and GSL in 6-observed years were 1415.5 mm ± 296.8 mm and 310 days ± 16.8 day, respectively. If P_G and GSL change 1σ, respectively, the annual ET changes 30.05 mm and 83.45 mm, respectively from the mean year. Therefore, ET was more influenced by the variance of GSL than that of P_G.

The clear seasonal changed of LAI was observed in this study site. The seasonal changes of LAI influenced energy partitioning between the canopy and the soil surface, and decided the soil evaporation and transpiration. Although, zero plane displacement and the roughness length were little influenced by LAI. The value of Scmax did not change with changing LAI. Consequently, contribution of GSL to evapotranspiration was relatively large than other factors.

References

Almeida, A. C., Soares, J. V., Landsberg, J. J., & Rezende, G. D. (2007). Growth and water balance of Eucalyptus grandis hybrid plantations in Brazil during a rotation for pulp production. *Forest Ecology and Management*, *251*(1-2), 10–21. doi:10.1016/j.foreco.2007.06.009

Aston, A. R. (1979). Rainfall interception by eight small trees. *Journal of Hydrology*, *42*(3-4), 383–396. doi:10.1016/0022-1694(79)90057-X

Aubinet, M., Heinesch, B., Longdoz, B. (2002). Estimation of the carbon sequestration by a heterogeneous forest: night flux corrections, heterogeneity of the site and inter-annual variability. *Global Change Biology*, *8*(11), 1053–1071. doi:10.1046/j.1365-2486.2002.00529.x

Barr, A. G., Black, T. A., Hogg, E. H., Griffis, T. J., Morgenstern, K., KLJUN, N., Theede, A., Nesic. Z. (2007). Climatic controls on the carbon and water balances of a boreal aspen forest. *Global Change Biology*, *13*(3), 561–576. doi:10.1111/j.1365-2486.2006.01220.x

Berbigier, P., Bonnefond, J. M., Loustau, D., Ferreira, M. I., David, J. S., & Pereira, J. S. (1996). Transpiration of a 64-year old maritime pine stand in Portugal. *Oecologia*, *107*(1), 43–52. doi:10.1007/BF00582233

Bruijnzeel, L. A., Sampurno, S. P., & Wiersum, K. F. (1987). Rainfall interception by a youngAcacia auriculiformis (a. cunn) plantation forest in West Java, Indonesia: Application of Gash's analytical model. *Hydrological Processes*, *1*(4), 309–319. doi:10.1002/hyp.3360010402

Calder, I. (1986). Water use of eucalypts - A review with special reference to south India. *Agricultural water management*, *11*, 333–342.

Cabral, O. M. R., Rocha, H. R., Gash, J. H. C., Ligo, M. a. V., Freitas, H. C., & Tatsch, J. D. (2010). The energy and water balance of a Eucalyptus plantation in southeast Brazil. *Journal of Hydrology*, *388*(3-4), 208–216. doi:10.1016/j.jhydrol.2010.04.041

Carlyle-Moses, D. E., & Price, A. G. (2007). Modelling canopy interception loss from a Madrean pine-oak stand, northeastern Mexico. *Hydrological Processes*, *21*(19), 2572–2580. doi:10.1002/hyp.6790

Carrara, A., Kowalski, A. S., Neirynck, J., Janssens, I. A., Yuste, J. C., & Ceulemans, R. (2003). Net ecosystem CO_2 exchange of mixed forest in Belgium over 5 years. *Agricultural and Forest Meteorology*, *119*(3-4), 209–227. doi:10.1016/S0168-1923(03)00120-5

Deguchi, A., Hattori, S., & Park, H.-T. (2006). The influence of seasonal changes in canopy structure on interception loss: Application of the revised Gash model. *Journal of Hydrology*, *318*(1-4), 80–102. doi:10.1016/j.jhydrol.2005.06.005

Denmead, O. T., & McIlroy, I. C. (1970). Measurements of non-potential evaporation from wheat. *Agricultural Meteorology*, *7*(1970), 285–302. doi:10.1016/0002-1571(70)90024-5

Dickinson, R. E., Henderson-Sellers, A., Rosenzweig, C., & Sellers, P. J. (1991). Evapotranspiration models with canopy resistance for use in climate models, a review. *Agricultural and Forest Meteorology*, *54*(2-4), 373–388. doi:10.1016/0168-1923(91)90014-H

Fisher, J. B., Malhi, Y., Bonal, D., Da Rocha, H. R., De AraãšJo, A. C., Gamo, M., Goulden, M. L., et al. (2009). The land-atmosphere water flux in the tropics. *Global Change Biology*, *15*(11), 2694–2714. doi:10.1111/j.1365-2486.2008.01813.x

Gash, J., & Morton, a. (1978). An application of the Rutter model to the estimation of the interception loss from Thetford Forest. *Journal of Hydrology*, *38*(1-2), 49–58. doi:10.1016/0022-1694(78)90131-2

Giambelluca, T., Martin, R., Asner, G., Huang, M., Mudd, R., Nullet, M., Delay, J., et al. (2009). Evapotranspiration and energy balance of native wet montane cloud forest in Hawai'i. *Agricultural and Forest Meteorology*, *149*(2), 230–243. doi:10.1016/j.agrformet.2008.08.004

Goulden, M. L., Mcmillan, A. M. S., Winston, G. C., Rocha, A. V., Manies, K. L., Harden, J. W., Lamberty, B. P. (2010). Patterns of NPP, GPP, respiration, and NEP during boreal forest succession. *Global Change Biology*, no–no. doi:10.1111/j.1365-2486.2010.02274.x

Granier, A., & Loustau, D. (1994). Measuring and modelling the transpiration of a maritime pine canopy from sap-flow data. *Agricultural and Forest Meteorology*, *71*(1-2), 61–81. doi:10.1016/0168-1923(94)90100-7

Granier, A., Reichstein, M., Bréda, N., Janssens, I.A., Falge, E., Ciais, P., Grünwald, T., Aubinet, M., Berbigier, P., Bernhofer, C., Buchmann, N., Facini, O., Grassi, G., Heinesch, B., Ilvesniemi, H. Keronen, P., Knohl, A., Köstner, B., Lagergren, F., Lindroth, A., Longdoz, B., Loustau, D., Mateus, J., Montagnani, L., Nys, C., Moors, E., Papale, D., Peiffer, M., Pilegaard, K., Pita, G., Pumpanen, J., Rambal, S., Rebmann, C., Rodrigues, A., Seufert, G., Tenhunen, J., Vesala, T., Wang, Q. (2007). Evidence for soil water control on carbon and water dynamics in European forests during the extremely dry year: 2003. *Agricultural and Forest Meteorology*, *143*(1-2), 123–145. doi:10.1016/j.agrformet.2006.12.004

Hattori, S. (1985). Explanation on Derivation Process of Equations to Estimate Evapotranspiration and Problems on the Application to Forest Stand. *Bulletin of the Forestry and Forest Products Research Institute*, *332*, 139–165.

Herwitz, S. R. (1985). Interception storage capacities of tropical rainforest canopy trees. *Journal of Hydrology*, *77* (1-4), 237–252. doi:10.1016/0022-1694(85)90209-4

Hirata, R., Hirano, T., Saigusa, N., Fujinuma, Y., Inokai, K., Kitamori, Y., Takahashi, Y., Yamamote, S., (2007). Seasonal and interannual variations in carbon dioxide exchange of a temperate larch forest. *Agricultural and Forest Meteorology*, *147*(3-4), 110–124. doi:10.1016/j.agrformet.2007.07.005

Jackson, N. a. (2000). Measured and modelled rainfall interception loss from an agroforestry system in Kenya. *Agricultural and Forest Meteorology*, *100*(4), 323–336. doi:10.1016/S0168-1923(99)00145-8

Jarvis, P. G. (1976). The Interpretation of the Variations in Leaf Water Potential and Stomatal Conductance Found in Canopies in the Field. *Philosophical Transactions of the Royal Society B: Biological Sciences*, *273*(927), 593–610. doi:10.1098/rstb.1976.0035

Kelliher, F., Leuning, R., Raupach, M. R., & Schulze, E.-D. (1995). Maximum conductances for evaporation from global vegetation types. Agricultural and Forest Meteorology, 73(1-2), 1–16. doi:10.1016/0168-1923(94)02178-M

Kosugi, Y., Kobashi, S., Shibata, S., (1995). Modelling stomatal conductance in leaves of several temperate evergreen broadleaf trees. J. Jpn. Soc. Reveget. Tech. 20, 158–167 (in Japanese with English summary).

Komatsu, H., Cho, J., Matsumoto, K., & Otsuki, K. (2012). Simple modeling of the global variation in annual forest evapotranspiration. *Journal of Hydrology*, *420-421*, 380–390. doi:10.1016/j.jhydrol.2011.12.030

Kondo, J., Watanabe, T., Nakazono, M., Ishii, M., (1992). Estimation of forest rainfall interception [in Japanese]. Tenki (the Bulletin Journal of the. Meteorological Society of Japan) 39, 159–167.

Kume, T., Tanaka, N., Kuraji, K., Komatsu, H., Yoshifuji, N., Saitoh, T. M., Suzuki, M., Kumagai, T.,. (2011). Ten-year evapotranspiration estimates in a Bornean tropical rainforest. *Agricultural and Forest Meteorology*, *151*(9), 1183–1192. doi:10.1016/j.agrformet.2011.04.005

Kuraji, K., & Tanaka, N. (2003). Rainfall Interception Studies in the Tropical Forests. [in Japanese]. *Journal of the Japanese Forestry Society*, *85*(1), 18–28.

Lafleur, P. M., Hember, R. a., Admiral, S. W., & Roulet, N. T. (2005). Annual and seasonal variability in evapotranspiration and water table at a shrub-covered bog in southern Ontario, Canada. *Hydrological Processes*, *19*(18), 3533–3550. doi:10.1002/hyp.5842

Li, Z., Zhang, Y., Wang, S., Yuan, G., Yang, Y., & Cao, M. (2010). Evapotranspiration of a tropical rain forest in Xishuangbanna, southwest China. *Hydrological Processes*, *24*(17), 2405 – 2416. doi:10.1002/hyp.7643

Lloyd, C. R., Gash, J. H. C., Shuttleworth, W. J., & De O. Marques F, A. (1988). The measurement and modelling of rainfall interception by Amazonian rain forest. *Agricultural and Forest Meteorology*, *43*(3-4), 277–294. doi:10.1016/0168-1923(88)90055-X

Lloyd, J. (1991). Modelling Stomatal Responses to Environment in Macadamia integrifolia. *Australian Journal of Plant Physiology*, *18*(6), 649. doi:10.1071/PP9910649

Loescher, H. W., Gholz, H. L., Jacobs, J. M., Oberbauer, S. F. (2005). Energy dynamics and modeled evapotranspiration from a wet tropical forest in Costa Rica. *Journal of Hydrology*, *315*(1-4), 274–294. doi:10.1016/j.jhydrol.2005.03.040

Lohammar, T., Larsson, S., Linder, S., & Falk, S. O. (1980). FAST: Simulation Models of Gaseous Exchange in Scots Pine. *Ecological Bulletins*, (32), 505–523. doi:10.2307/20112831

Matsumoto, K., Ohta, T., Nakai, T., Kuwada, T., Daikoku, K., Iida, S., Yabuki, H., et al. (2008). Responses of surface conductance to forest environments in the Far East. *Agricultural and Forest Meteorology*, *148*(12), 1926–1940.

Manfroi, O. J., Kuraji, K., Suzuki, M., Tanaka, N., Kume, T., Nakagawa, M., Kumagai, T., et al. (2006). Comparison of conventionally observed interception evaporation in a 100-m2 subplot with that estimated in a 4-ha area of the same Bornean lowland tropical forest. *Journal of Hydrology*, *329*(1-2), 329–349. doi:10.1016/j.jhydrol.2006.02.020

Malhi, Y., Pegoraro, E., Nobre, A. D., Pereira, M. G. P., Grace, J., Culf, A. D., & Clement, R. (2002). Energy and water dynamics of a central Amazonian rain forest. *Journal of Geophysical Research*, *107*(D20), 1–17. doi:10.1029/2001JD000623

Nielson, R., & Jarvis, P. (1975). Photosynthesis in Sitka Spruce (Picea sitchensis (Bong.) Carr.): VI. Response of Stomata to Temperature. *Journal of Applied Ecology*, *12*(3), 879–891.

Monteith, J. L., & Unsworth, M. H. (1990). *Principles of Environmental Physics*. Arnold, London

Mulder, J. (1985). *Simulating interception loss using standard meteorological data*. (B. A. Hutchison & B. B. Hicks, Eds.) (pp. 177–196). Oak Ridge, TN: D. Reidel Publishing Company.

Nobuhiro, T. (2009). Evapotranspiration Characteristics of a Lowland Dry Evergreen Forest in Central Cambodia Examined Using a Multilayer Model. *Journal of Water Resource and Protection*, *01*(05), 325–335. doi:10.4236/jwarp.2009.15039

Oren, R., & Pataki, D. E. (2001). Transpiration in response to variation in microclimate and soil moisture in southeastern deciduous forests. *Oecologia*, *127*(4), 549–559. doi:10.1007/s004420000622

Pearce, A. J., & Rowe, L. K. (1981). Rainfall Interception In A Multi-Storied, Evergreen Mixed Forest: Estimates Using Gash's Analytical Model. *Journal of Hydrology*, *49*(3-4), 341–353. doi:10.1016/S0022-1694(81)80018-2

Pitman, J. I. (1989). Rainfall interception by bracken in open habitats — Relations between leaf area, canopy storage and drainage rate. *Journal of Hydrology*, *105*(3-4), 317–334. doi:10.1016/0022-1694(89)90111-X

Priestley, C. H. B., & Taylor, R. J. (1972). On the Assessment of Surface Heat Flux and Evaporation Using Large-Scale Parameters. *Monthly Weather Review*, *100*(2), 81–92. doi:10.1175/1520-0493(1972)100<0081:OTAOSH>2.3.CO;2

Rutter, A. J., Morton, A. J., & Robins, P. C. (1975). A Predictive Model of Rainfall Interception in Forests. II. Generalization of the Model and Comparison with Observations in Some Coniferous and Hardwood Stands. *Journal of Applied Ecology*, *12*(1), 367–380. doi:10.2307/2401739

Saigusa, N., Yamamoto, S., Murayama, S., Kondo, H., & Nishimura, N. (2002). Gross primary production and net ecosystem exchange of a cool-temperate deciduous forest estimated by the eddy covariance method. *Agricultural and Forest Meteorology*, *112*(3-4), 203–215. doi:10.1016/S0168-1923(02)00082-5

Sato, T., Igarashi, Y., Tanaka, N., Yoshifuji, N., Tantashirin, C., Suzuki, M., (2009). Turbulent statistics and roughness parameters of leafed and leafless canopy of tropical monsoon forest. Abstract of ISAM 2008 International Symposium . p97 [in Japanease]

Scatena, F. N. (1990). Watershed scale rainfall interception on two forested watersheds in the Luquillo Mountains of Puerto Rico. *Journal of Hydrology*, *113*(1-4), 89–102. doi:10.1016/0022-1694(90)90168-W

Schmid, H. (2000). Measurements of CO_2 and energy fluxes over a mixed hardwood forest in the mid-western United States. *Agricultural and Forest Meteorology*, *103*(4), 357–374. doi:10.1016/S0168-1923(00)00140-4

Sharpe, P. J., & DeMichele, D. W. (1977). Reaction kinetics of poikilotherm development. *Journal of theoretical biology*, *64*(4), 649–70.

Shuttleworth, W. J. (1988). Evaporation from Amazonian Rainforest. *Proceedings of the Royal Society B: Biological Sciences*, *233*(1272), 321–346. doi:10.1098/rspb.1988.0024

Shuttleworth, W. J., Leuning, R., Black, T. A., Grace, J., Jarvis, P. G., Roberts, J., & Jones, H. G. (1989). Micrometeorology of Temperate and Tropical Forest [and Discussion]. *Philosophical Transactions of the Royal Society B: Biological Sciences*, *324*(1223), 299–334. doi:10.1098/rstb.1989.0050

Stewart, J. . (1988). Modelling surface conductance of pine forest. *Agricultural and Forest Meteorology*, *98*(1), 124–35. doi:10.1016/0168-1923(88)90003-2

Suzuki, M. (1980). Evapotranspiration from a small catchment in hilly mountains (I) Seasonal variations in evapotranspiration, rainfall interception and transpiration [in Japanease]. *Journal of the Japanese Forestry Society*, *62*(2), 46–53.

Tani, M. (2003). Long-term estimation of evapotranspiration from a tropical rain forest in Peninsular Malaysia. *Water Resources Systems - Water Availability and Global Change*, 267–274.

Thompson, F.B., (1972). Rainfall interception by oak coppice (Quercus robur, L.). In: Taylor, A. (Ed.), Research Papers in Forest Meteorology. Cambrian News Ltd., Aberystwyth, pp. 59–74

Toba, T., & Ohta, T. (2005). An observational study of the factors that influence interception loss in boreal and temperate forests. *Journal of Hydrology*, *313*(3-4), 208–220. doi:10.1016/j.jhydrol.2005.03.003

Watanabe, T., & Mizutani, K. (1996). Model study on micrometeorological aspects of rainfall interception over an evergreen broad-leaved forest. *Agricultural and Forest Meteorology*, *80*(2-4), 195–214. doi:10.1016/0168-1923(95)02301-1

White, M. A., Running, S. W., & Thornton, P. E. (1999). The impact of growing-season length variability on carbon assimilation and evapotranspiration over 88 years in the eastern US deciduous forest. *International Journal of Biometeorology*, *42*(3), 139–145. doi:10.1007/s004840050097

Wilson, K. B., & Baldocchi, D. D. (2000). Seasonal and interannual variability of energy fluxes over a broadleaved temperate deciduous forest in North America. *Agricultural and Forest Meteorology*, *100*(1), 1–18. doi:10.1016/S0168-1923(99)00088-X

Yoshifuji, N., Kumagai, T., Tanaka, K., Tanaka, N., Komatsu, H., Suzuki, M., & Tantasirin, C. (2006). Inter-annual variation in growing season length of a tropical seasonal forest in northern Thailand. *Forest Ecology and Management*, *229*(1-3), 333–339. doi:10.1016/j.foreco.2006.04.013

Yoshifuji, N., Komatsu, H., Kumagai, T., Tanaka, N., Tantasirin, C., & Suzuki, M. (2011). Interannual variation in transpiration onset and its predictive indicator for a tropical deciduous forest in northern Thailand based on 8-year sap-flow records. Ecohydrology, 4(2), 225–235. doi:10.1002/eco.219

Zhang, G., & Zeng, G. (2006). Modelling and measurement of two-layer-canopy interception losses in a subtropical evergreen forest of central-south China. *Hydrology and Earth System Sciences*, *10*, 65–77.

Chapter 5

Seasonality of water and carbon dioxide exchanges at a tropical deciduous forest in northern Thailand

5.1 Introduction

The examination of energy, water and carbon exchanges between vegetation and the atmosphere is critical in various research fields such as metrology, ecology and hydrology (e.g. Baldocchi et al., 2001; Pitman, 2003; Komatsu et al., 2008). In deciduous forests, energy, water and carbon exchange are influenced not only by meteorology but also by the timing and/or duration of phenology such as leaf-out and leaf-fall (White et al., 1999; Black et al., 2000; Aubinet et al., 2002; Carrara et al., 2003; Saigusa et al., 2005; Barr et al., 2006), as well as leaf age (Kitajima et al., 1997; Wilson et al., 2001). Understanding the interactions between these factors is a key to adequately characterizing the dynamics of energy, water and carbon exchanges within deciduous forests in Southeast Asia. In the chapter, to document the seasonality of energy, water and carbon exchanges especially transpiration, photosynthesis within a teak plantation using the eddy covariance method was objective. The relationship between energy, water and carbon exchanges and the timing of teak phenology such as leaf-out and leaf-fall, as well as leaf ageing were also discussed.

5.2 Materials and methods

The details of site descriptions, meteorological measurements, eddy covariance method and monitoring of LAI had shown in chapter 2. In this section, details of photosynthesis model were explained.

According to Twine et al. (2000), it was pointed out that energy imbalance affected to Fc. In general, Fc was corrected by the lack of the energy balance closure. For example, the value of corrected Fc was approximately 30 % larger than the value of uncorrected Fc, and. the ratio of correction related with energy balance closure. The energy balance closure differed

in daytime and night due to the low friction velocity and stable boundary condition (e.g., Anthoni et al., 1999; Blanken et al., 1997). And there is still much discussion on whether or not Fc should be corrected by the amount of the lack of closure (Saigusa et al., 2003). Therefore, the correction of energy balance for Fc was not applied in this study.

Analysis of seasonal variation Data for observed daytime NEE were fitted to the following equation based on a non-rectangular hyperbola relationship (Thornley, 1970 as a function of R_s (W m^{-2}):

$$f(R_s) = -\frac{\emptyset R_s + P_{max} - \sqrt{(\emptyset R_s + P_{max})^2 - 4\emptyset R_s P_{max} v}}{2v} + R_e \quad (5.1)$$

where P_{max} was the maximum rate of NEE (μ mol CO_2 m^{-2} s^{-1}), $\emptyset$ was the initial slope, v (= 0.9) was a dimentional curve parameter (Hirata et al., 2008) and Rd was a dark respiration (μ mol CO_2 m^{-2} s^{-1}), respectively. The regression coefficients P_{max}, R_e and $\emptyset$ were determined for every month using the least-squares method. Seasonal variation in the canopy duration period

5.3 Results and Discussion

5.3.1 Seasonality of sensible heat and latent heat flux with net ecosystem exchange

Fig. 5.1 (A) and (B) showed the seasonal progression of H and LE, and NEE with seasonal changes of LAI, respectively. The author had already mentioned LE was more prominent than H during the wet season, whereas in the dry season, the latter was the major form of energy emitted to the atmosphere (section 2.3.5 in Chapter 2). The reduction in LE in the dry season, when available R_s did not greatly decrease (Fig. 2.3), may have resulted from a lack of available water for evapotranspiration within the forest ecosystem due to a prolonged dry period. Such a reduction in LE in the dry season has not been reported for evergreen forest sites in mainland SE Asia. Tanaka et al. (2003) reported that at an upland evergreen forest site in Thailand, evapotranspiration in the hot dry season was considerably higher than during the wet season. Nobuhiro et al. (2009) also showed that at a lowland evergreen forest site in Cambodia, evapotranspiration in the hot dry season was higher than in the wet season. The seasonality in energy partitioning observed here also differs from typical tropical rain forests in SE Asia (Kumagai et al., 2004; Takanashi et al., 2010), where seasonal patterns in LE are often ambiguous. Due to the effects of Asian monsoons, differences in the seasonal variation of H and

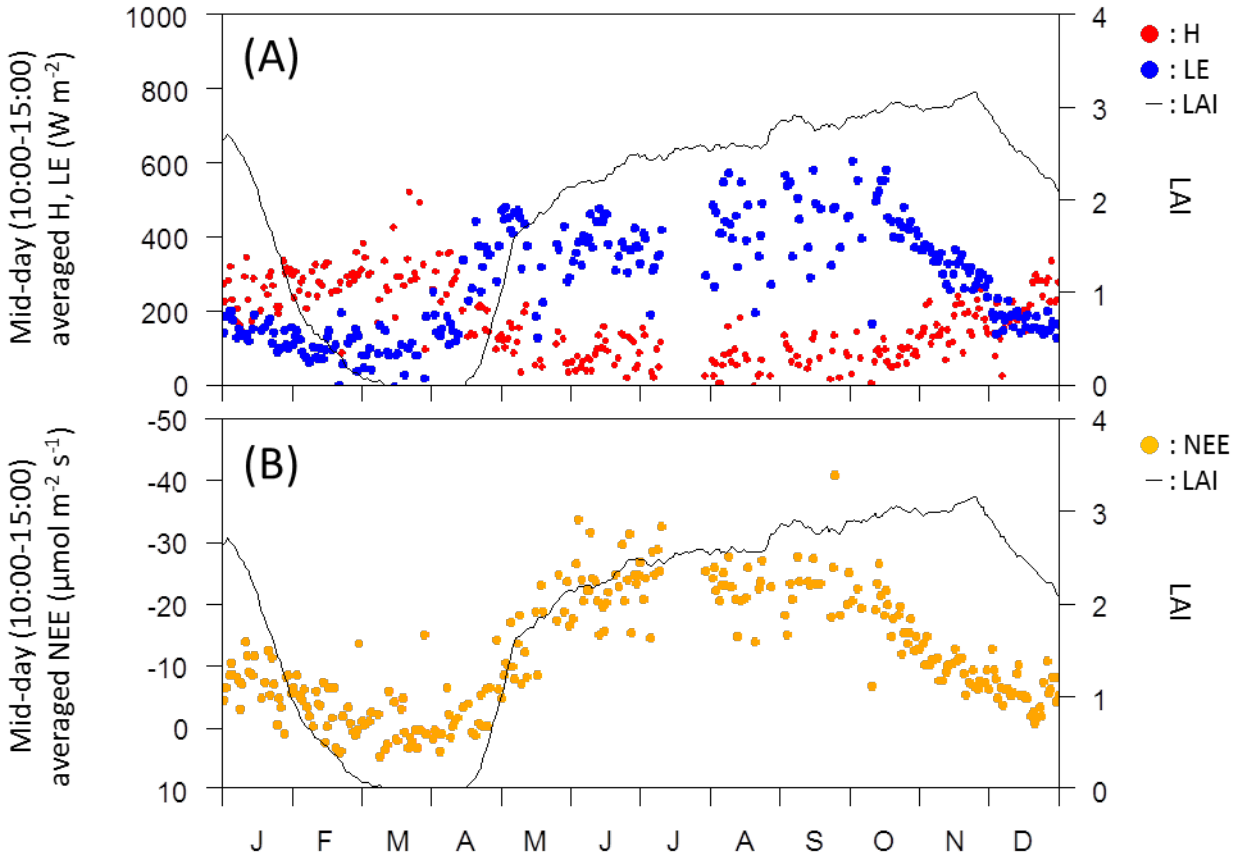

Fig. 5.1 (A) Seasonal variation of sensible heat flux, latent heat and LAI, (B) Seasonal variation of NEE and LAI

LE were influenced by differences in vegetation type between deciduous and evergreen forests. In contrast, the Amazon region, which experiences less than 1700 mm of precipitation and a longer dry season, exhibited clear evidence of reduced evaporation in the dry season. (e.g., Vourlitis *et al.*, 2008; da Rocha *et al.*, 2009). For example, at a *Eucalyptus* plantation in Brazil, more than 80% of available energy was utilized in evaporation in the summer (wet season), and 74% of the available energy was directed to sensible flux in the winter (dry season) (Cabral *et al.*, 2010). Such a clear seasonal contrast in the pattern of energy partitioning is often less pronounced in tropical rain forests in the Amazon (Carswell *et al.*, 2002; Malhi *et al.*, 2002; Hutyra *et al.*, 2007) and in SE Asia, as these sites are located close to the equator and the Intertropical Convergence Zone. As noted above, clear energy partitioning is not often observed at boreal or temperate deciduous forest sites (e.g., Greco and Baldocchi, 1996; Wilson and Baldocchi, 2000; Pejam *et al.*, 2006) because in the winter (corresponding to the dry season at our site), these sites receive much lower net radiation compared to the summer months (the wet season at our site).

Occasional increases in LE occurred during the hot dry season, when teak trees were almost leafless. These increases may have been caused by soil evaporation from the moist ground, as the above-mentioned rainfall events prior to the NLR onset were followed by the eventual increases in LE. Another possible explanation for the increases of LE involves transpiration by understory plants, such as shrubs and bamboos, which are patchily distributed at our site. Some of these plants had leaves throughout the dry season, and the energy available to them may have been sufficient because of the absence of light interception by teak leaves. However, because no corresponding increases were observed in the daytime uptake of CO_2 throughout the dry season, soil evaporation following the rainfall events might have played a major role in the occasional increases in LE.

LE appeared to decrease from the beginning of October, even though LAI remained high until the end of November. At the Mae Moh plantation, Yoshifuji et al. (2006) examined seasonal variability of sap flow velocity as well as the leaf amount of teak trees for 3 years; they found that in each year, the sap flow velocity began to decrease approximately 1 month earlier than leaf-fall initiation. The decline in LE in Fig. 5.1 (A) might also have been caused by reduced transpiration by teak trees.

Negative NEE values indicate daytime net uptake of CO_2 by the ecosystem, whereas positive NEE values indicate net release of CO_2 (ecosystem respiration). In the beginning of the wet season, NEE appeared to increase with increasing LAI (Fig. 5.1 B), indicating that CO_2

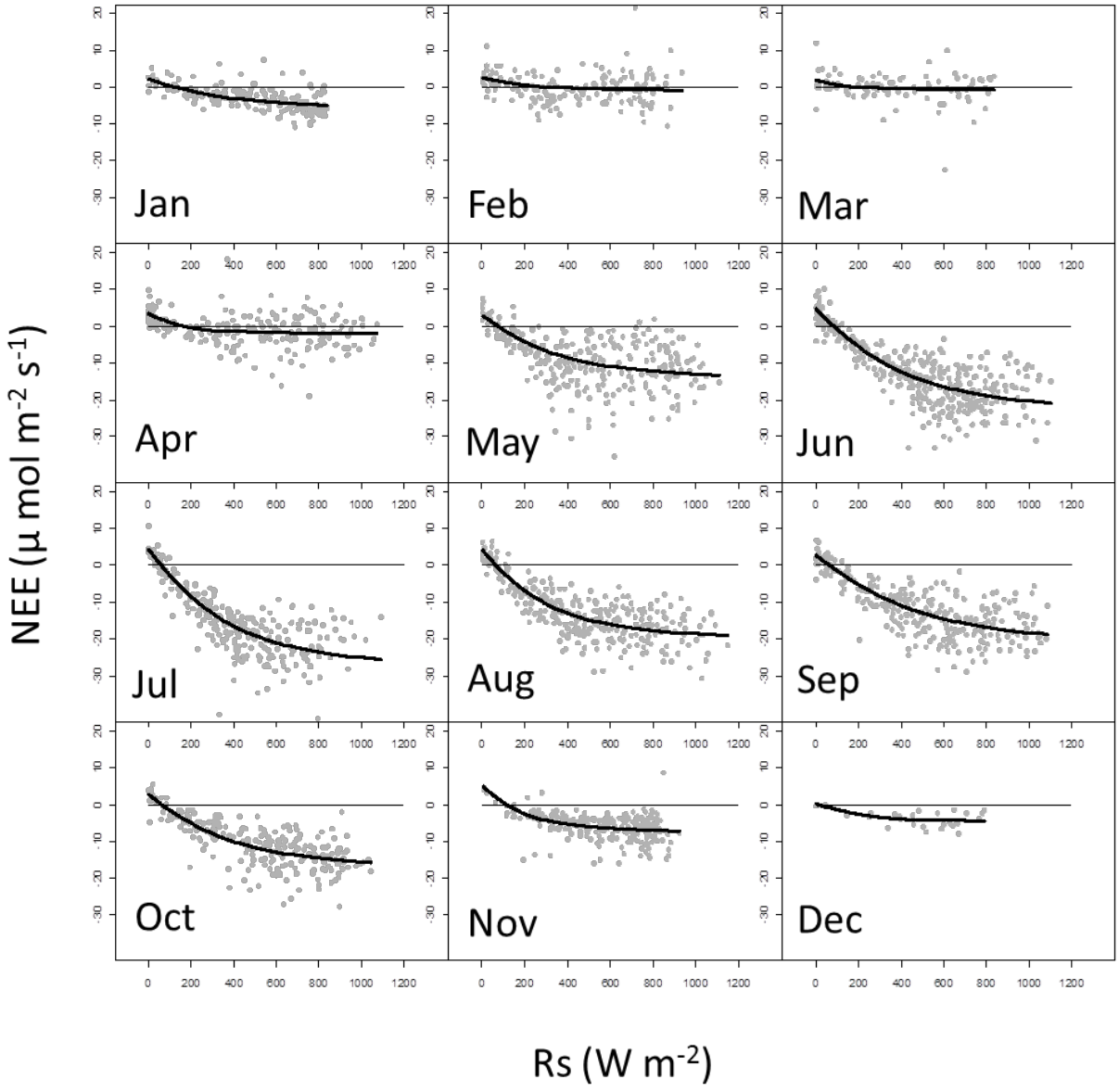

Fig 5.2 Relationship between the observed NEE (black) and estimated NEE (grey)

assimilation by photosynthesis of teak trees increased with increases in their leaf amount during this period. The maximum value of NEE uptake occurred in July and declined gradually thereafter. The decline NEE occurred approximately 3 months earlier than the start of LE decrease. The decline NEE was more pronounced after October. The seasonality of NEE at our deciduous forest site is discussed further in the following subsection. During the dry season, both daytime NEE and LAI were lower than in any other season, indicating that CO_2 uptake was more restricted under conditions of a leafless teak canopy.

5.3.2 Seasonality of Pmax and LAI

Fig. 5.2 showed the relationship between incident shortwave radiation and NEE for each month. The curves are nonlinear regressions (fitted by the least-squares method) of the non-rectangular hyperbolas (see Eq. 5.1). Table 5.1 showed the list of the non-rectangular hyperbola parameters for each month. Among the parameters listed in Table 5.1, P_{max} might be the most important parameter indicating the photosynthetic capacity of this forest ecosystem. Fig. 5.3 compares the seasonality of P_{max} and LAI. The maximum value of P_{max} (42.4 μmol m^{-2} s^{-1}) took place in July, whereas minimum P_{max} (5.6 μmol m^{-2} s^{-1}) occurred in March. P_{max} increased linearly from April to July, but this pattern did not closely parallel that of LAI. In fact, P_{max} increased in parallel with LAI during the April–June period but not after July.

Wilson et al. (2001) reported that for temperate deciduous tree species in the northeastern United States, the maximum carboxylation rate of individual leaves increased gradually with time, i.e., with the maturing of flushed leaves. This relationship may help to explain the increase in P_{max} with an increase in the leaf amount of teak trees at our tropical deciduous forest site. Similarly, in a physiological study in a Panamanian tropical deciduous forest, Kitajima et al. (1997) found that the leaf-level photosynthetic capacity of five tree species peaked approximately 1 month after canopy closure of the study stand. Our P_{max} data also suggest that a mature canopy forms about 1 month after stand-scale canopy closure in June.

P_{max} decreased steadily during the August–November period, despite the absence of substantial changes in LAI. During this period (August–October 2006), leaf age was likely the major factor causing decreases in the photosynthetic capacity of teak trees after maturation. Because, clear seasonal trends in soil water content, net radiation, or water vapor pressure (Fig. 2.2) were not observed. And, this seasonal trend of P_{max} was different that of canopy conductance and stomatal conductance (Fig. 3.3). For temperate deciduous species, the maximum carboxylation rates of mature individual leaves are often strongly controlled by leaf

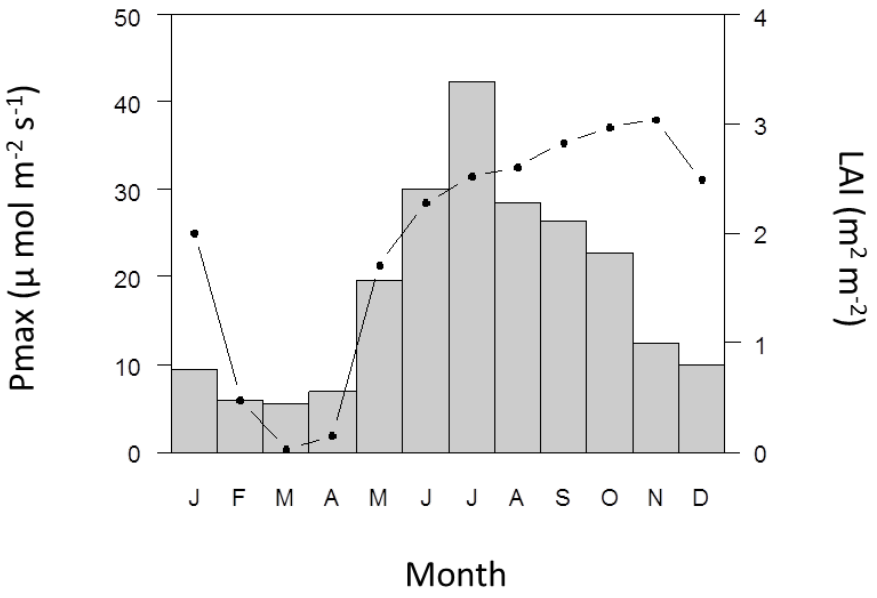

Fig. 5.3 Seasonality of monthly averaged LAI and Pmax. Gray bar represents Pmax. Solid line and dots represent LAI.

Table 5.1 Parameters of non-rectangular hyperbolas.

Month	Jan	Feb	Mar	Apr	May	Jun	Jul	Aug	Sep	Oct	Nov	Dec
P_{max} (μmol CO_2 m^{-2} s^{-1})	9.4	5.8	5.6	6.9	19.5	30	42.4	28.5	26.3	22.7	12.3	9.9
R_e (μmol CO_2 m^{-2} s^{-1})	2.1	2.4	1.9	3.4	2.9	4.6	4.2	4.2	2.7	2.6	5.3	0.2
∅	0.019	0.012	0.015	0.03	0.042	0.059	0.074	0.068	0.045	0.045	0.055	0.019

age rather than ambient environmental factors (Wilson et al., 2001). Kitajima et al. (2002) also showed that photosynthetic capacity decreased with leaf age in a seasonally dry forest in Panama.

Yoshifuji et al. (2006) demonstrated that variation in the canopy duration and transpiration period ranged between 40 and 60 days; this range is much larger than the interannual variation previously reported for temperate deciduous forests and may have a profound impact on interannual variation in energy, water, and carbon exchanges in this forest ecosystem. The consistent decline in P_{max} during the late growing season points to drastic decreases in the water-use efficiency of teak in the corresponding season, as LE at this site remained high at least until the end of October (Fig. 5.2). The decoupling of the seasonality of water and carbon exchanges may be particularly important when modeling the ecohydrology of evergreen forests as well as this tropical deciduous forest.

5.4 Conclusion

In this chapter, the seasonal progression of H and LE, and NEE with seasonal changes of LAI were showed. About the seasonality of NEE, in the beginning of the wet season, NEE appeared to increase with increasing LAI, indicating that CO_2 assimilation by photosynthesis of teak trees increased with increases in their leaf amount during this period. The maximum value of NEE uptake occurred in July and declined gradually thereafter. Essentially, the decline NEE occurred approximately 3 months earlier than the start of LE decrease.

P_{max} that was the most important parameter indicating the photosynthetic capacity of this forest ecosystem and seasonality of LAI was compered. The maximum value of P_{max} appeared in July, whereas minimum P_{max} appeared in March. P_{max} increased linearly from April to July, but this pattern did not closely parallel that of LAI. In fact, P_{max} increased in parallel with LAI during the April–June period but not after July. P_{max} decreased steadily during the August–November period, despite the absence of substantial changes in LAI. During this period (August–October 2006), leaf age was likely the major factor causing decreases in the photosynthetic capacity of teak trees after maturation. Because, clear seasonal trends in soil water content, net radiation, or water vapor pressure (Fig. 2.3) were not observed. The consistent decline in P_{max} during the late growing season points to drastic decreases in the water-use efficiency of teak in the corresponding season, as LE at this site remained high at least until the end of October (Fig. 5.2). The decoupling of the seasonality of water and carbon exchanges may be particularly important when modeling the ecohydrology of evergreen forests as well as this tropical deciduous forest.

References

Aubinet, M., Heinesch, B., Longdoz, B,. (2002). Estimation of the carbon sequestration by a heterogeneous forest: night flux corrections, heterogeneity of the site and inter-annual variability. *Global Change Biology* **8**(11): 1053-1071. doi: 10.1046/j.1365-2486.2002.00529.x.

Baldocchi, D., Falge, E., Gu, L., Olson, R., Hollinger, D., Running, S., Anthoni, P., Bernhofer, C., Davis, K., Evans, R., Fuentes, J., Goldstein, A., Katul, G., Law, B., Lee, X., Malhi, Y., Meyers, T., Munger, W., Oechel, W., Paw, KT., Pilegaard, K., Schmid, HP., Valentini, R., Verma, S., Vesala, T., Wilson, K., Wofsy, S. (2001). FLUXNET: a new tool to study the temporal and spatial variability of ecosystem-scale carbon dioxide, water vapor, and energy flux densities. *Bulletin of the American Meteorological Society* **82**(11): 2415–2434. doi: 10.1175/1520-0477(2001)082<2415:FANTTS>2.3.CO;2.

Barr, A. G., Black, T. A., Hogg, E. H., Griffis, T. J., Morgenstern, K., Kljun, N., Theede, A., Nesic, Z., (2006). Climatic controls on the carbon and water balances of a boreal aspen forest, 1994–2003. *Global Change Biology* **13**(3): 561-576. doi: 10.1111/j.1365-2486.2006.01220.x

Black, T. A., Chen, W. J., Barr, A. G., Arain, M. A., Chen, Z., Nesic, Z., Hogg, EH., Neumann, HH., Yang, P. C. (2000). Increased carbon sequestration by a boreal deciduous forest in years with a warm spring. *Geophysical Research Letters* **27**(9): 1271. doi: 10.1029/1999GL011234

Bonan, G. B. (2008). Forests and climate change: forcings, feedbacks, and the climate benefits of forests. Science, 320(5882), 1444–1449. doi:10.1126/science.1155121

Cabral, O. M. R., Rocha, H. R., Gash, J. H. C., Ligo, M. a. V., Freitas, H. C., & Tatsch, J. D. (2010). The energy and water balance of a Eucalyptus plantation in southeast Brazil. Journal of Hydrology, 388(3-4), 208–216. doi:10.1016/j.jhydrol.2010.04.041

Carrara, A., Kowalski, A. S., Neirynck, J., Janssens, I. A., Yuste, J. C., & Ceulemans, R. (2003). Net ecosystem CO_2 exchange of mixed forest in Belgium over 5 years. Agricultural and Forest Meteorology, 119(3-4), 209–227. doi:10.1016/S0168-1923(03)00120-5

Carswell, F. E., Costa, A. L., Palheta, M., Malhi, Y., Meir, P., Costa, J. de P. R., Ruivo, M. de L., et al. (2002). Seasonality in CO_2 and H_2O flux at an eastern Amazonian rain forest. Journal of Geophysical Research, 107(D20), 8076. doi:10.1029/2000JD000284

da Rocha, H. R., Manzi, A. O., Cabral, O. M., Miller, S. D., Goulden, M. L., Saleska, S. R., R.-Coupe, N., et al. (2009). Patterns of water and heat flux across a biome gradient from tropical forest to savanna in Brazil. Journal of Geophysical Research, 114(G1), G00B12. doi:10.1029/2007JG000640

Davis, K. J., Bakwin, P. S., Yi, C., Berger, B. W., Zhao, C., Teclaw, R. M., & Isebrands, J. G. (2003). The annual cycles of CO_2 and H_2O exchange over a northern mixed forest as observed from a very tall tower. Global Change Biology, 9(9), 1278–1293. doi:10.1046/j.1365-2486.2003.00672.x

Greco, S., & Baldocchi, D. D. (1996). Seasonal variations of CO_2 and water vapour exchange rates over a temperate deciduous forest. Global Change Biology, 2(3), 183–197. doi:10.1111/j.1365-2486.1996.tb00071.x

Hashimoto, S., Tanaka, N., Suzuki, M., Inoue, A., Takizawa, H., Kosaka, I., Tanaka, K., et al. (2004). Soil respiration and soil CO_2 concentration in a tropical forest, Thailand. Journal of Forest Research, 9(1), 75–79. doi:10.1007/s10310-003-0046-y

Hashimoto, S. (2005). Temperature sensitivity of soil CO_2 production in a tropical hill evergreen forest in northern Thailand. Journal of Forest Research, 10(6), 497–503. doi:10.1007/s10310-005-0168-5

Hutyra, L. R., Munger, J. W., Saleska, S. R., Gottlieb, E., Daube, B. C., Dunn, A. L., Amaral, D. F., et al. (2007). Seasonal controls on the exchange of carbon and water in an Amazonian rain forest. Journal of Geophysical Research, 112(G3), 1–16. doi:10.1029/2006JG000365

Kanae, S., Oki, T., & Musiake, K. (2001). Impact of Deforestation on Regional Precipitation over the Indochina Peninsula. Journal of Hydrometeorology, 2(1), 51–70. doi:10.1175/1525-7541(2001)002<0051:IODORP>2.0.CO;2

Kitajima, K., Mulkey, S. S., Samaniego, M., & Joseph Wright, S. (2002). Decline of photosynthetic capacity with leaf age and position in two tropical pioneer tree species. American journal of botany, 89(12), 1925–32. doi:10.3732/ajb.89.12.1925

Kitajima, K., Mulkey, S. S., & Wright, S. J. (1997). Decline of Photosynthetic Capacity with Leaf Age in Relation to Leaf Longevities for Five Tropical Canopy Tree Species. American Journal of Botany, 84(5), 702 – 708.

Komatsu, H., Kume, T., & Otsuki, K. (2008). The effect of converting a native broad-leaved forest to a coniferous plantation forest on annual water yield: A paired-catchment study in northern Japan. Forest Ecology and Management, 255(3-4), 880–886. doi:10.1016/j.foreco.2007.10.010

Kosugi, Y., Takanashi, S., Ohkubo, S., Matsuo, N., Tani, M., Mitani, T., Tsutsumi, D., et al. (2008). CO_2 exchange of a tropical rainforest at Pasoh in Peninsular Malaysia. Agricultural and Forest Meteorology, 148(3), 439–452. doi:10.1016/j.agrformet.2007.10.007

Krishnapillay, B. (2000). Silviculture and management of teak plantations. Unasylva, 201(51), 14–21.

Kumagai, T., Katul, G. G., Porporato, A., Saitoh, T. M., Ohashi, M., Ichie, T., & Suzuki, M. (2004). Carbon and water cycling in a Bornean tropical rainforest under current and future climate scenarios. Advances in Water Resources, 27(12), 1135–1150. doi:10.1016/j.advwatres.2004.10.002

Lean, J., & Warrilow, D. A. (1989). Simulation of the regional climatic impact of Amazon deforestation. Nature, 342(6248), 411–413. doi:10.1038/342411a0

Lean, J., & Warrilow, D. A. (1989). Simulation of the regional climatic impact of Amazon deforestation. Nature, 342(6248), 411–413. doi:10.1038/342411a0

Malhi, Y., Pegoraro, E., Nobre, A. D., Pereira, M. G. P., Grace, J., Culf, A. D., & Clement, R. (2002). Energy and water dynamics of a central Amazonian rain forest. Journal of Geophysical Research, 107(D20), 1–17. doi:10.1029/2001JD000623

Monsi, M., & Saeki, T. (1953). ÜUber den Lichtfaktor in den Pflanzengesellschaften und seine Bedeutung fur die Stoffproduktion. Japanese Journal of Botany, 14(1), 22–52. [In German].

Nobuhiro, T. (2009). Evapotranspiration Characteristics of a Lowland Dry Evergreen Forest in Central Cambodia Examined Using a Multilayer Model. Journal of Water Resource and Protection, 01(05), 325–335. doi:10.4236/jwarp.2009.15039

Pattey, E., Strachan, I. B., Desjardins, R. L., & Massheder, J. (2002). Measuring nighttime CO_2 flux over terrestrial ecosystems using eddy covariance and nocturnal boundary layer methods. Agricultural and Forest Meteorology, 113(1-4), 145–158. doi:10.1016/S0168-1923(02)00106-5

Pejam, M. R., Arain, M. A., & McCaughey, J. H. (2006). Energy and water vapour exchanges over a mixedwood boreal forest in Ontario, Canada. Hydrological Processes, 20(17), 3709–3724. doi:10.1002/hyp.6384

Pitman, A. J. (2003). The evolution of, and revolution in, land surface schemes designed for climate models. International Journal of Climatology, 23(5), 479–510. doi:10.1002/joc.893

Saigusa, N., Yamamoto, S., Murayama, S., Kondo, H. (2005). Inter-annual variability of carbon budget components in an AsiaFlux forest site estimated by long-term flux measurements. Agricultural and Forest Meteorology, 134(1-4), 4–16. doi:10.1016/j.agrformet.2005.08.016

Saigusa, N., Yamamoto, S., Hirata, R., Ohtani, Y., Ide, R., Asanuma, J., Gamo, M., et al. (2008). Temporal and spatial variations in the seasonal patterns of CO_2 flux in boreal, temperate, and tropical forests in East Asia. Agricultural and Forest Meteorology, 148(5), 700–713. doi:10.1016/j.agrformet.2007.12.006

Santisuk, T. (1988). An Account of the Vegetation Northern Thailand. Wiesbaden GmbH, Stuttgart: Franz Steiner Verlag.

Takanashi, S., Kosugi, Y., Ohkubo, S., Matsuo, N., Tani, M., & Nik, A. R. (2010). Water and heat fluxes above a lowland dipterocarp forest in Peninsular Malaysia. Hydrological Processes, 24(4), 472–480. doi:10.1002/hyp.7499

Tanaka, K., Takizawa, H., Tanaka, N., Kosaka, I., Yoshifuji, N., Tantasirin, C., Piman, S., et al. (2003). Transpiration peak over a hill evergreen forest in northern Thailand in the late dry season: Assessing the seasonal changes in evapotranspiration using a multilayer model. J. Geophys. Res., 108(D17), 4533. doi:10.1029/2002JD003028

Tanaka, K., Yoshifuji, N., Tanaka, N., Shiraki, K., Tantasirin, C., & Suzuki, M. (2009). Water budget and the consequent duration of canopy carbon gain in a teak plantation in a dry tropical region: Analysis using a soil–plant–air continuum multilayer model. Ecological Modelling, 220(12), 1534–1543. doi:10.1016/j.ecolmodel.2009.03.023

Tanaka K, Yoshifuji N, Tanaka N, Shiraki K, Tantasirin C, Suzuki M. 2009. Water budget and the consequent duration of canopy carbon gain in a teak plantation in a dry tropical region: analysis using a soil–plant–air continuum multilayer model. *Ecological Modelling* **220**(12): 1534–1543. doi: 10.1016/j.ecolmodel.2009.03.023.

Tanaka, K., Tantasirin, C., Suzuki, M. (2011). Interannual variation in leaf expansion and outbreak of a teak defoliator at a teak stand in northern Thailand. Ecological Applications, 21(5), 1792–1801. doi:10.1890/10-1165.1

Tanaka, N., Kume, T., Yoshifuji, N., Tanaka, K., Takizawa, H., Shiraki, K., Tantasirin, C., et al. (2008). A review of evapotranspiration estimates from tropical forests in Thailand and adjacent regions. Agricultural and Forest Meteorology, 148(5), 807–819. doi:10.1016/j.agrformet.2008.01.011

Thornley, J. H. M. (1976). Mathematical models in plant physiology. London: Academic Press.

Twine, T. E., Kustas, W. P., Norman, J. M., Cook, D. R., Houser, P. R., Meyers, T. P., Prueger, J. H., et al. (2000). Correcting eddy-covariance flux underestimates over a grassland. Agricultural and Forest Meteorology, 103(3), 279–300. doi:10.1016/S0168-1923(00)00123-4

Vourlitis George, De Souza Nogueira, J., De Almeida Lobo, F., Sendall, K. M., De Paulo, S. R., Antunes Dias, C. A., Pinto, O. B., et al. (2008). Energy balance and canopy conductance of a tropical semi-deciduous forest of the southern Amazon Basin. Water Resources Research, 44(3), 1–14. doi:10.1029/2006WR005526

White, M. A., Running, S. W., & Thornton, P. E. (1999). The impact of growing-season length variability on carbon assimilation and evapotranspiration over 88 years in the eastern US deciduous forest. International Journal of Biometeorology, 42(3), 139–145. doi:10.1007/s004840050097

Wilson, K. B., & Baldocchi, D. D. (2000). Seasonal and interannual variability of energy fluxes over a broadleaved temperate deciduous forest in North America. Agricultural and Forest Meteorology, 100(1), 1–18. doi:10.1016/S0168-1923(99)00088-X

Wilson, K. B., Baldocchi, D. D., & Hanson, P. J. (2001). Leaf age affects the seasonal pattern of photosynthetic capacityand net ecosystem exchange of carbon in a deciduous forest. Plant, Cell and Environment, 24(6), 571–583. doi:10.1046/j.0016-8025.2001.00706.x

Wilson, K., Goldstein, A., Falge, E., Aubinet, M., Baldocchi, D., Berbigier, P., Bernhofer, C., Ceulemans, R., Dolman, H., Field, C., Grelle, A., Ibrom, A., Law, B. E., Kowalski, A., Meyers, T., Moncrieff, J., Monson, R., Oechel, W., Tenhunen, J., Valentini, R., Verma, S. (2002). Energy balance closure at FLUXNET sites. Agricultural and Forest Meteorology, 113(1-4), 223–243. doi:10.1016/S0168-1923(02)00109-0

Yoshifuji, N., Kumagai, T., Tanaka, K., Tanaka, N., Komatsu, H., Suzuki, M., Tantasirin, C. (2006). Inter-annual variation in growing season length of a tropical seasonal forest in northern Thailand. Forest Ecology and Management, 229(1-3), 333–339. doi:10.1016/j.foreco.2006.04.013

Zhang, Y., Li, T., Wang, B., & Wu, G. (2002). Onset of the Summer Monsoon over the Indochina Peninsula: Climatology and Interannual Variations. Journal of Climate, 15(22), 3206–3221. doi:10.1175/1520-0442(2002)015<3206:OOTSMO>2.0.CO;2

Chapter 6

Summary and conclusion

This study aimed to reveal heat, water and carbon exchanges between atmosphere and tropical deciduous forest in Southeast Asia. To this aim, eddy covariance measurements were conducted at a teak plantation in Northern Thailand where long-time meteorological measurements and LAI monitoring have been already measured. Furthermore, the author estimated 6-years evapotranspiration by using a big-leaf model, and revealed the effect of rainfall and growing season length to of evapotranspiration at a tropical deciduous forest in Southeast Asia.

Chapter 1 emphasized the importance of assessing evapotranspiration, and the relationship between water and carbon exchanges in tropical deciduous forest in Southeast Asia. In recent studies, measurement and modeling of water and carbon exchanges based on eddy covariance measurements have been widely used as a powerful technique. However, studies on the canopy-atmosphere heat, water and carbon exchanges at a tropical deciduous forest are less relative to that in other vegetation types. Therefore, it was showed that requirement of investigating heat, water and carbon exchanges of tropical deciduous forests and their response to the environmental variables based on the field measurements.

Chapter 2 showed a site description, and seasonal and interannual variation of meteorological variables, LAI and eddy fluxes. Measurements were conducted in an even-aged teak (*Tectona grandis* Linn. f.) stand planted in 1968 in Mae Moh plantation, Lampang province, northern Thailand (18 ° 25 N, 99 ° 43E, 380 m above sea level). Teak is one of the major deciduous tree species of Southeast Asia, and its plantation are widely distributed over tropical Asia. Simple species components and forest structure of plantation provides an advantage to evaluate the energy, water and carbon exchanges between atmosphere to forest. For these reasons, this study site was chosen. Annual summed rainfall and mean temperature with standard deviation during 6-observed-years were 1415.5 ± 296.8 mm and 25.2 ± 0.5 °C, respectively. Clear seasonality of rainfall was observed. T_a, VPD and $\Theta_{0\text{-}60}$ had a clear senility corresponded with seasonality of rainfall. R_s showed a seasonal variation caused by the changes of solar elevation. Seasonality of this site could be roughly divided into the wet season and the dry season. The dry season can be divided into the cool and hot dry season, respectively. Mean maximum LAI value was 3.0 ± 0.2 (m^2 m^{-2}) during from 2006 to 2011 and interannual variation of maximum LAI was insignificant. The mean growing season length was 310 ± 16.8 (days) and growing season length was corresponded to timing of onset and offset of wet season. The difference the number of

annual rainfall event was mainly caused by the number of small rainfall event (< 10mm) although the difference annual rainfall was mainly caused the amount of heavy rainfall event (> 40mm) because about half of rainfall was supplied by the heavy intensity rainfall event (> 40 mm). To remove the noise due to rainfall, over range output of USA-1 and LI7500 and unstationality data, quality control was conducted. After quality control, 8703 (16.79 %) eddy flux data was used in analysis in this study. For after quality controlled dataset, spectral and co-spectrum analyses were conducted. Each normalized spectra converged to a $-2/3$ line at a high-frequencies and each generalized co-spectrum also converged to a $-4/3$ line at a high-frequencies. These results showed that each variable of flux easements is measured appropriately in this study site. Footprint analysis also examined. Among the after quality control data (n = 8703), 7037 data sets (80.86 %) were plotted inside the boundary line of this study site. It was considered that the source of observed eddy flux at tower was almost within the range of site boundary line. The relationship between available energy ($R_n - G$) and sum of sensible heat (H) and latent heat (LE) fluxes was examined. As a results, regression slope and regression coefficient were 0.673 and 0.635, respectively (n = 8703). The regression line of within site boundary line data (n = 7037) was 0.690 (R^2 = 0.711) and slightly larger. The difference of energy balance ratio between after quality controlled all data and within site boundary line data was insignificant. The energy imbalance in this site was 31 - 33 % although energy balance closure in this study was within the range reported by Wilson et al. (2002). IBR was smaller and was more depend on u^* when u^* < 0.2 (m s^{-1}) although IBR was increasing with increasing u^* in linearly when u^* > 0.2 (m s^{-1}). In this study, the seasonal and inter annual variation of energy balance closure was also examined. In each LAI levels, IBR showed insignificant difference. IBR did not have bias in specific LAI, season of wet and dry, and observed year. Based on these findings, it was considered that, although energy imbalance occurred, eddy flux measurement was conducted as appropriately and sufficient data for analysis the seasonal and interannual variation of heat, water and carbon flux between forest and atmosphere was observed in this study. Clearly seasonal variation of H and LE was observed. LE was more prominent than H during the wet season, whereas in the dry season, the latter was the major form of energy emitted to the atmosphere. Occasional increases in LE occurred during the hot dry season, when teak trees were almost leafless. These increases may have been caused by soil evaporation from the moist ground, as the above-mentioned rainfall events prior to the beginning of leaf-out were followed by the eventual increases in LE. Another possible explanation for the increases of LE involves transpiration by understory plants, such as shrubs and bamboos, which are patchily distributed at this site. Based on these findings in this chapter, the ratio of sensible and

latent heat flux showed largely seasonal changes due to the seasonality of rainfall with following the seasonal variation of leaf area index.

In Chapter 3, seasonal and interannual variation of G_s, G_c and g_s and its controlling factors were examined. To evaluate g_s observed LE was decomposed into transpiration from teak and soil evaporation using developed soil evaporation model and LAI. The seasonal and interannual variation of G_s, G_c and g_s were estimated and the averaged g_s in mid-growing season showed a interannual variation despite the maximum LAI was almost constant in every year. The value of g_s was increasing with increasing of LAI. The value of g_s in mid-growing season was the highest in a year, and g_s in leaf-out season was higher than that of leaf senescence season despite of the same LAI level. The relationship between monthly g_{sref} and m was almost plotted near Oren's line although data in mid-growing season tended to be plotted below the line The value of g_{sref} was significant higher in the growing season than other season. But insignificant difference of m/g_{sref} was observed throughout a year. To clarify the controlling factor to decide a magnitude of g_s, the response of g_{sref} to controlling factors was examined. The seasonality of g_{sref} mainly correlated with soil water contents. On the other hand, the significant relationship between LAI and g_{sref} was also observed just only the period in growing season and leaf-senescence season. As results, it was implied that the effect of physiological changes like a maturing and aging of teak leaves (allocation and reallocation of nitrogen) affected to the relationship between g_{sref} and LAI in mid-growing season and leaf-senescence season, respectively. In addition, seasonality of LAI was strongly influenced by the seasonal changes of soil moisture contents in this study site

In Chapter 4, modeling of stomatal conductance and six-year estimation of evapotranspiration based on the big-leaf model were conducted to evaluate the seasonal and interannual variation evapotranspiration at a teal plantation in Northern Thailand. The values of roughness length (z_0) and zero plane displacement (d) were estimated from the friction velocity, which was determined using the sonic anemometer under near-neutral condition, $|z/L| < 0.05$. The value of d and z_0 that were calculated using all data were 20.73 m and 1.93 m, respectively and the effect of seasonal changes of LAI was not clear. To calculate big-leaf model's canopy conductance, Jarvi-type stomatal conductance model was chosen. The parameter values of Jarvis conductance model to minimize the root mean square error (RMSE) between the observed and predicted values of g_s under the constraint that the function line did not fit to a lower position than the upper boundary of the scatter of observed g_s values. The model function of R_s, VPD and Θ_{0-60} was selected as a best fitting model. The relationship between observed LE and modeled LE that was sum of canopy transpiration and soil evaporation during dry canopy showed good agreement. The accuracy

of soil evaporation was already examined in Chapter 3. In this study, Rutter type interception model parameter was examined. Based on the through-fall and stemflow measurements, annual summed interception during 2006 (period from January to December) was 106.2 mm (Tanaka, private communication). It should be noted that interception rate was constant through the year, and the effect of seasonal changes of LAI to interception rate was not clear. Optimum S_{cmax} that canopy storage capacity was calculated as to minimize the residual between observed interception (= 106.2 mm) and modeled interception and optimum S_{cmax} that was to minimize the residual between observed interception and modeled interception was estimated 0.26 mm LAI^{-1}. As a result of big-leaf model calculation, 6-year averaged ET, E_{tc}, E_{ts} and EI were 1154.6 mm, 792.1 mm, 256.6 mm, and 105.9 mm, respectively. The result of interception of this study, EI, canopy interception (E_{i}) and trunks interception (E_{it}) were 7.5 %, 6.2 % and 1.3 % of annual rainfall, respectively. Compared to previous studies, it was shown that the interception rate in this site was relatively small. It can be considered that heavy rainfall, less rainfall events and small basal area made small interception as a reason of small interception in this study. In this study site, the value of annual ET was changed with P_{G} and GSL, respectively. The mean and standard deviation of P_{G} and GSL in 6-observed years were 1415.5 ± 296.8 mm and 310 ± 16.8 days, respectively. If P_{G} and GSL change 1σ, the annual ET changes 30.05 mm and 83.45 mm, respectively from the mean year. Therefore, ET was more influenced by the variance of GSL than that of P_{G}. The clear seasonality of LAI influenced energy partitioning between the canopy and the soil surface, and decided the soil evaporation and transpiration. Although, zero plane displacement and the roughness length were little influenced by LAI. The value of Scmax did not change with changing LAI. Consequently, contribution of GSL to evapotranspiration was relatively large than other factors.

In Chapter 5, the seasonal progression and relation of H and LE, and NEE with seasonal changes of LAI were showed. About the seasonality of NEE, in the beginning of the wet season, NEE appeared to increase with increasing LAI, indicating that CO_2 assimilation by photosynthesis of teak trees increased with increases in their leaf amount during this period. The maximum value of NEE uptake occurred in July and declined gradually thereafter. Essentially, the decline NEE occurred approximately 3 months earlier than the start of LE decrease. The value of P_{max} that was the most important parameter indicating the photosynthetic capacity of this forest ecosystem and seasonality of LAI was compered. The maximum value of P_{max} appeared in July, whereas minimum P_{max} appeared in March. P_{max} increased linearly from April to July, but this pattern did not closely parallel that of LAI. In fact, P_{max} increased in parallel with LAI during the April–June period but not after July. P_{max} decreased steadily during the August – November period, despite the absence of

substantial changes in LAI. During this period (August – October 2006), leaf age was likely the major factor causing decreases in the photosynthetic capacity of teak trees after maturation. Because, clear seasonal trends in soil water content, net radiation, or water vapor pressure were not observed. The consistent decline in P_{max} during the late growing season points to drastic decreases in the water-use efficiency of teak in the corresponding season, as LE at this site remained high at least until the end of October. The decoupling of the seasonality of water and carbon exchanges may be particularly important when modeling the ecohydrology of evergreen forests as well as this tropical deciduous forest.

As mentioned above, this study revealed that the interannual variation of evapotranspiration and seasonality of heat, water and carbon exchanges between atmosphere and tropical deciduous forest in Southeast Asia. Again, the author revealed that not only annual rainfall but also growing season length plays an important role for interannual variation of evapotranspiration, and decoupling of the seasonality of water and carbon exchanges. These findings in this study emphasized that the importance of LAI dynamics for more complex numerical model for water and carbon cycle in tropical deciduous forest under the Asian monsoon influence, and also will allow further understandings of hydro-ecological responses to environmental changes in tropical deciduous forest.

Acknowledgements

First, the author would like to appreciate Professor Dr. Masakazu Suzuki (The University of Tokyo), who provided the opportunity to conduct field observation of hydro-physiological studies in tropical deciduous forest in Northern Thailand, helpful suggestion, critical comments and encouragements.

The author would like to express great thanks to Dr. Natsuko Yoshifuji (Kyoto Univ.), Mr. Takanori Sato, Dr. Nobuaki Tanaka (The University of Tokyo), Dr. Katsunori Tanaka (Japan Agency for Marine-Earth Science and Technology), and all the other Japanese researchers and students from The University of Tokyo for their great help for conducting the field observations, providing the data, many discussion and suggestions and enjoyable time in a filed in Thailand. The author also grateful to Dr. Nipon Tangtham and Dr. Chatchai Tantasirin (Kasetsart University) for providing the opportunity to conduct the field measurements and the assistance to continue the research in Thailand. Dr. Masatoshi Aoki and the Staff of Thai Forest Industry Organization MaeMoh office also supported the filed study in teak plantation in MaeMoh. Ms. Ae, Mr. Che and Mr. Min (in Chaing Mai) and Mr. Swan and Mr. Ei (in MaeMoh) also supported the activity at the field and the downtown in Chaing Mai and Lampang city, I would like to express sincere thanks to them, too.

The author appreciates to Assoc. Professor Dr. Nobuhito Ohte, Dr. Tomoki Oda, Dr. Norifumi Hotta, Dr. Tomonori Kume and Dr. Kumagai Tomo'omi for suggesting me some analysis and to write a paper included in this thesis. I also thank Dr. Takehiko Ohta for suggesting me to study and research in The University of Tokyo.

This study was supported by CREST (Core Research for Evolutional Science Technology, PI: Prof. Masakazu Suzuki) of Japan Science and Technology Agency and GCOE (Global Center of Excellence, PI: Prof. Tetsukazu Yahara).

Finally, the author wishs to express my heartfelt thanks to my friends and also my family. And, my friends that I had meet and know for the last seven years in Tokyo whom I will greatly missed as we part to go on our own journey. It was an interesting chapter of my life journey, where I have met and forge friendship with few friends that often "bring laughter and joy" into my life especially Rie Fuji.